Programme Area: Carbon Capture and Storage

Project: Storage Appraisal

Title: Representative Structure Modelling of Diping Open Saline Aquifers

Abstract:

This document is a supporting document to deliverable MS6.1 UK Storage Appraisal Final Report.

Context:

This £4m project produced the UK's first carbon dioxide storage appraisal database enabling more informed decisions on the economics of CO2 storage opportunities. It was delivered by a consortium of partners from across academia and industry - LR Senergy Limited, BGS, the Scottish Centre for Carbon Storage (University of Edinburgh, Heriot-Watt University), Durham University, GeoPressure Technology Ltd, Geospatial Research Ltd, Imperial College London, RPS Energy and Element Energy Ltd. The outputs were licensed to The Crown Estate and the British Geological Survey (BGS) who have hosted and further developed an online database of mapped UK offshore carbon dioxide storage capacity. This is publically available under the name CO2 Stored. It can be accessed via www.co2stored.co.uk.

UKSAP

Appendix A5.3

Representative Structure Modelling of Dipping Open Saline Aquifers

Conducted for

The Energy Technologies Institute

By

RPS Energy

Author	Jeff Masters .....
Technical Audit	Eugene F Balbinski .....
Quality Audit	.....
Release to Client	Grahame Smith .....
Date Released	28th October 2011 (final) .....

File Location
Appendix A5.3 - Representative Structure Modelling of Dipping Open Saline Aquifers.doc

Executive Summary

Open aquifers have potentially large storage capacity as they are less constrained by fracture pressure limits than pressure cells and pressure can bleed off over time. However, as injected CO_2 may migrate updip large distances in thin plumes, storage security may be an issue and they are challenging to model, requiring large computing resources. Although there is some analytic work in the literature modelling this behaviour, it is hard to apply to obtain quantitative dynamic estimates of storage capacity. The literature is also lacking in numerical reservoir simulation studies which can readily be applied to UKCS open aquifers, so this project conducted its own Representative Structure and Exemplar studies. This Appendix describes in detail the Representative Structure modelling on open aquifers.

A project workshop was held to consider how to model the large dipping open aquifers identified on the UKCS and defining parameters were agreed. The representative model consisted of a large tilted slab with some transverse curvature to enhance channelling, but with a smooth dipping top surface. The trapping mechanisms modelled were residual and dissolution, but heterogeneity and structural trapping from surface topology were not included, as these were to be investigated using the more detailed Exemplar models.

Dynamic estimates of storage capacity require some constraint determining when the store is 'full', which may depend on the type of store under consideration. An operational definition for dipping open aquifers, applicable to numerical simulation, was developed based on the existing UK/EU guidelines.

Typically CO_2 injected into this model formed a thin tongue under the overlying seal and migrated updip tens of kms over thousands of years due to its density being lower than the surrounding brine. During this time injected CO_2 which had remained near the point of injection gradually became residually trapped, though this took several thousand years. As run times for these models were beyond the limit of what was practical for a study requiring many cases to be run, it was not possible to represent a typical full aquifer unit requiring multiple injectors with these models alone. Therefore a computer program using a pressure upscaling technique and utilising symmetry and superposition was written to estimate the extent of the pressure footprint from multiple injectors. The dynamic capacity was then calculated from the volume required for a single injector, combined with the number of injection sites which could be accommodated in the aquifer, taking into account pressure interference between neighbouring injection sites.

Almost 100 separate cases were then investigated using these models. These included many cases covering the range of sensitivities identified at the modelling workshop such as the role and importance of key properties such as dip, permeability, depth, porosity, thickness, vertical to horizontal permeability anisotropy, trapped gas saturation and salinity. When data from actual UKCS storage Units became available in CarbonStore a further group of cases were simulated in order to ensure that coverage of the full range of UKCS open aquifers was obtained.

Representative permeability and mean dip were found to be the most important factors affecting storage security and dynamic storage capacity in dipping open aquifers, as they strongly influence the speed of updip CO_2 migration. In order to facilitate storage capacity estimation, it proved useful to classify the simplified modelled open aquifers into three broad storage regimes using these two key factors:

- Regime 1 has poor well injectivity, but good storage security and is characterised by a low representative permeability.
- Regime 2 is characterised by both good CO_2 injectivity and good storage security and therefore typically has higher storage capacities.
- Regime 3 has good CO_2 injectivity, but storage capacities are strongly constrained by the tendency of CO_2 to migrate updip due to buoyancy forces. Such stores are characterised by either a high representative permeability or significant mean dip, or both.

For each of these storage regimes a range and most likely value of storage capacity were estimated. Typical storage capacities obtained were equivalent to significantly less than the 2% of pore volume figure originally assumed from the literature, for initial CarbonStore estimates. These results which were then compared with those from the open aquifer Exemplar model and a combined set of results agreed for use in CarbonStore. These results were also compared with other studies. Whilst no similar study was available for a good comparison, the results produced in this project are consistent with other published results where relevant.

Contents

List of Tables

List of Figures

1 Introduction

For CO_2 injection into saline aquifers, the interaction between gravity and viscous forces determines in large part how much CO_2 can be trapped by capillary forces, see, for example, (Kovscek, 2006). Trapping requires that CO_2 saturations decrease, either at the trailing edge of CO_2 that is migrating upward, or because redistribution of water causes CO_2 to flow into a region with already high CO_2 saturations. Additional CO_2 is trapped if high CO_2 saturations are subsequently reduced. When gravity dominates the flow, a thin tongue of injected CO_2 flows just under the top boundary of the aquifer. CO_2 saturations reach high levels there, but dissolution and, possibly, mineralisation, are the only mechanisms acting during the post-injection period which might reduce CO_2 saturations. When viscous forces dominate the long period of post-injection redistribution of CO_2 by gravity-driven flow allows significant trapping. For the dipping open aquifers considered in this project, typically gravity dominates so injected CO_2 forms a thin tongue under the overlying seal and migrates tens of kms updip over thousands of years, see **Figure A1.1**. During this time injected CO_2 which remains near the point of injection gradually becomes residually trapped, though this takes several thousand years.

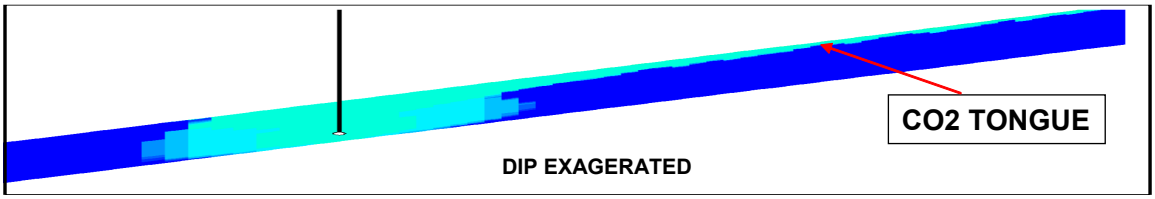

Figure A1.1: Typical Behaviour of Injected CO_2 in Dipping Open Aquifers

Open aquifers have potentially large storage capacity as they are less constrained by fracture pressure limits than pressure cells and pressure can bleed off over time. However, as injected CO_2 may migrate updip large distances, storage security may be an issue and they are challenging to model, requiring large computing resources. Although there is some analytic work in the literature modelling this behaviour, it is hard to apply to obtain quantitative dynamic estimates of storage capacity, see section 8. The literature is also lacking in numerical reservoir simulation studies which can readily be applied to UKCS open aquifers, so this project conducted its own Representative Structure and Exemplar studies. This Appendix describes in detail the Representative Structure modelling on open aquifers.

A project workshop was held to consider how to model the large dipping open aquifers identified on the UKCS. This workshop considered a number of relevant issues including the following:

- Should limits be placed on the distance CO_2 can migrate from the point of injection?
- Should there be limits on the CO_2 migration rate across a virtual boundary?
- How long to model after the end of CO_2 injection?

Dynamic estimates of storage capacity require some constraint determining when the store is ‘full’, which may depend on the type of store under consideration. The conclusions from the workshop discussions were used to construct an operational definition, applicable to numerical simulation, of when dipping open aquifers might be considered ‘full’, based on existing UK/EU guidelines. This is described in section 5.

The workshop also defined parameters for the Representative Structure model, see section 0. The model consisted of a large tilted slab with some transverse curvature to enhance channelling, but with a smooth dipping top surface, as described in section 4. It was recognised that this model was unrealistic in some respects. For example, in reality, CO_2 might be trapped in small scale undulations in the top structure, or due to heterogeneities, for example shale barriers. However, it was considered that such deficiencies were better addressed through the modelling of an actual geology in a detailed Exemplar model. The results from the Representative Structure modelling might then be revised accordingly. The trapping mechanisms included in the Representative Structure model were residual and dissolution.

Running times for these models were beyond the limit of what was practical for a study requiring many cases to be run, so it was not possible to represent a typical full aquifer Unit, requiring multiple injectors, with these models alone. Therefore a computer program using a novel pressure upscaling technique and utilising symmetry, the method of images and superposition, was written to estimate the extent of the pressure footprint from multiple injectors. This is described in section 5. The dynamic capacity was then calculated from the volume required for a single injector, combined with the number of injection sites which could be accommodated in the aquifer, taking into account pressure interference between neighbouring injection sites.

Almost 100 separate cases were then investigated using these models. These included scoping grid sensitivity and boundary condition cases which are described in section 3. These cases also covered the range of sensitivities identified at the modelling workshop, such as the role and importance of key properties such as dip, permeability, depth, porosity, thickness, vertical to horizontal permeability anisotropy, trapped gas saturation and salinity, see section 6. When data from actual UKCS storage Units became available in CarbonStore, a further group of cases were modelled in order to ensure that coverage of the full range of UKCS open aquifers was obtained, see section 7. The results obtained are compared with some from other relevant studies in section 8.

2 Simulation Model Parameters

A simple simulation model, motivated by the key features of the Palaeocene fans, was constructed to represent CO_2 storage in dipping open aquifers. It has constant dip in the Y-direction (longitudinal) whilst the X direction (transverse) has a curved (parabolic) top surface, to enhance channelling, characterised by the dip from the centre of the model to the outer edge. The model has a smooth top surface top surface (no structural trapping) and a constant width. The length of the model is determined by specifying the depth at which CO_2 is injected and the longitudinal dip. The updip extent of the model is typically curtailed at a depth of 1000 m although some models have been extended to a depth of 800 m. Typically 50 km of aquifer is modelled downdip from the point of injection although some simulations only include 10 km of aquifer (see section 5). Typical cross sections through the simulation model are shown in **Figure A2.1**

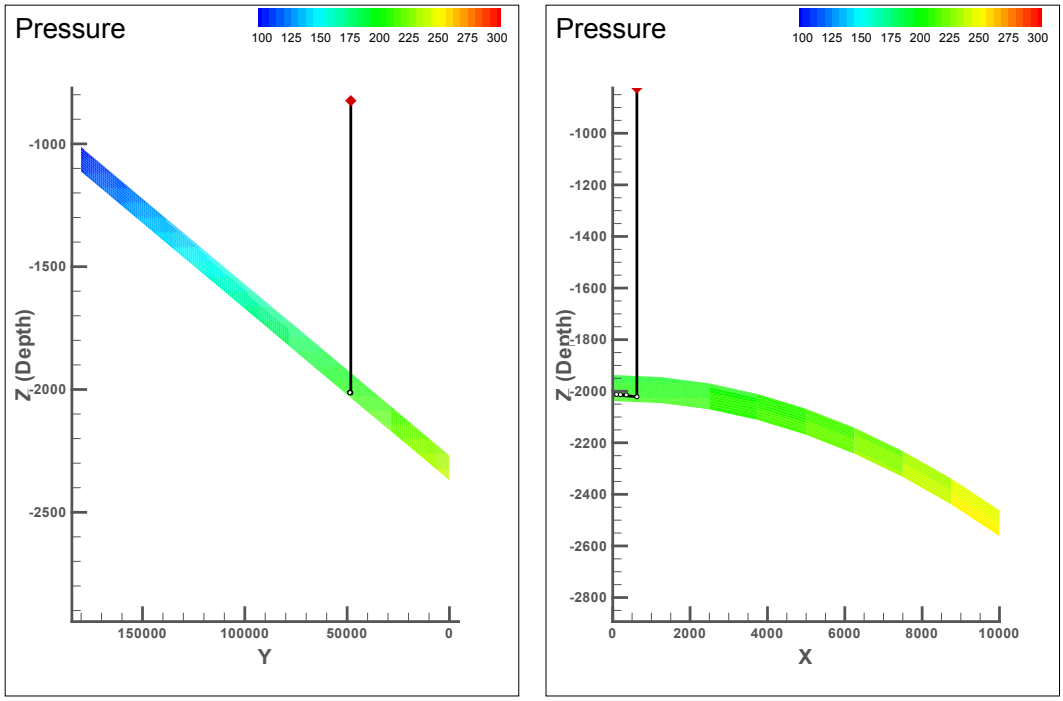

Figure A2.1: Longitudinal and Transverse Cross Sections through Simulation Model

The range of parameters and the base case values were discussed at the workshop, which included a number of industry experts, and modelling update meetings (Smith 2010a, Smith 2010b). A representative model with defining parameters was agreed (**Table A2.1**). The base case model parameters correspond to a store with good injectivity and security, storage regime 2 in section 7.2, justifying the chosen parameter set as suitable for CO_2 storage.

The trapping mechanisms modelled were residual and dissolution, but heterogeneity and structural trapping from surface topology were not included, as these were to be investigated using the more detailed Exemplar models.

Almost 100 separate cases were investigated using these models. These included many cases covering the range of sensitivities identified at the modelling workshop (**Table A2.1**). When data from actual UKCS storage Units became available in CarbonStore, a further group of cases were simulated in order to ensure that coverage of the full range of UKCS open aquifers was obtained. This included extending the permeability range to 12 -D.

Property	Minimum	Base Case	Maximum
Length (km)	23	180	180
Width (km)	5	20	40
Depth (m)	1000	2000	3000
Longitudinal dip (°)	0.1	0.4	5.7
Curved transverse top surface mean dip (°)	1	3	5
Longitudinal Permeability (mD)	5	300	3000
Transverse Permeability (mD)	3.8	30	3000
Permeability anisotropy (ratio)	1	10	100
Vertical Permeability (mD)	0.3	30	300
k_v:k_h ratio	0.001	0.1	1
Porosity (may decrease with depth)	0.06	0.27	0.33
Thickness (m)	25	100	400
NTG (fraction)	1.0	1.0	1.0
Salinity (ppm)	50000	100000	200000
Trapped Gas Saturation (fraction)	0.15	0.3	0.45
Rock compressibility (1/MPa)	$5.8x10^{-4}$	$5.8x10^{-4}$	$15x10^{-4}$
Geothermal gradient (°C/km)		30	
Hydrostatic pressure gradient (psi/ft)		0.45	
Well Length (m)	100	900	1000
Well bore radius (m)		0.1	
Open updip and downdip boundaries	Closed	Open	

Table A2.1: Range of Parameters to Simulate using DOA Model

Other features of the simulation model are:

- ECLIPSE100™ black oil;
- Hysteresis Model (Carlson or Killough);
- Downdip injection;
- Well orientation horizontal (transverse and parallel to dip), vertical;
- Horizontal well trajectory 1/5 of thickness from bottom surface;
- Fifty years of continuous CO_2 injection subject to;
    - maximum BHP calculated as 90% of the fracture gradient of 0.8 psi/ft;
    - maximum injection rate of 4 Mt/year.

3 Simulation Model Construction

The simulator used for this work was ECLIPSE100™ as recommended from a previous phase of this project (see Appendix A5.1). An extended black oil representation was used to account for CO_2 dissolution and brine vaporisation. The data was generated from the TOUGH2™-ECO2N module. In this model the brine is represented by the oil component and the CO_2 by the gas. Salt precipitation plus geochemical and geomechanical processes were ignored. A companion task considered these issues as part of an injectivity study (see Appendix A5.8).

3.1 Grid Size Sensitivity

The results of numerical simulation of flow in aquifers may be sensitive to the size of grid block chosen to discretise the model (Mattax and Dalton, 1990). Typically discretisation errors (numerical diffusion) increase as the grid block dimensions are increased. As a preliminary step to performing simulation a grid sensitivity study was undertaken in which the areal size of the grid was varied between 50 and 500 m. The grid sensitivity study used a truncated version of the base case model described in section 4 which was only 50 km long. Most of these preliminary simulations were run for 10,000 years except for the finest grid size which was stopped after approximately 3,000 years due to excessive computer run time.

The vertical layering was selected to ensure that free CO_2 plume occupied at least two layers in the simulation model once it has migrated significant distances (tens of kilometres) from the point of injection (see section 4). This resulted in varying vertical grid thickness from 0.5 m at the top to approximately 5 m at the bottom.

The impact of the areal grid block size on the migration distance and velocities of the injected CO_2 is shown in **Figures A3.1 to A3.3**. These plots show how far a fixed percentage of the CO_2 has migrated from the point of injection. The migration velocity of the limit of CO_2 is also plotted in **Figure A3.1**. The 99% limit in **Figure A3.2** indicates that 99% of the injected CO_2 is contained within the plotted distance from the injection well and the migration velocity corresponds to the rate of advance of the limit of this fraction of the injected CO_2.

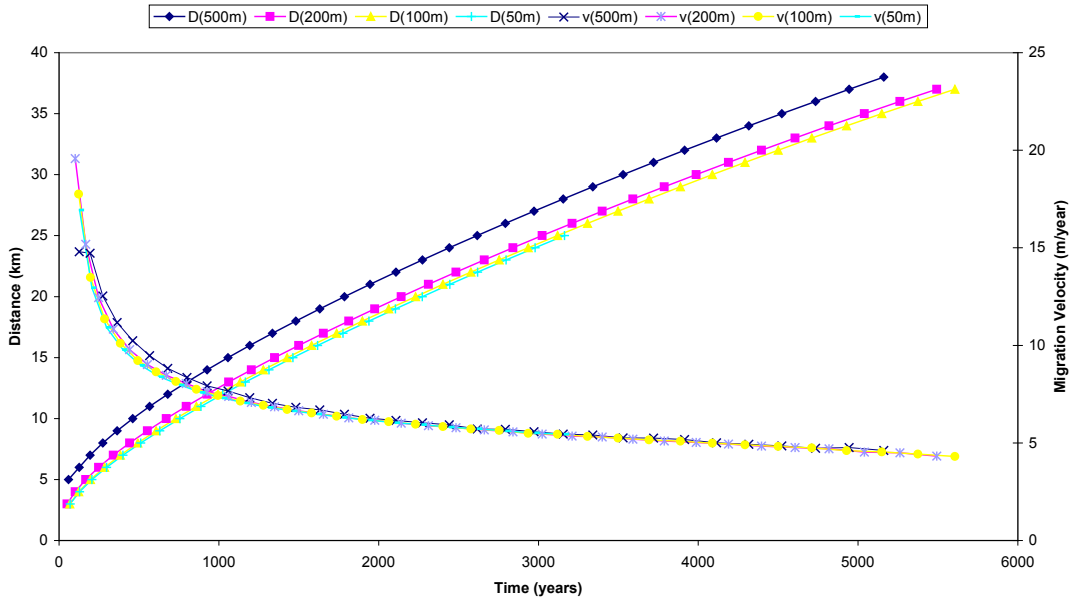

Figure A3.1: Variation of the Migration of 99.999% Limit of Injected CO_2 with Grid Size

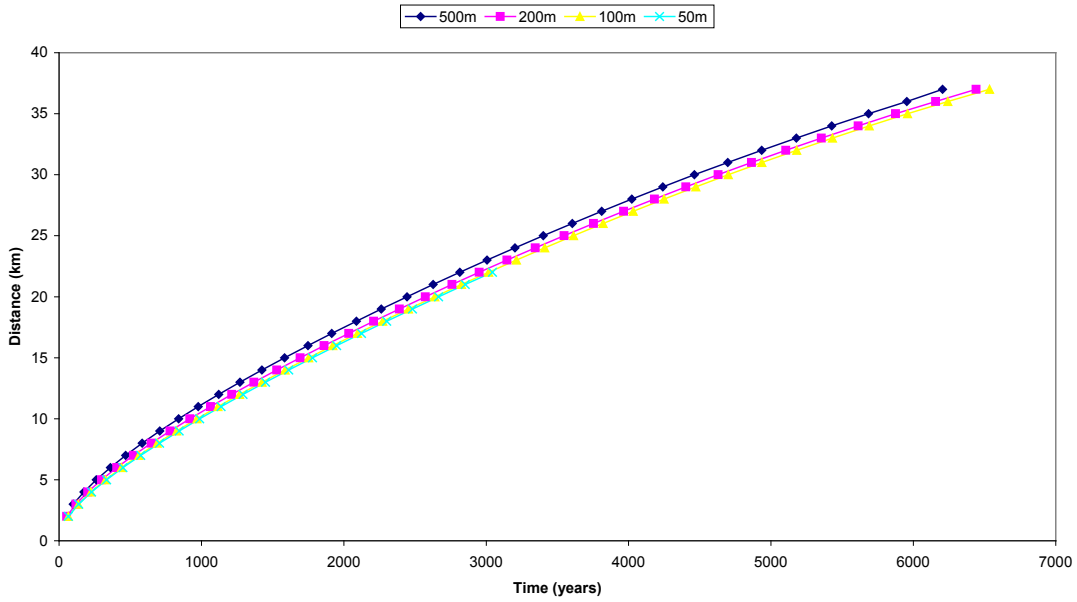

Figure A3.2: Variation of the Migration of 99% Limit of Injected CO_2 with Grid Size

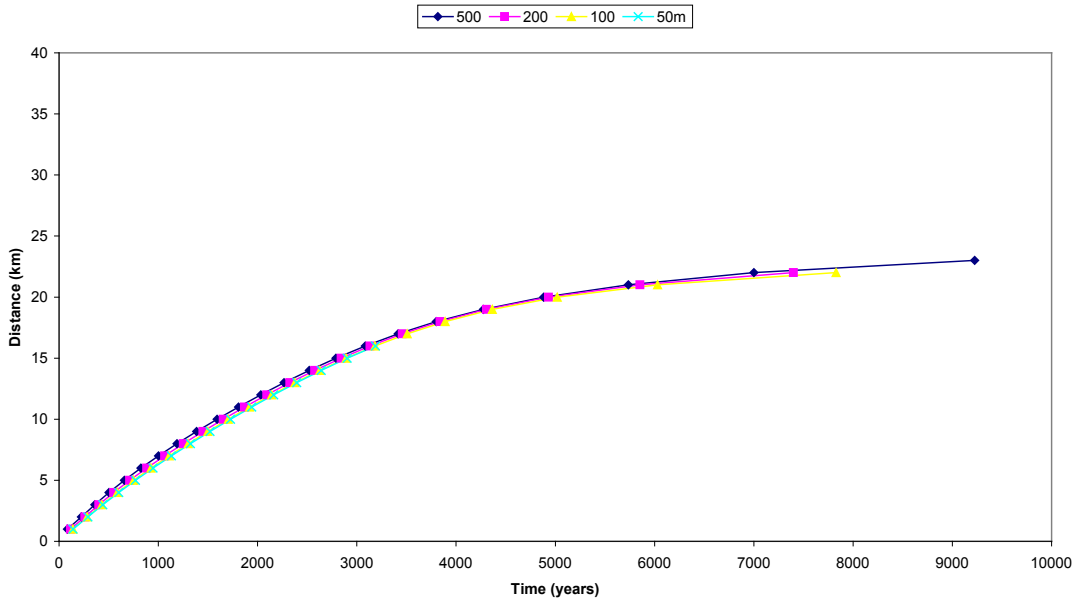

Figure A3.3: Variation of the Migration of 90% Limit of Injected CO_2 with Grid Size

Figures A3.1 to A3.3 show increasing difference in migration distances with grid size with the limit of larger fractions of the injected CO_2. The bulk of the injected CO_2 (90%) was quite well represented using the 500 m grid. However, the tip of the CO_2 plume had migrated approximately 5% further for the 500 m grid. The migration distances for the various fractions were very similar for the smaller grid sizes with differences only occurring at the very tip of the CO_2 plume. This effect can also be appreciated from the spatial distribution of CO_2 (**Figures A3.4 and A3.5**). In these figures, the CO_2 is injected at the 10 km point. Differences mainly occurred at the limit of CO_2 migration and were typically small for grid sizes of 200 m or less.

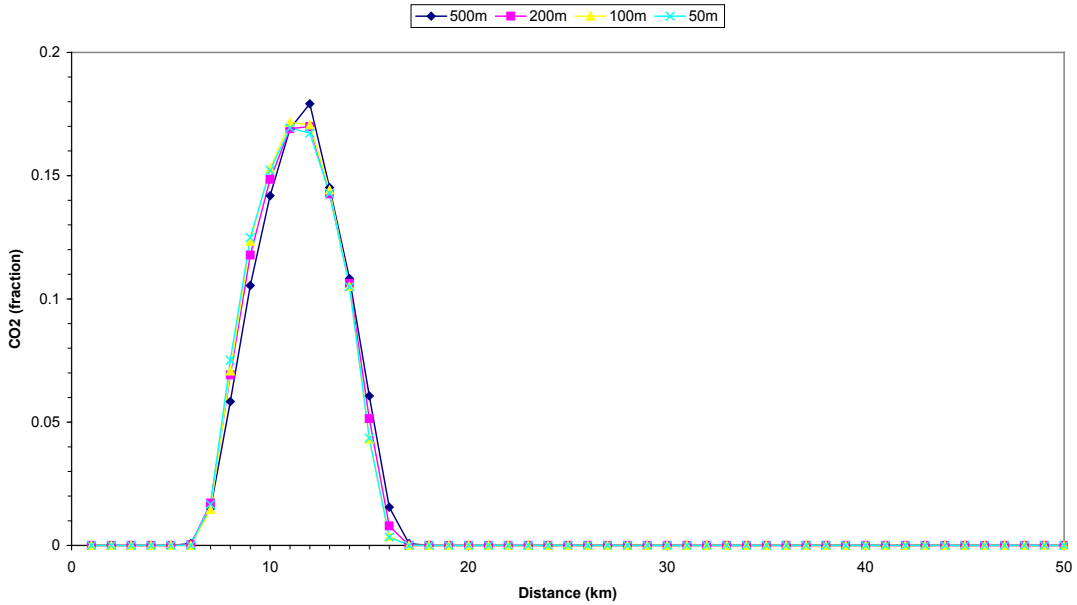

Figure A3.4: Spatial Distribution of Injected CO_2 at the end of Injection

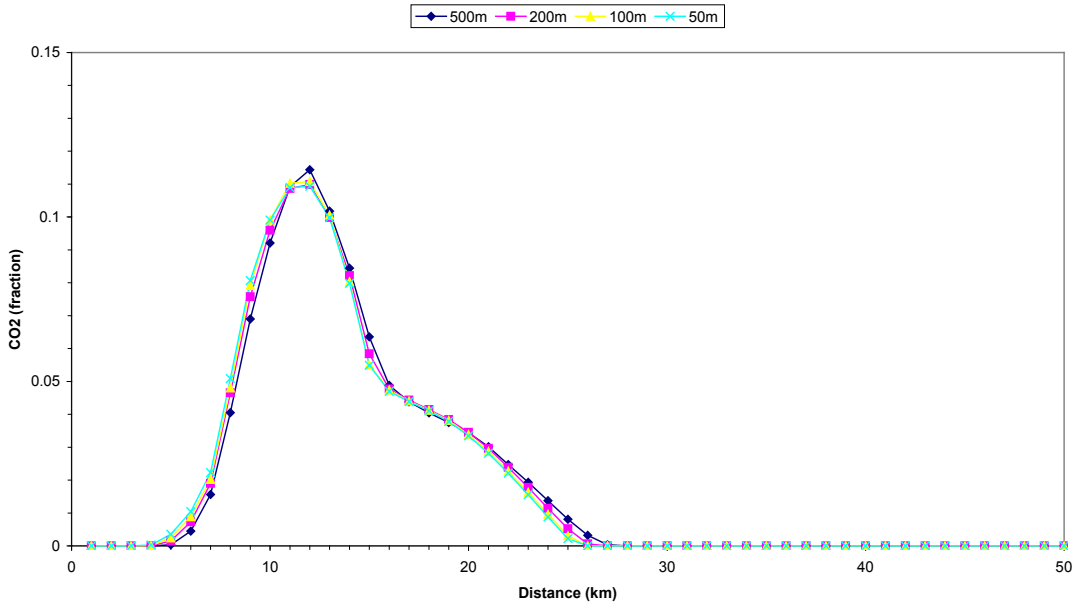

Figure A3.5: Spatial Distribution of CO_2 after 1000 Years

A storage factor was defined as the fraction of the pore volume occupied by the injected CO_2 where the pore volume is defined as the smallest cuboid which contains 99% of the injected CO_2. The storage factor is shown in **Figure A3.6**.

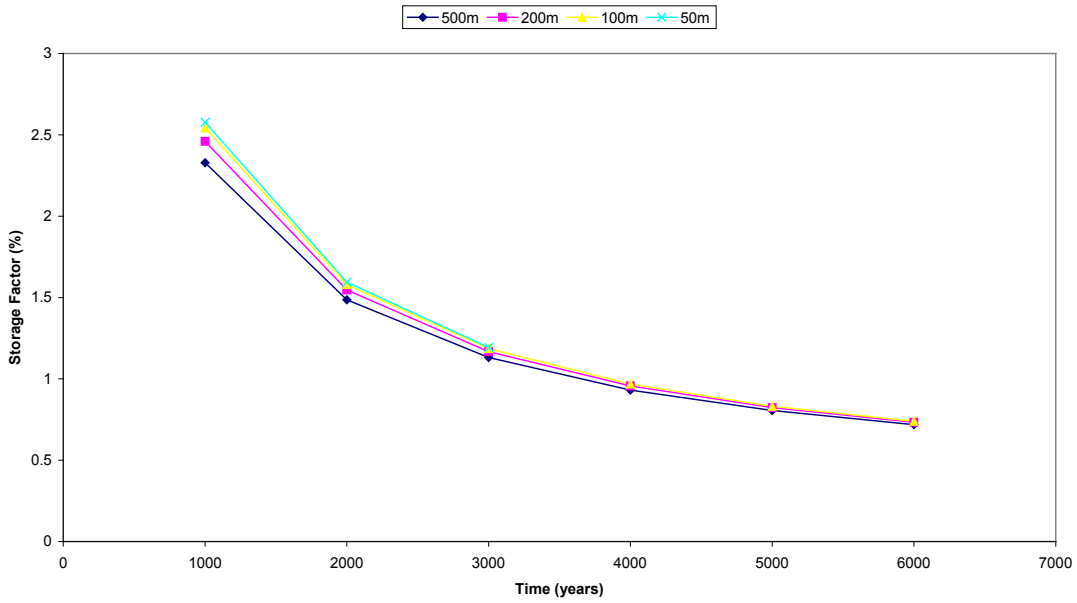

Figure A3.6: Variation of Storage Factor with Grid Block Size

For this definition, the storage factor decreases with time as the injected CO_2 migrates further updip increasing the total pore volume of the store. **Figure A3.6** shows a small difference in the calculated storage factors at 1,000 years which decreases with increasing time. At 1,000 years, the difference between the 500 and 50 m grids was approximately 10%, the difference between the 200 and 50 m grids was approximately 4% and the difference between the 100 and 50 m grid size was approximately 1%.

The computing run time increased significantly with decreasing grid size due to more grid blocks in the simulation model as shown in **Figure A3.7**. The increase is roughly parabolic and the 50 m case would have taken around 270 hours if run through to 10,000 years.

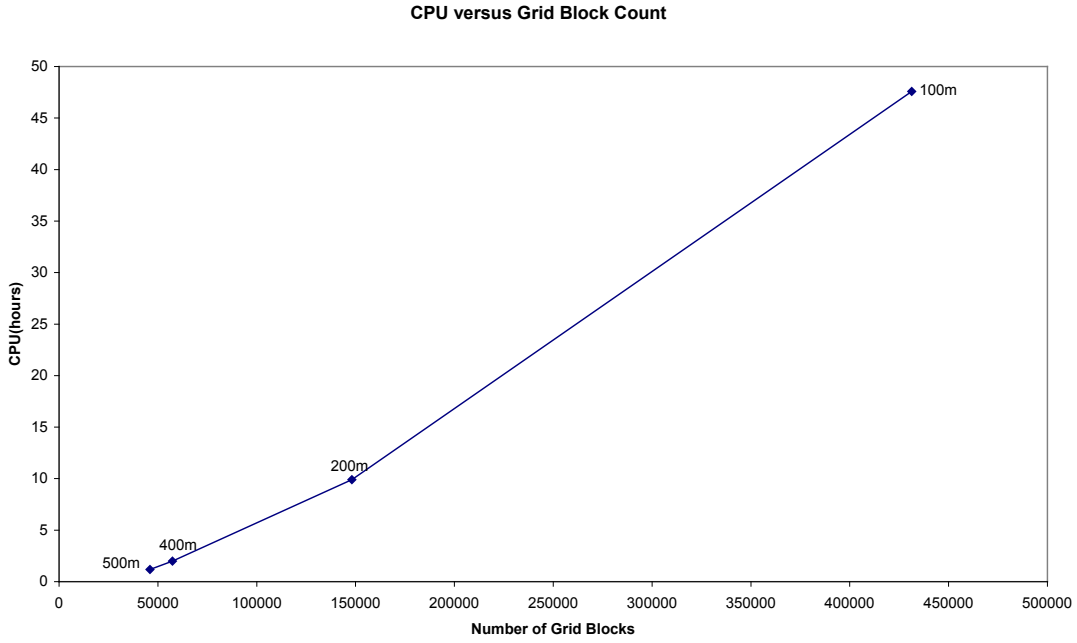

Figure A3.7: CPU Requirement versus Grid Block Count

The final choice of grid size is a compromise between modelling accuracy and computer run time. From this sensitivity study, it was concluded that the 200 m grid size would be adequate for modelling open aquifers in that the results that would be obtained using finer grids would not significantly change their interpretation and would still provide reasonable accuracy for the generated storage factors. Using coarser grids may result in a significant loss of accuracy in modelling the CO_2 plume. This would be undesirable because the pore volume utilisation depends on the total store volume which depends on the plume extent.

However, using a 200 m grid typically resulted in excessive run times for the base case of approximately 40 hours to simulate 1,000 years. The only practical option to significantly reduce this computing requirement is to drastically reduce the grid block count. A symmetry element, representing one half of the model had already been used to half the grid cell count. To further reduce the grid count it was decided to coarsen the grid in regions not contacted by the injected CO_2. This was achieved by first setting up a global grid with areal cell dimensions of 1 km by 1 km and vertical thicknesses of typically 5 to 10 m and then using local grid refinement (ECLIPSE100^{TM}, 2008) to reduce the cell size to 200 m areally. The vertical resolution was as described above and ensured no CO_2 crossed the boundaries between the coarse and fine grids, other than through gravity slumping of CO_2 dissolved in brine. This typically resulted in the number of grid blocks being reduced by a factor of 8. The final cell count in the base case model was approximately 150,000. The run time for the base case was reduced to 11.5 hours for 1,000 years and 28 hours for 10,000 years. At the modelling update meeting, it was agreed that only 1,000 years would be simulated (Smith, 2010b).

3.2 Boundary Conditions

The transverse edges of the model corresponded to no flow boundaries. As such they either represent the lateral limit of the aquifer or can be considered to be part of a pattern flood with comparable injection occurring to the side(s). Narrower pattern elements were run but it is shown in section 5 that they can be extrapolated from a wider model using the method of images and superposition of pressure transients.

The updip and downdip boundaries were considered to be open. They were modelled using a large pore volume grid block which essentially gave a constant pressure boundary condition. The significance of this choice has been investigated by varying the boundary from open to closed by changing the pore volume of the bounding blocks.

It was found that the proximity of the well to the boundary can significantly reduce the injection bottom hole pressure and so affect results when upscaling to multiple wells. Consequently, the injection well for most cases was placed a minimum of 50 km (updip geometry permitting) from the constant pressure boundary. The proximity of the downdip boundary was not found to significantly affect the distance CO_2 migrated updip from the point of injection (see section 5).

4 Base Case Detailed Description and Analysis

The base case simulation model properties are listed in **Table A4.1**. As described in section 2, the model was agreed at a Consortium workshop at which industry experts agreed the base properties as typical of potential UKCS stores. The base case model parameters correspond to a store with good injectivity and security, storage regime 2 in section 7.2 and are therefore typical of a good storage site.

Property	Base Case
Length (km)	180
Width (km)	20
Depth (m)	2000
Longitudinal dip (°)	0.4
Curved transverse top surface mean dip (°)	3
Longitudinal Permeability (mD)	300
Transverse Permeability (mD)	30
Vertical Permeability (mD)	30
k_v:k_h ratio	0.1
Porosity (fraction)	0.27
Thickness (m)	100
NTG (fraction)	1.0
Salinity (ppm)	100,000
Trapped Gas Saturation (fraction)	0.3
Rock compressibility (1/MPa)	5.8×10^{-4}
Temperature at injection depth (°C)	60
Pressure at injection depth (MPa)	20.35
Well Length (m)	900
Well bore radius	0.1
Updip and downdip boundary conditions	Open
Injection rate (Million tonnes/year)	4
Injection time (years)	50
Limiting BHP (90% of fracture pressure) (MPa)	32.58
Relative permeability	Viking 2 linearly extended to $S_{br}=0$, $k_{rCO2}=1$
PVT	Eclipse black oil tables (PVT_T_60_S_100000ppm.inc)

Table A4.1: Base Case Simulation Model Parameters

The length of 180 km allowed a model to be constructed with a depth variation of 1250 m. Initially the well was set 10 km from the downdip edge at a depth of 2000 m. The updip boundary was at a depth of approximately 900 m.

CO_2 was injected continuously at a rate of 4 Mt per year for 50 years. The development of the CO_2 plume is shown in **Figures A4.1 to A4.5**. Typically, the CO_2 migrated upwards until it reached the top surface of the model and then migrated updip as a long thin tongue.

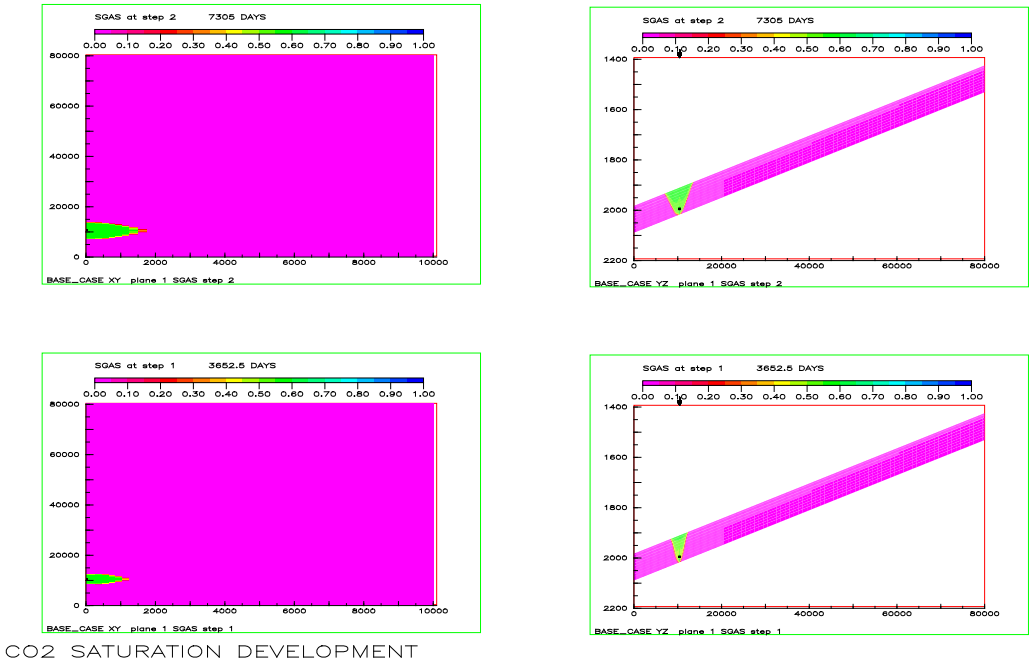

Figure A4.1: CO_2 Distribution during Injection after 10 and 20 Years

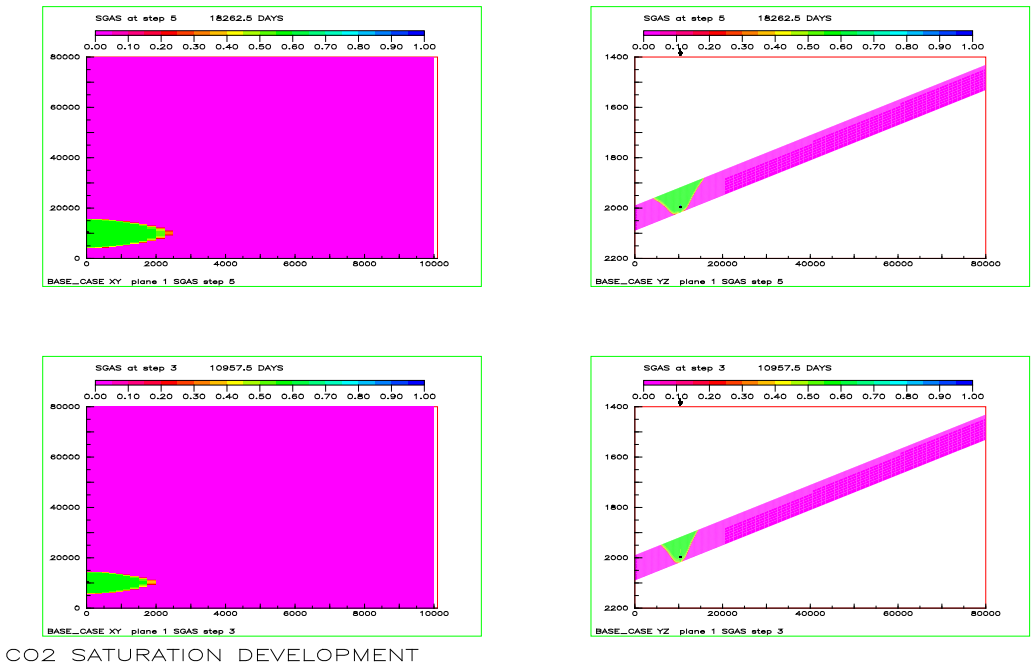

Figure A4.2: CO_2 Distribution during Injection after 30 and 50 Years

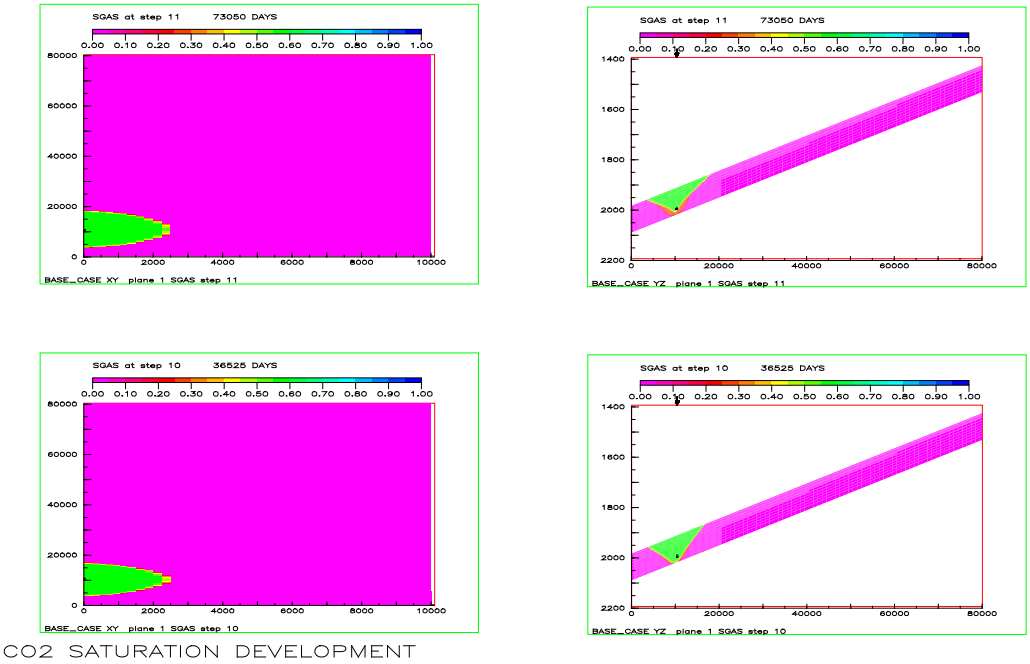

Figure A4.3: Post Injection CO_2 Distribution after 100 and 200 Years

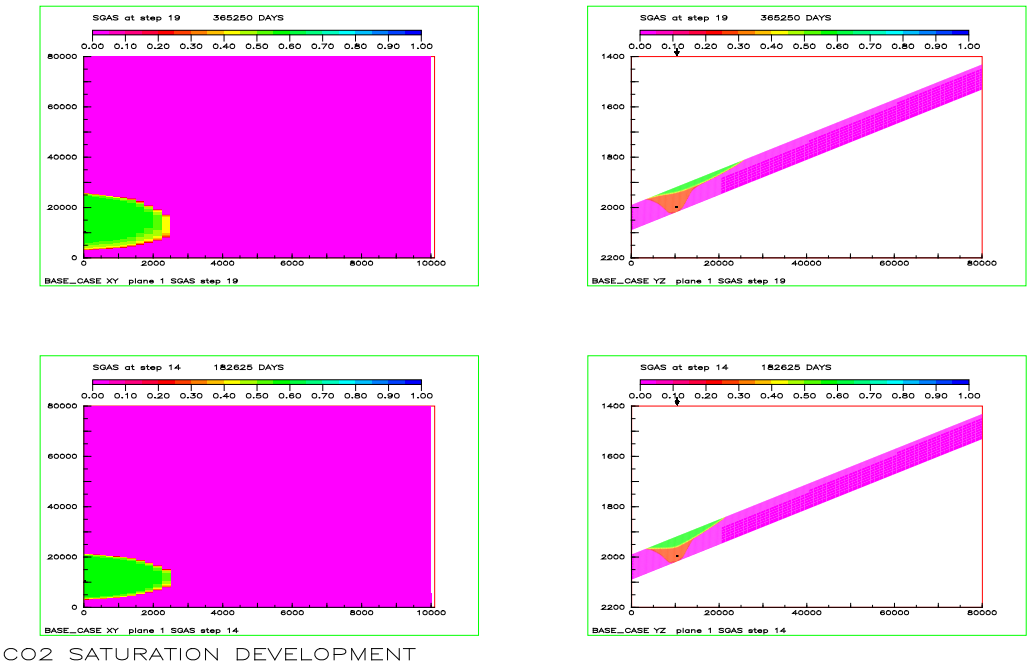

Figure A4.4: Post Injection CO_2 Distribution after 500 and 1000 Years

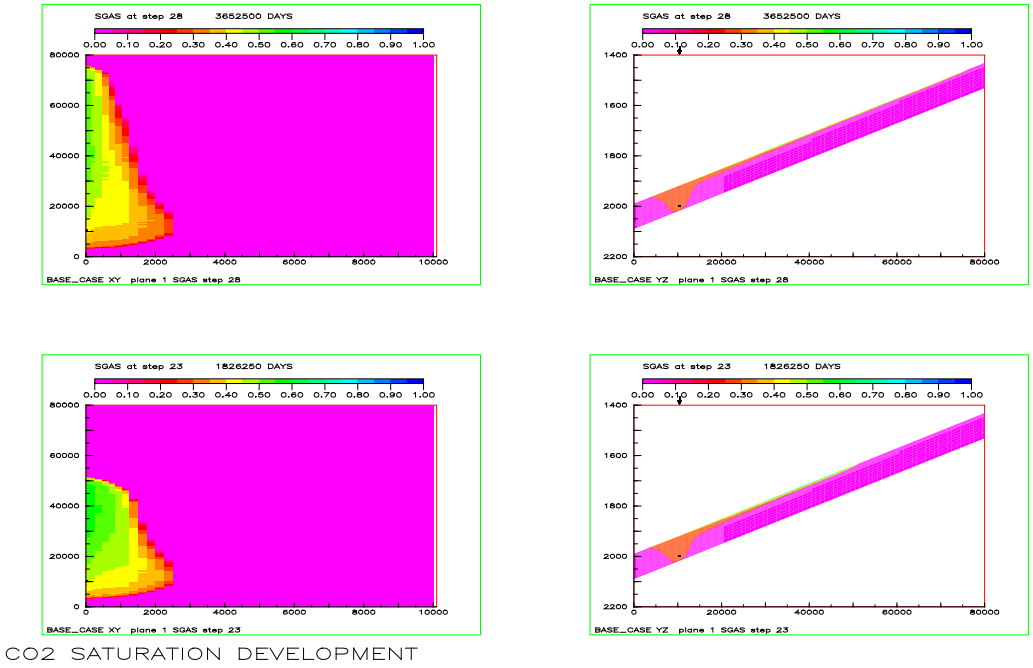

Figure A4.5: Post Injection CO_2 Distribution after 5000 and 10000 Years

At the end of injection, the injected CO_2 was contained within a 5.5 km distance from the injection well (**Figures A4.6 and A4.7**). However, the CO_2 became more dispersed with time with the limit of CO_2 migrating 65 km after 10,000 years. Whilst **Figure A4.6** shows considerable dispersion of the CO_2 after 10,000 years, in fact 50% of the injected CO_2 was contained within 2.3 km from the point of injection.

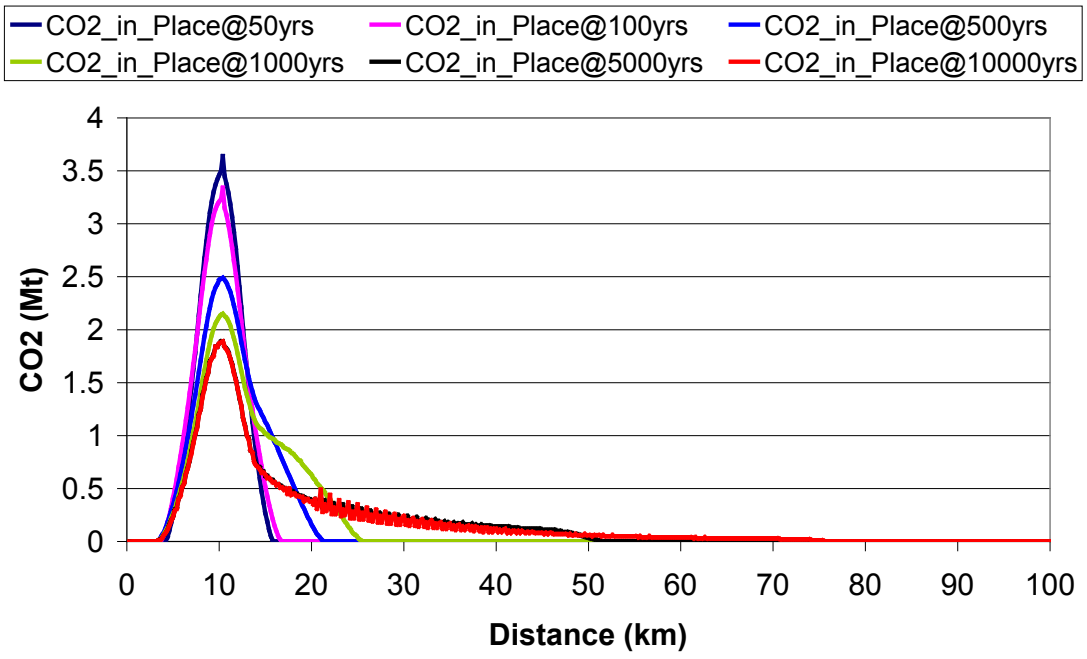

Figure A4.6: CO_2 Distribution along the Simulation Model

Figure A4.7 shows that 75% of the injected CO_2 was contained within 12 km whilst 99% of the injected CO_2 was contained within 56 km. In this and subsequent figures, the percentile limit is defined as the boundary containing the relevant fraction of the injected CO_2.

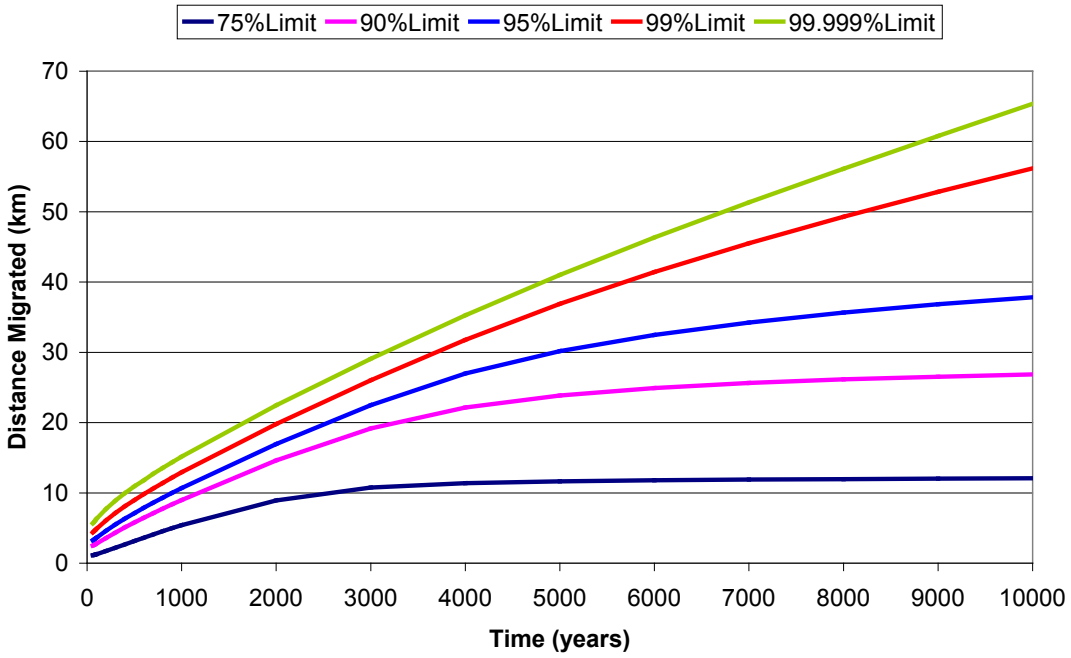

Figure A4.7: Distance Migrated By Injected CO_2

The movement of the CO_2 was fairly slow as shown in **Figure A4.8** which shows that approximately 75% of the injected CO_2 ceased to migrate after approximately 6,000 years during which time it had migrated only 12 km. The 90% boundary limit of CO_2 had practically ceased to migrate after 10,000 years being contained within 27 km from the point of injection. However the remaining 10% of injected CO_2 (20 Mt) continued to migrate at a rate of 4.6 m/year.

At 1,000 years, the 99% boundary limit of CO_2 had travelled 13 km and had a migration velocity of 7.5 m/yr.

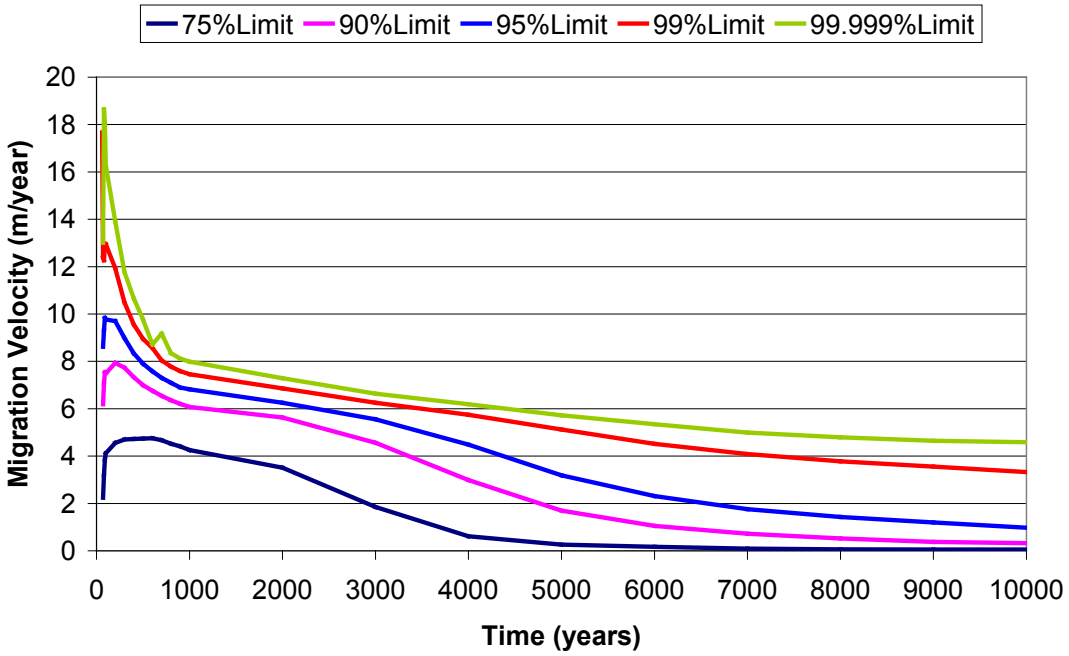

Figure A4.8: Migration Velocity of Injected CO_2

The distribution of the injected CO_2 can be understood by considering its relative permeability which is shown in **Figures A4.9 and A4.10**. **Figure A4.9** shows the relative permeability at the end of injection and after 1,000 years. At the end of injection, all of the injected CO_2 was essentially mobile. However, after 1,000 years, only CO_2 towards the top surface of the model was mobile. CO_2 distributed around the injection well (see also **Figure A4.4**) had become trapped through hysteresis effects. At later times the region of trapped CO_2 increased and there was only a relatively small fraction of the injected CO_2 still migrating (**Figure A4.10**). **Figure A4.11** shows the fraction of injected CO_2 which was effectively capillary trapped (relative permeability less than 0.00001). The fraction rose from 34% after 1,000 years to 60% after 10,000 years.

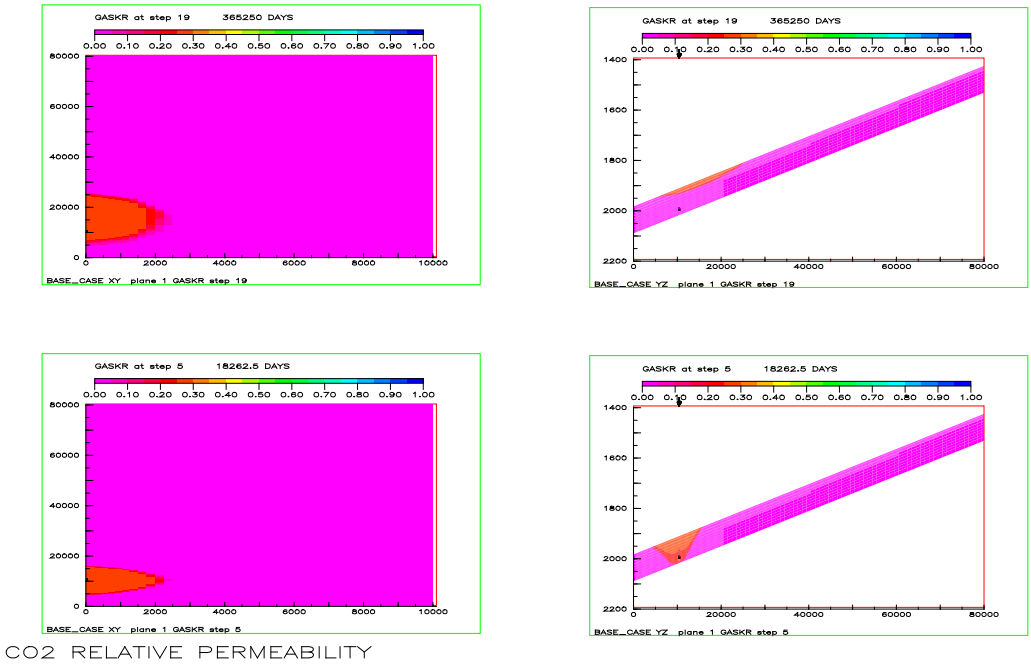

Figure A4.9: CO_2 Relative Permeability After 50 and 1,000 Years

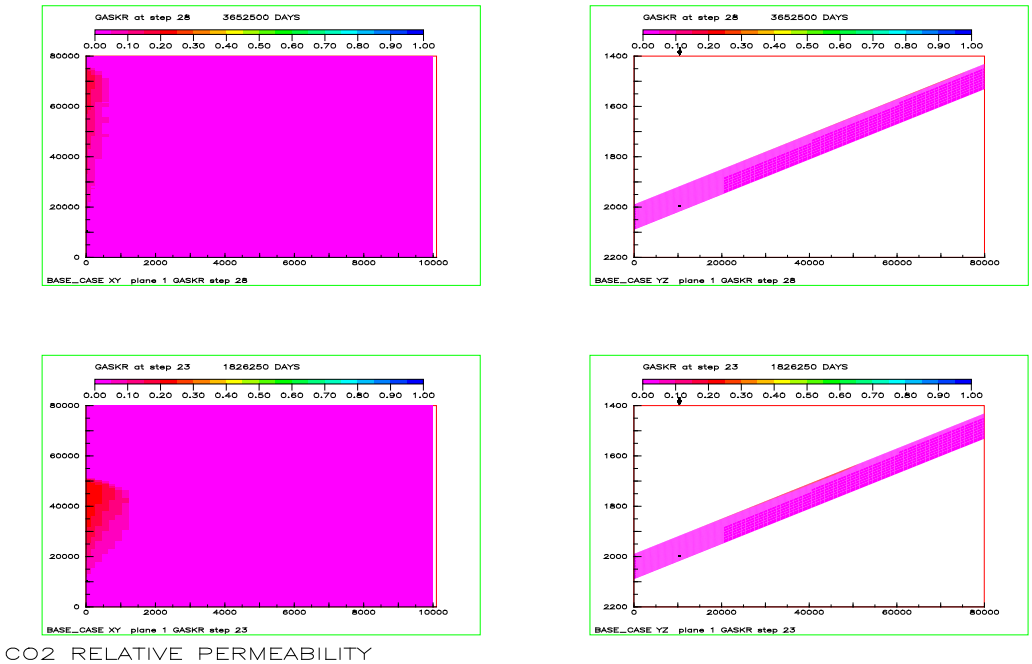

Figure A4.10: CO_2 Relative Permeability After 5,000 and 10,000 Years

CO_2 also became trapped through dissolution. The importance of this process is shown in **Figure A4.11** where it is compared to capillary trapping. After 1,000 years, approximately 10% of the injected CO_2 had dissolved in the brine increasing to 26% after 10,000 years. **Figure A4.12** shows the history of the CO_2 dissolved in the brine, revealing the development of convection cells which increased the fraction of CO_2 dissolved, but only after thousands of years.

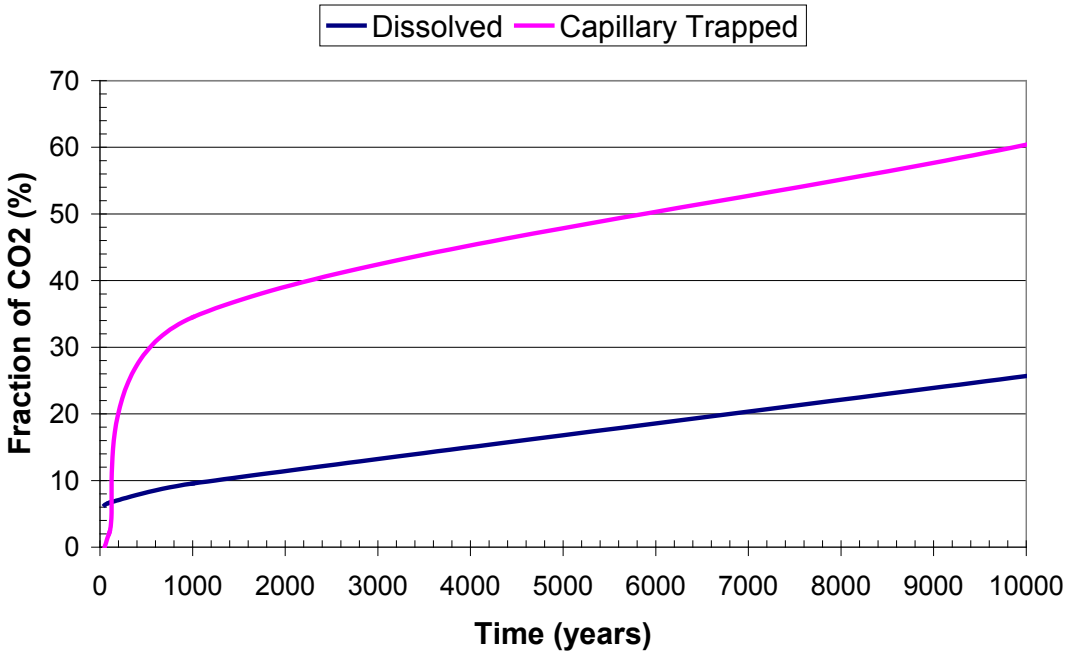

Figure A4.11: Distribution of Trapped CO_2

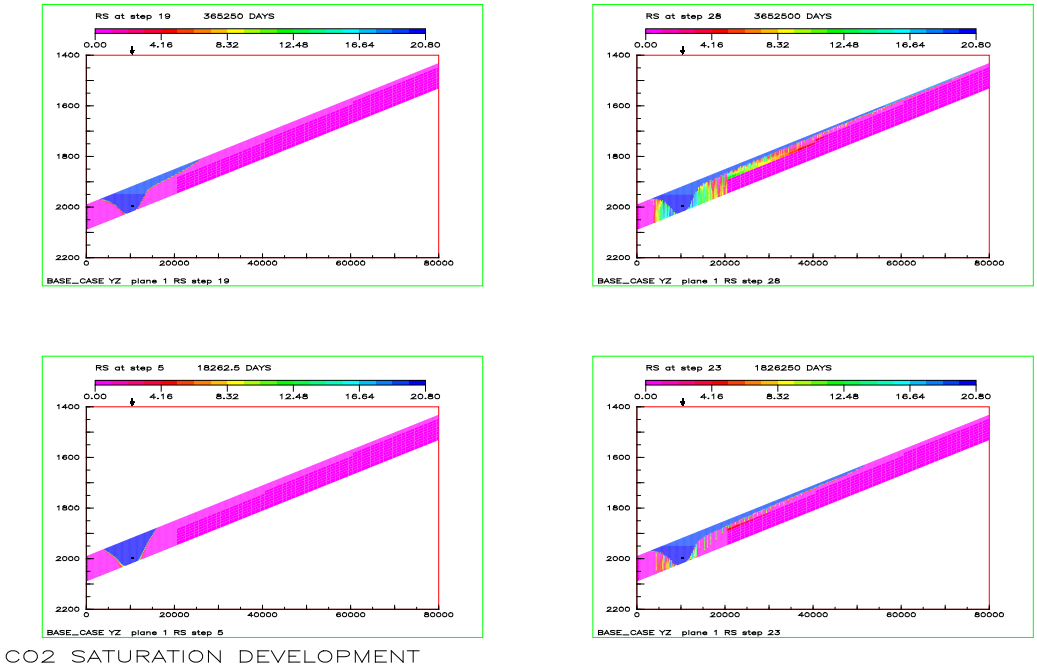

Figure A4.12: Dissolved CO_2 Brine Ratio

Figure A4.13 shows the change in pressure (DP) from the initial hydrostatic conditions with time. Step 5 corresponded to the end of injection (50 years) and shows the maximum increase in the pressure during the simulation. DP 6 and DP 7 represent the pressure transient after 60 and 70 years (10 and 20 years after injection) which was still larger than 0.5

MPa although the peak had moved significantly updip. The pressure transient had decayed to about 0.25 MPa after 100 years (step 10) and largely dissipated after 1,000 years (step 19).

The pressure transient at the end of injection was clearly influenced by the presence of the constant pressure boundary 10 km downdip and this will have resulted in lower pressure transients, and lower injection bottom hole pressure, being calculated. To investigate this effect, the simulation was repeated but with the well moved 50 km from the downdip boundary. This was achieved by extending the model downdip whilst truncating the updip part of the model, so that a model length of 180 km was still utilised. The pressure transients are shown in **Figure A4.14**, where it can be seen that the pressure transient at the end of injection was typically 50% higher than in **Figure A4.13**. The decay of the pressure transient was also much slower with a pressure transient of over 1 MPa still remaining after 100 years, but had still effectively dissipated after 1,000 years.

The presence of the constant pressure boundary clearly impacted the pressure footprint of the injected CO_2. It was decided to situate the pressure boundary 50 km away from the point of injection, because this potentially represents a more realistic scenario and is conservative in that it resulted in larger injection sites (well spacing) and consequently lower pore volume utilisations (see section 5).

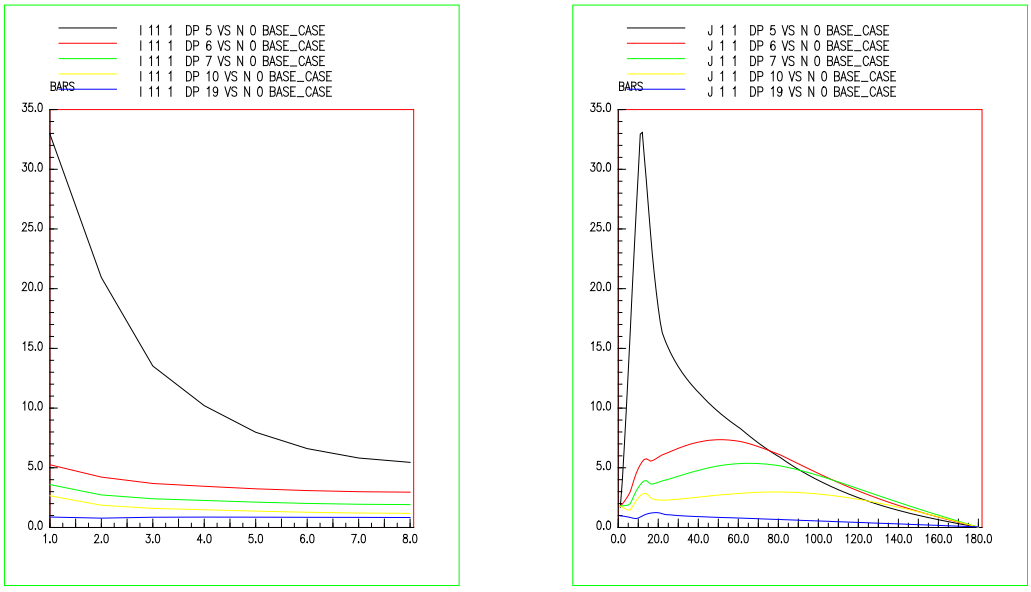

Figure A4.13: Pressure Transients Parallel and Perpendicular to Injection Well

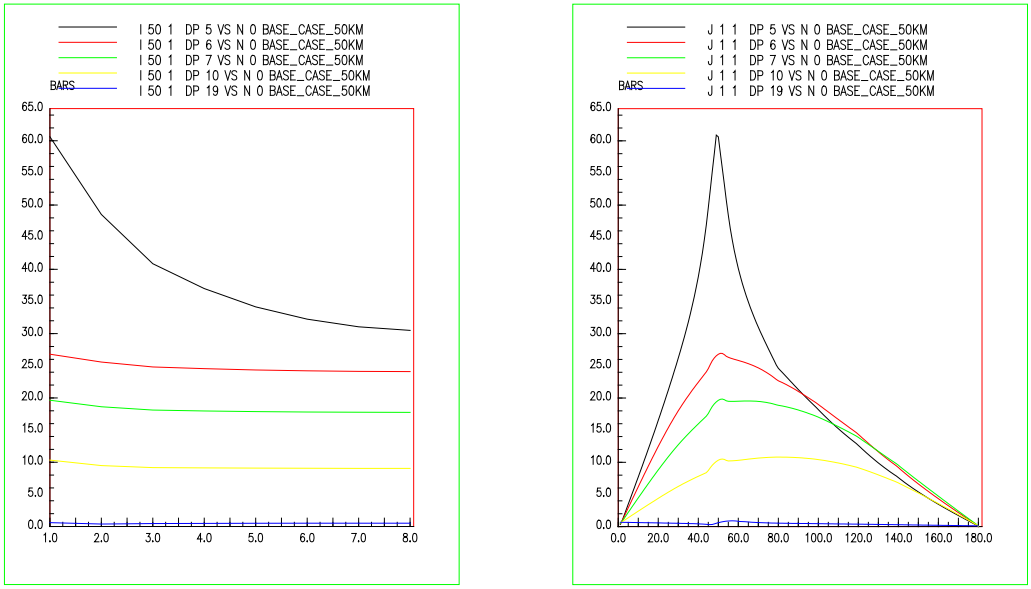

Figure A4.14: Revised Pressure Transients Parallel and Perpendicular to Injection Well

Revised plots for the CO_2 distribution, migration distances and velocities are given in **Figures A4.15 – A4.17**. The migration distances and velocities are also given in **Tables A4.2 – A4.3**. These plots show migration distances and velocities which are essentially the same as for the original simulation indicating that whilst the pressure footprint was significantly affected by the proximity of the constant pressure boundary, the migration of CO_2 seems to be unaffected by it. A comparison of **Figure A4.14** and **Figure A4.15** shows that the pressure footprint at 50 years was much larger than the CO_2 plume after 1,000 years.

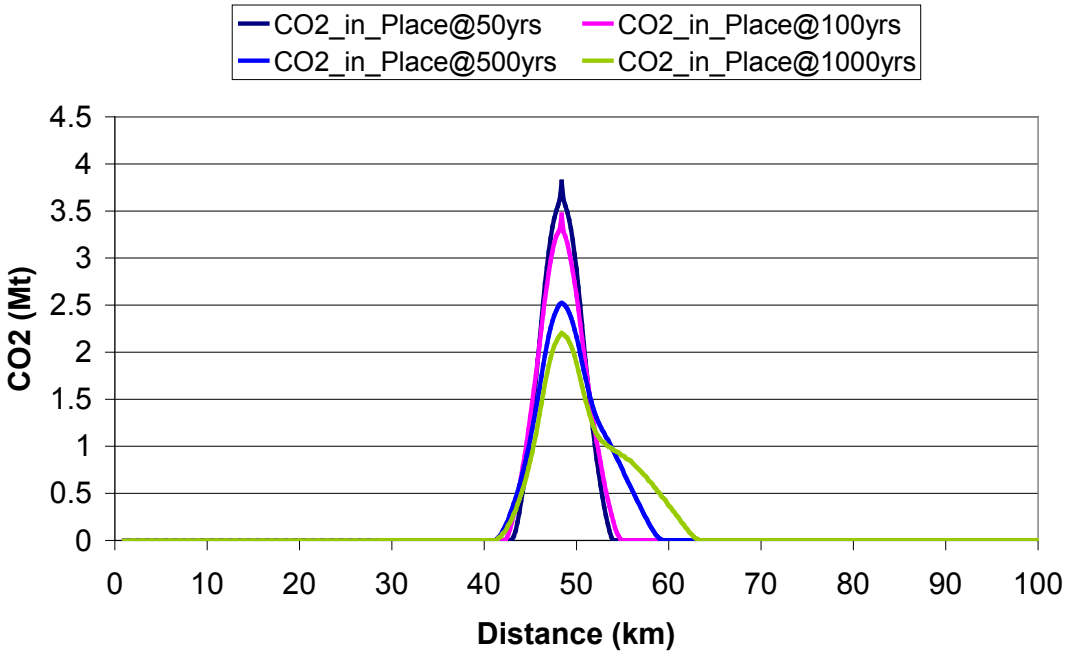

Figure A4.15: CO_2 Distribution along the Revised Simulation Model

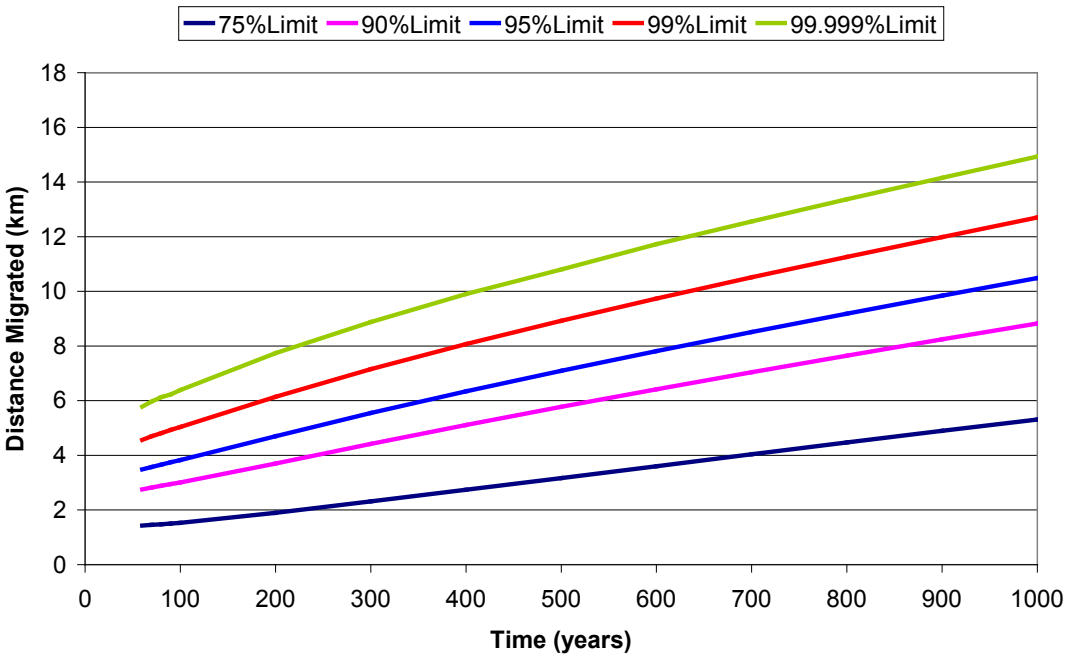

Figure A4.16: Revised Distance Migrated by Injected CO_2

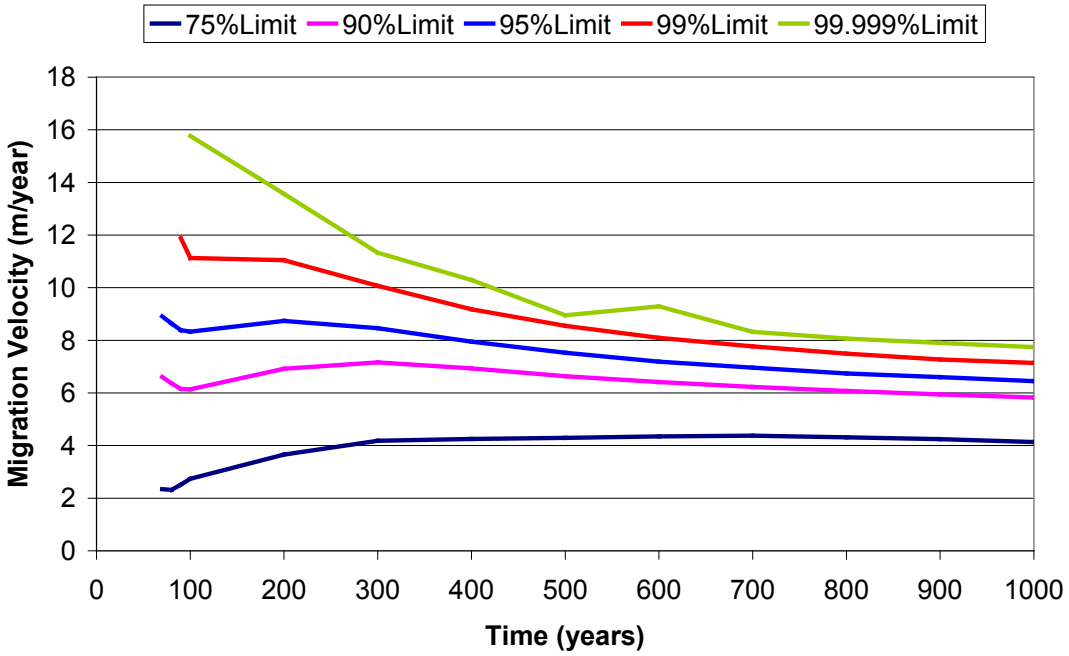

Figure A4.17: Migration Velocity of Injected CO_2

Time (years)	Velocity (m/year)				
	75%	90%	95%	99%	99.999%
60	5.4	12.3	15.9	20.8	21.5
70	2.3	6.6	8.9	12.9	18.2
80	2.3	6.4	8.6	11.2	16.3
90	2.5	6.2	8.4	11.9	9.7
100	2.7	6.1	8.3	11.1	15.8
200	3.7	6.9	8.7	11.0	13.6
300	4.2	7.2	8.5	10.1	11.3
400	4.2	6.9	7.9	9.2	10.3
500	4.3	6.6	7.5	8.6	8.9
600	4.3	6.4	7.2	8.1	9.4
700	4.4	6.2	7.0	7.8	8.3
800	4.3	6.1	6.7	7.5	8.1
900	4.2	5.9	6.6	7.3	7.9
1000	4.1	5.8	6.4	7.1	7.7

Table A4.2: Migration Velocity of Injected CO_2 – Well 50 km from Constant Pressure Boundary

Time (years)	Plume width (km)	Distance (km)				
		75%	90%	95%	99%	99.999%
50	2.5	1.4	2.635	3.3	4.4	5.6
60	2.75	1.4	2.758	3.5	4.6	5.8
70	2.75	1.5	2.824	3.6	4.7	6.0
80	2.75	1.5	2.888	3.7	4.8	6.1
90	2.75	1.5	2.949	3.7	4.9	6.2
100	2.75	1.5	3.011	3.8	5.0	6.4
200	2.75	1.9	3.702	4.7	6.1	7.7
300	2.75	2.3	4.418	5.5	7.2	8.9
400	2.75	2.7	5.112	6.3	8.1	9.9
500	2.75	3.2	5.776	7.1	8.9	10.8
600	2.75	3.6	6.417	7.8	9.7	11.7
700	2.75	4.0	7.04	8.5	10.5	12.6
800	2.75	4.5	7.648	9.2	11.3	13.4
900	2.75	4.9	8.242	9.8	12.0	14.2
1000	2.75	5.3	8.825	10.5	12.7	14.9

Table A4.3: Migration Distance and Plume Width of Injected CO_2– Well 50 km from Constant Pressure Boundary

The well injection bottom hole pressure is shown in **Figure A4.18** along with the cumulative CO_2 injection. The injection rate of 4 Mt of CO_2 per year corresponded to an injection rate of 5.85 Mm^3/day or 206.6 Mscf/day. The well BHP limit was not encountered during the 50 years of injection. No tubing performance modelling was incorporated within this work.

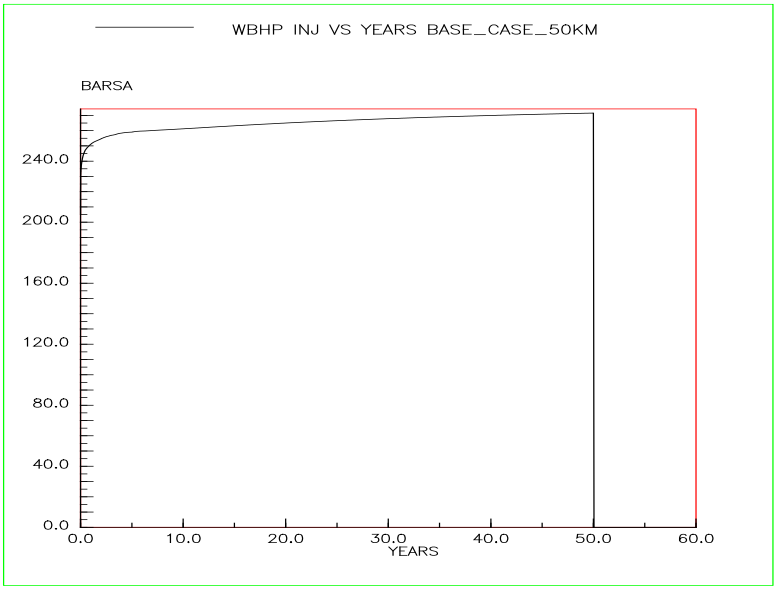

Figure A4.18: Injection Bottom Hole Pressure

5 CO_2 Storage Capacity Estimation Method

5.1 Calculation of Storage Capacity

In section 4 a scenario was described in which the majority of CO_2 remained close to the point of injection, whilst a small fraction typically migrated tens of kilometres over thousands of years. Not all of the injected CO_2 was trapped (capillary or dissolution) even after 1,000 years and some of it could have migrated to the surface. As some estimate of open aquifer potential was required it, was agreed to define CO_2 storage in open aquifers in the following way. Tajen from the European directive on geological storage of CO_2 guidance documents (European Commission, 2011) the following criteria were applied to establish safe storage:

- Injected CO_2 must not reach the surface (implemented as must not migrate above a depth of 800 m);
- 'Long term stability' of CO_2 plume within storage complex.

It should be noted that this does not preclude all movement of CO_2. Lateral migration of metres/ year could be acceptable, provided the rate is declining and accompanied by no significant risk of leakage.

In order to make estimates of CO_2 storage potential from these simple models for a single injection site the following definitions and constraints were adopted consistent with the EU guidance:

- the extent of the storage boundary in the dip direction is that boundary encompassing 99% of injected CO_2 after 1000 years;
- providing the maximum CO_2 migration velocity at 1000 years is less than 10 metres/year and declining;
- and providing pressures remain less than 90% of the estimated fracture pressure limit.

The dip direction boundary was motivated by discussion in a special IPCC report on carbon capture and storage for policymakers which considered that it should be likely that at least 99% of injected CO_2 should be retained after 1000 years (IPCC, 2005). The remainder is within bounds of uncertainty and unmodelled heterogeneities or trapping mechanisms may make this definition conservative (to be modelled in Exemplar).

The dynamic capacity of a single injection site is calculated from the extent of the CO_2 plume and its pressure footprint as defined above and the number of injection sites which can be accommodated in the aquifer (**Figure A5.1**). The utilisation is then given by the mass of CO_2 which can be injected divided by the mass of CO_2 required to fill the unit.

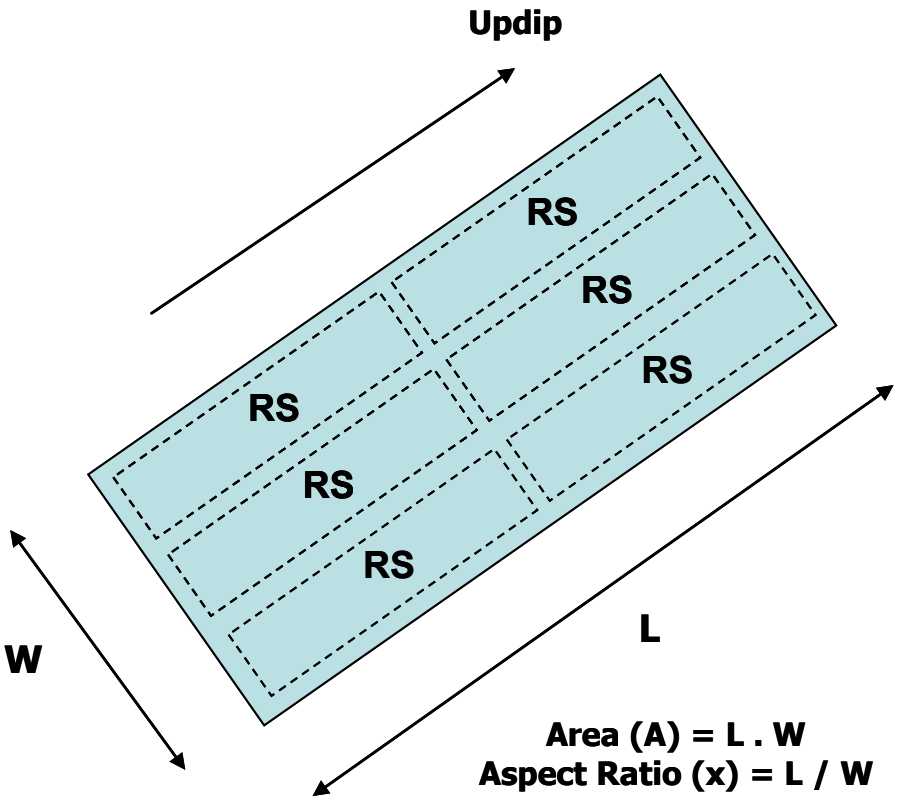

Figure A5.1: Areal 'stacking' of RS to Account for Multiple Injection Points

In section 4 it was noted that the pressure footprint is larger than the CO_2 plume. The pressure footprints from neighbouring sites interfere resulting in higher injection pressures. Superposition of pressure transients and the method of images (symmetry) can be used to approximate the multi-injector pressure footprint as shown in **Figure A5.2** (Earlougher, 1977).

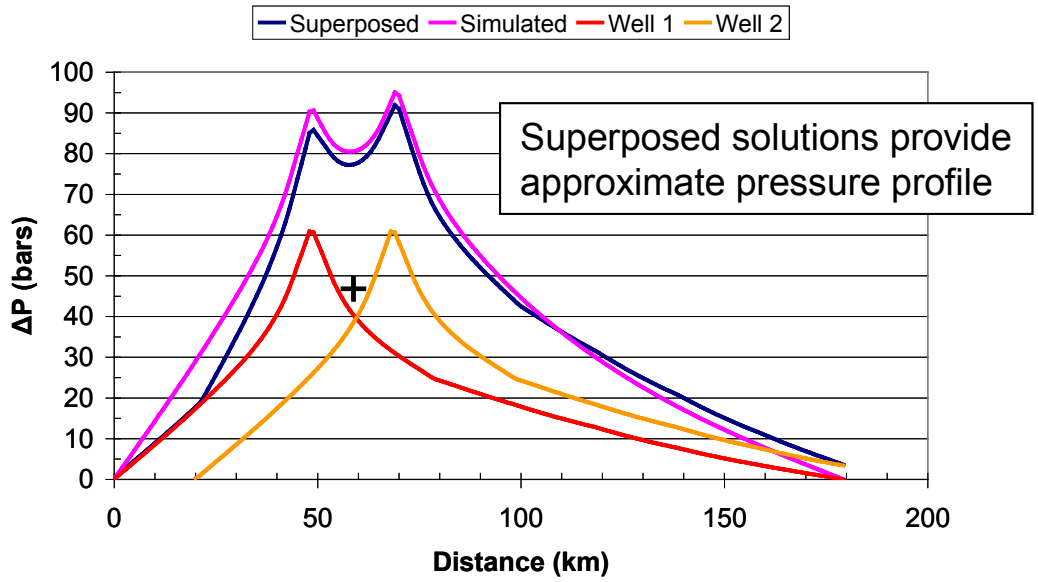

Figure A5.2: Superposed Pressure Profiles

The injection site spacing can be estimated by ensuring that the combined pressure transients remain below 90% of the fracture pressure limit.

The transverse injection site spacing was considered by combining the pressure transients from a single well. The pressure solutions from the base case (equivalent to 20 km well spacing) were superimposed to determine the pressure transient for two wells which, using the Method of Images, is equivalent to the pressure transient for a single well in a 10 km wide model. The pressure transients were combined again to obtain the pressure transient for a 5km model. The combined pressure transients in the transverse direction are shown in **Figure A5.3** where they are compared to simulation with good agreement. Reducing the well separation increases the pressure transient and may result in the fracture pressure limit being exceeded.

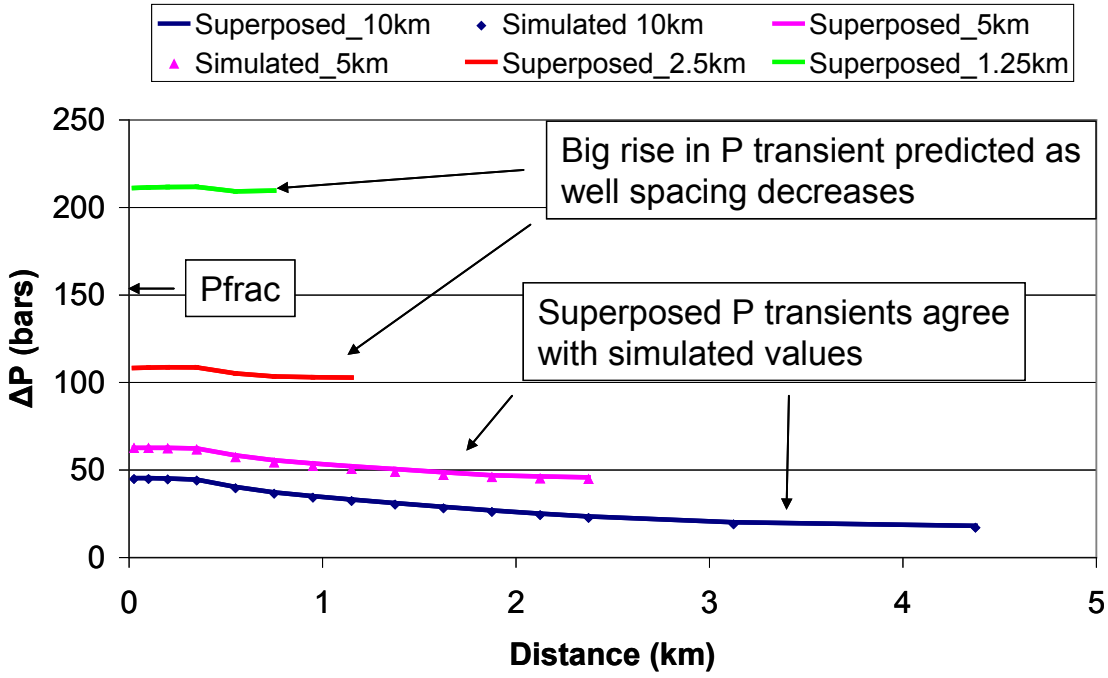

Figure A5.3: Transverse Pressure Transients from Method of Images

Figure A5.4 shows the superposed longitudinal pressure transients which result from decreasing the transverse well spacing. The superposed solutions are again compared to simulation with good agreement.

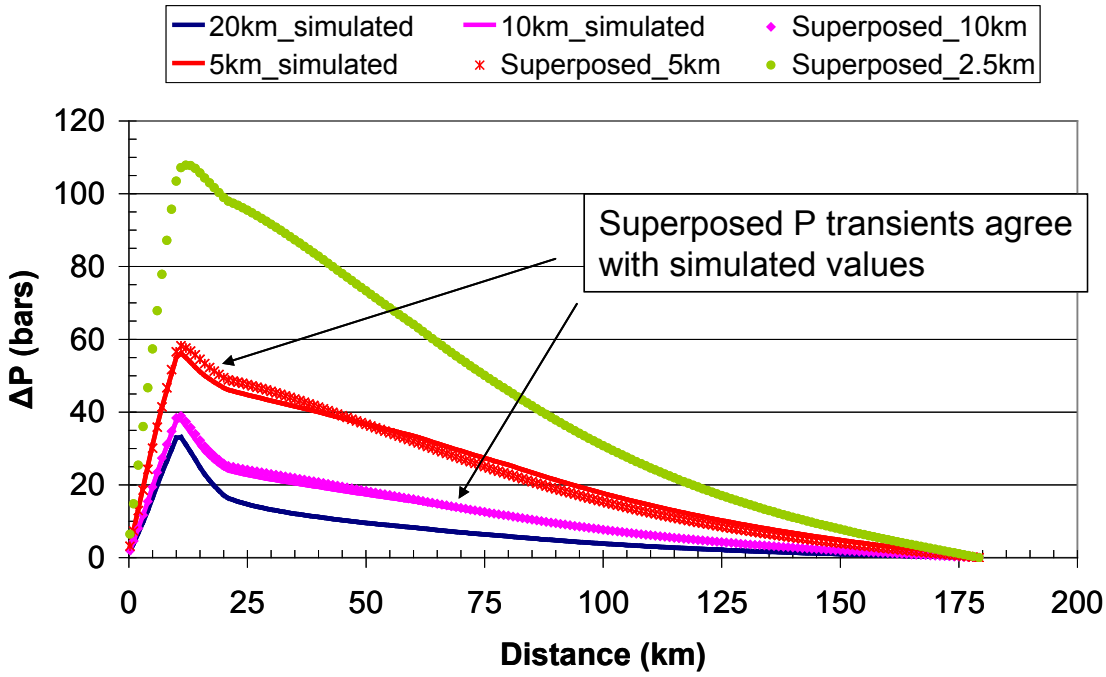

Figure A5.4: Longitudinal Pressures from Method of Images

All superposed pressure transients in **Figures A5.3 and A5.4** were generated from a 20 km wide model.

The longitudinal pressure transient for the base case is shown in **Figure A5.5**. The procedure for estimating the pressure transient due to two injection sites is shown in **Figure A5.2**, where it can be seen that superposed pressure transient is a good approximation to the actual (simulated) transient. **Figure A5.6** shows the impact of successive injection sites on the pressure transient until the fracture pressure limit is exceeded.

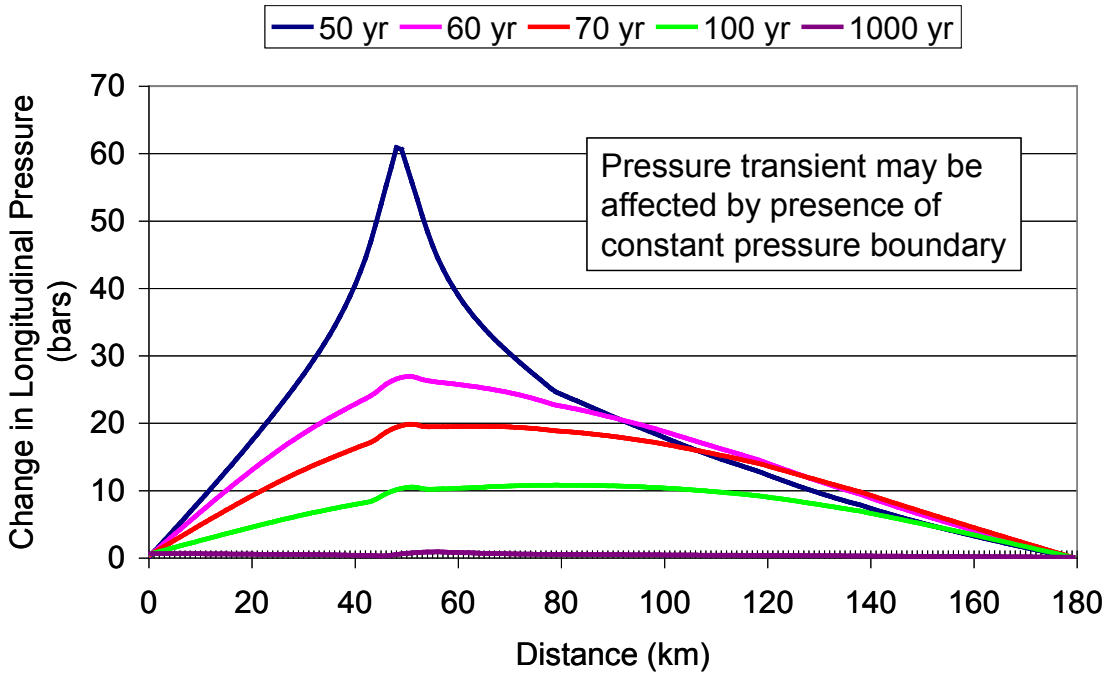

Figure A5.5: Single Well 50 km Away From Constant Pressure Boundary

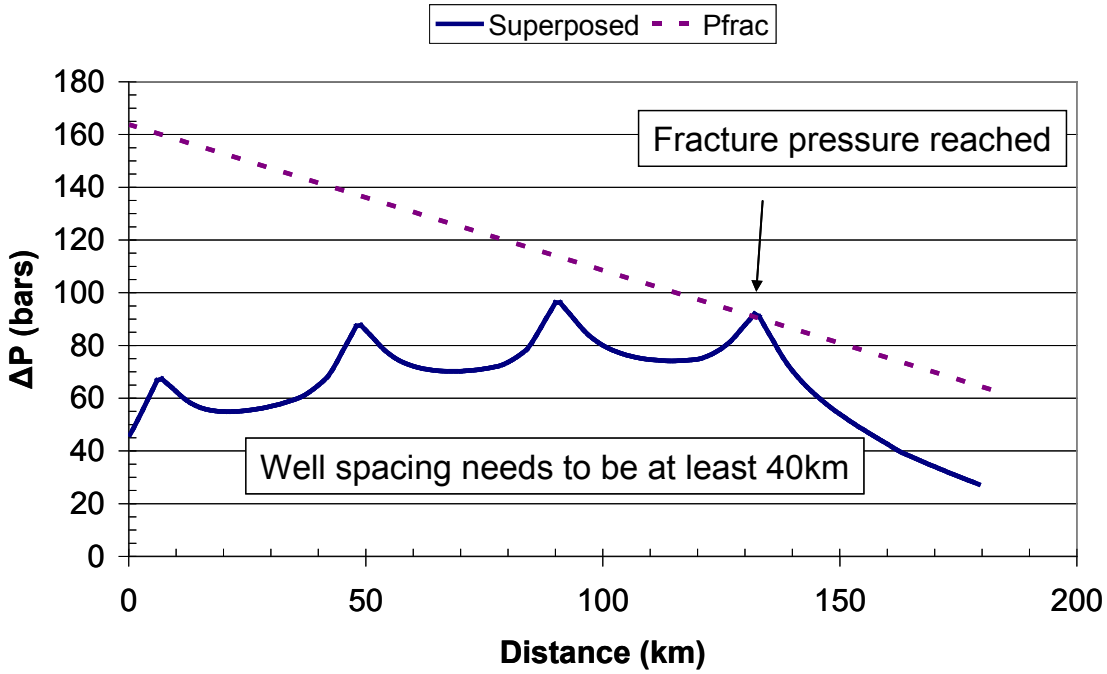

Figure A5.6: Superposition of Four Wells – 50 km from CP boundary

The algorithm used to populate the aquifer with injection sites places the first well at a distance of half of the CO_2 plume from the lower boundary of the model. Successive wells are added at a separation equal to the CO_2 plume length until the fracture pressure is exceeded.

The algorithm is then repeated for increasing well separation although in general this does not permit more injection sites because the fracture pressure decreases significantly as wells move updip.

The algorithm is then repeated by halving the transverse spacing. The halving continues whilst the width remains greater than the transverse dimension of the CO_2 plume.

This procedure does not attempt to optimise the number of injection sites, but just to provide a reasonable estimate of the total storage capacity in the whole aquifer.

5.2 Verification of Method

Several simulations were run with multiple wells to verify the proposed upscaling methodology.

The first case utilised the base case model but with five wells 22 km apart. The resulting pressure transient at the end of injection is shown in **Figure A5.7**. The superposed pressure transient was calculated from the single well base case model. It can be seen that the superposed solution overestimates the downdip pressure transient whilst providing a reasonable estimate of the pressure transient updip. The downdip pressure for the simulation model was significantly affected by the presence of the constant pressure boundary which for the first well was only 11 km from the point of injection whilst the superposed curve was based on a pressure transient for which the well was located 50 km from the constant pressure boundary.

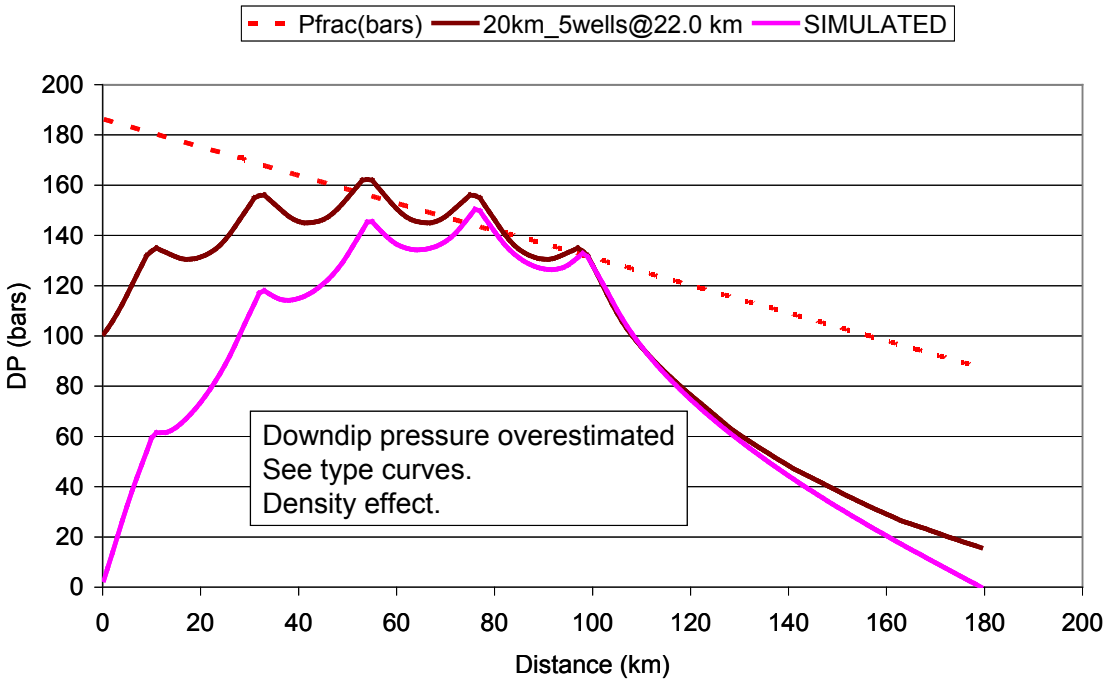

Figure A5.7: Base Case with Five Wells

The base case model was modified by increasing the thickness from 100 to 400 m and simulation performed with eight wells spaced 22 km apart. A single well simulation was also performed with the well 50 km from the constant pressure boundary and an eight well

pressure profile calculated using superposition. The pressure transients are compared in **Figure A5.8**.

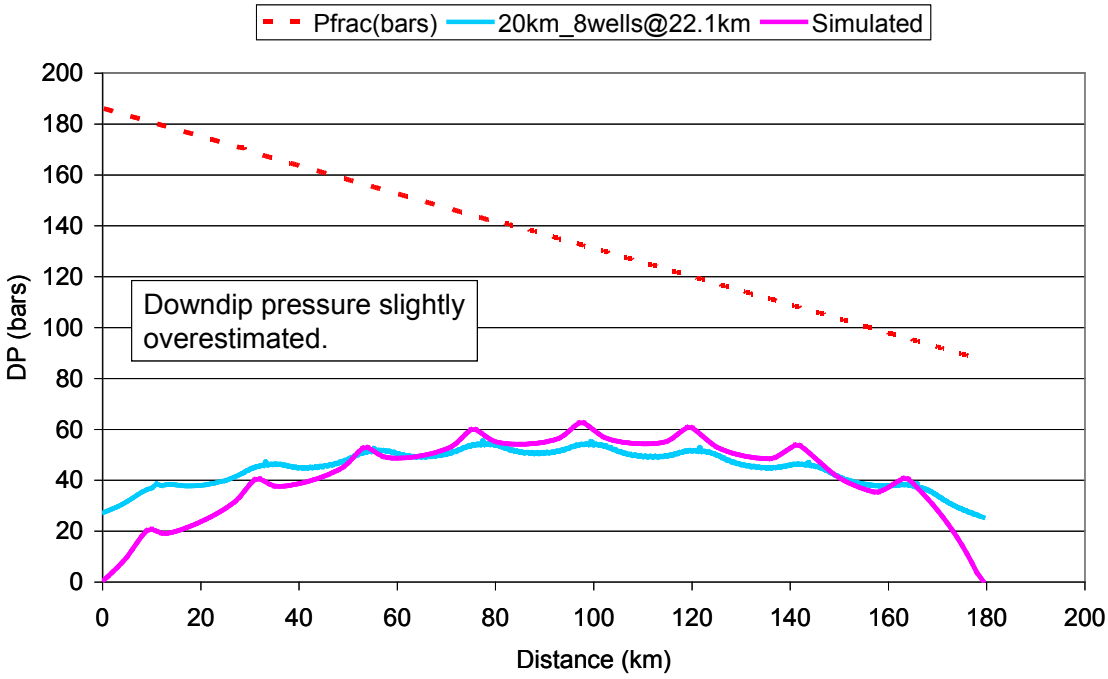

Figure A5.8: Example with Eight Wells

This again shows good estimates of pressure transient for the updip wells whilst the pressure downdip is less well matched because the simulation results were affected by the constant pressure boundary which resulted in lower downdip pressures in the simulation model.

A final example considered four wells in the base case model with a transverse spacing of 5 km. The simulated and superposed pressure transients at the end of injection are shown in **Figure A5.9**.

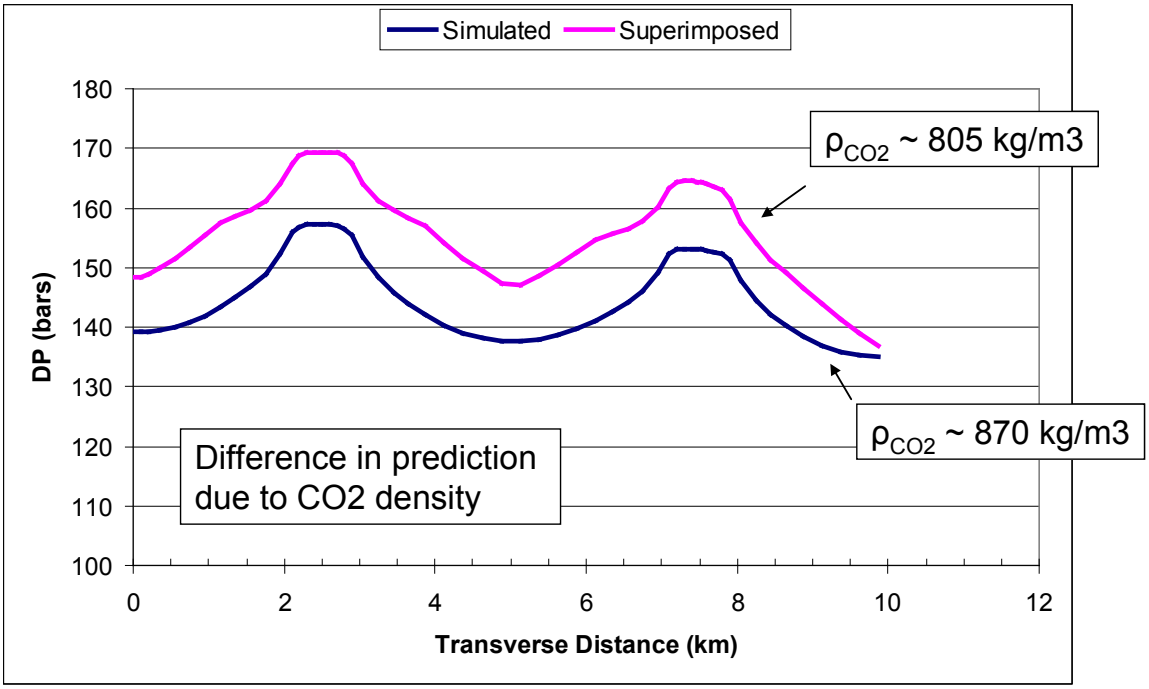

Figure A5.9: Base Case – Four Wells Transverse

The simulated case had a pressure increase of up to 15.5 MPa where as the base case single well simulation had a pressure increase of 6.7 MPa. Consequently the superposed line effectively assumed a lower CO_2 density (higher reservoir volume of CO_2) and so predicted higher pressures.

The validation simulations suggest that superposition of pressure transients can provide a good estimate of well spacing. It is noted that the larger the pressure change from the underlying type curve (single well pressure transient), the more inaccurate the method becomes. The results probably imply greater well spacing than may be needed in practice (lower storage capacity).

5.3 Application to Base Case

The upscaling method is applied to the base case in this section to estimate the size of storage site and the associated storage capacity (see section 4).

For the case with the well located 10 km from the constant pressure boundary the size of the CO_2 plume and the minimum storage site separation are given in **Table A5.1**. The corresponding pressure transient is shown in **Figure A5.10**. The velocity of the 99% limit boundary was 7.4 m/year and declining, whilst the boundary limit only migrated 12.9 km from the point of injection, so the storage criteria were satisfied. The maximum number of injection sites was estimated to be six resulting in a pore volume utilisation of 1.7%. This could be implemented as either six sites spaced longitudinally 20.3 km with a transverse separation of 20 km between sites, or as three sites spaced longitudinally 20.3 km with a transverse separation of 10 km. Although the model is 180 km long, only the deepest 120 km (assuming 20 km transverse spacing) is able to accommodate 200 Mt injection sites. Halving the transverse separation to 10 km, only the deepest 60 km is utilised. The fact that it may be possible to operate smaller storage sites updip combined with the conservative nature of the pressure footprint calculation suggests this upscaling methodology provides an underestimate

of storage capacity. It is not possible to have injection sites 5 km apart because of the plume width limitation.

CO_2 Plume Dimensions after 1000 years				
Half Plume Width	**Downdip Limit of injected CO_2**	**Updip Limit of 99% of injected CO_2**	**Velocity of 99% limit of CO_2**	**CO_2 Density at Centroid**
2.75 km	7.3 km	12.9 km	7.4 m/year	721.6 kg/m3
Maximum Number of wells in 180 km				
Number of wells	**Longitudinal well spacing**	**Transverse well spacing**	**Maximum number of Injection Sites**	
6	20.3 km	20 km	6	
3	20.3 km	10 km	6	
0	20.3 km	5km	0	

Table A5.1Base Case – Well 10 km Updip

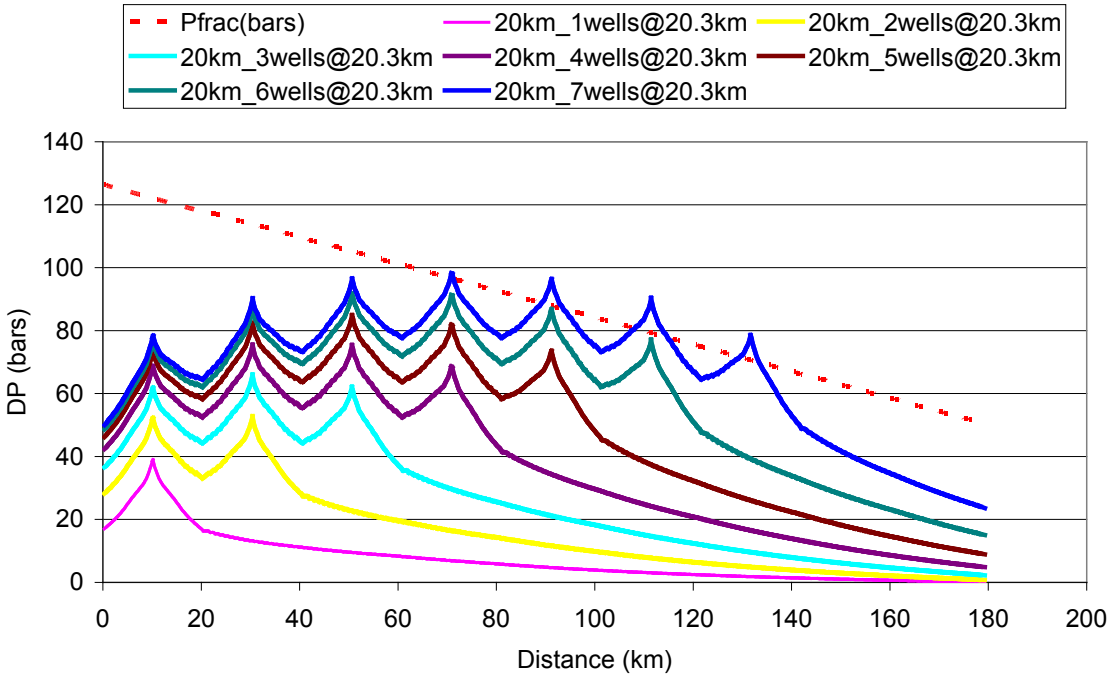

Figure A5.10: Base Case – Well 10 km Updip

For the case with the well located 50 km from the constant pressure boundary the size of the CO_2 plume and the minimum storage site separation are given in **Table A5.2**. The corresponding pressure transient is shown in **Figure A5.11**. The velocity of the 99% boundary limit was 7.1 m/year and declining, whilst the boundary limit only migrated 12.7 km from the point of injection, so the storage criteria were again satisfied. The maximum number of injection sites was determined to be three resulting in a utilisation of 0.85%. This could only be implemented using three sites spaced longitudinally 20.1 km with a transverse separation of 20 km between sites. Reducing the transverse separation to 10 km resulted in less overall storage sites. Although the model was 180 km long, only the deepest 60 km (assuming 20 km transverse spacing) was able to accommodate 200 Mt injection sites. Halving the transverse

separation to 10 km, only the deepest 20 km was utilised. It is again not possible to have injection sites 5 km apart because of plume width and pressure limitations.

CO_2 Plume Dimensions				
Half Plume Width	**Downdip Limit of injected CO_2**	**Updip Limit of 99% of injected CO_2**	**Velocity of 99% limit of CO_2**	**CO_2 Density at Centroid**
2.5 km	7.4 km	12.7 km	7.1 m/year	724.3 kg/m3
Maximum Number of wells in 180 km				
Number of wells	**Longitudinal well spacing**	**Transverse well spacing**	**Maximum number of Injection Sites**	
3	20.1 km	20 km	3	
1	20.1 km	10 km	2	
0	20.1 km	5km	0	

Table A5.2: Base Case – Well 50 km Updip

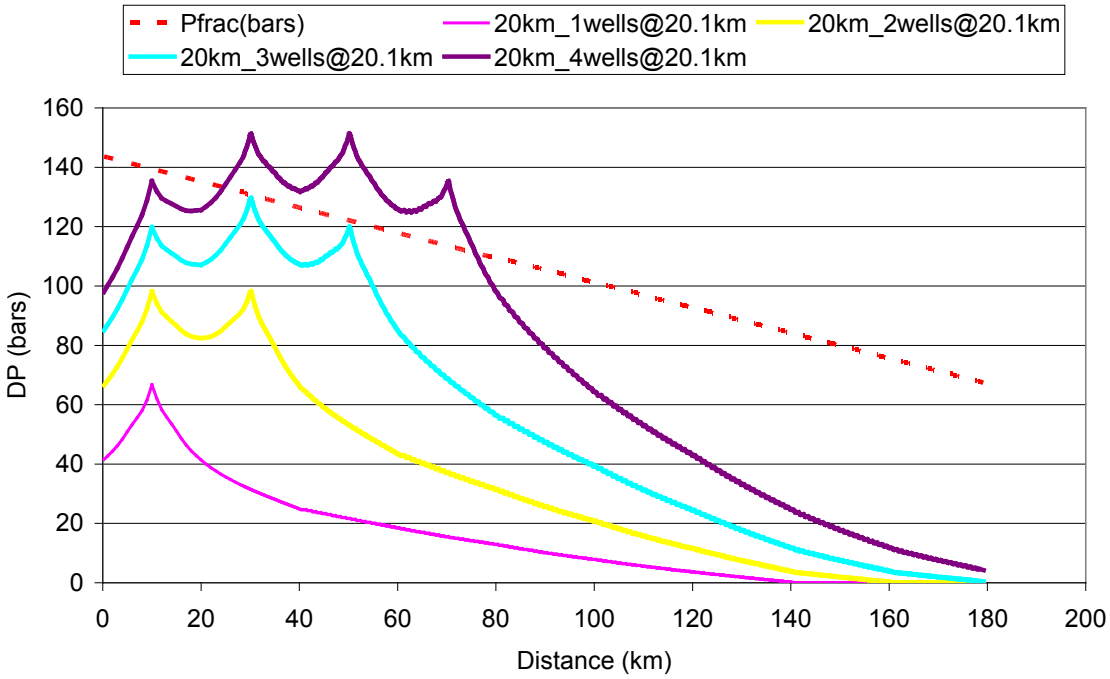

Figure A5.11: Base Case – Well 50 km Updip

The constant pressure boundary had a significant impact on the pore volume utilisation because the magnitude of the pressure transient determines how may injection sites can be accommodated updip. A transient based on a well close to a constant pressure boundary is much smaller than for a well located at some distance.

It is unlikely that an injector would be positioned close to a constant pressure boundary, so all pressure transients used for storage capacity estimation were determined assuming a distance of 50 km from the downdip boundary. The distance to the updip constant pressure boundary depended on the dip of the aquifer and the depth of the centroid. Typically the aquifer was not modelled above 800 m and so for high dip shallow aquifers the updip

constant pressure boundary could be of the order of 10 km. However, in these cases the CO_2 is likely to migrate above 800 m (assuming reasonable permeability) and so the proximity of the updip boundary has generally not been regarded as significant as the CO_2 migrates comparable distance from the well when either close to or remote from the boundary.

Many of the initial simulations were run with the downdip boundary 10 km from the well. The base case indicated that this has a small effect on the migration of CO_2, but a large effect on the pressure transient. These initial cases were compared to determine which had comparable pressure transients. For example, salinity was found to have only a small effect on the pressure transient and so these cases were not rerun with the 50 km boundary, but the pressure transient from the base case was used when calculating pore volume utilisation. However, where necessary, cases were rerun with the 50 km distant boundary to determine new pressure transients. The comparison method used was to examine the flowing bottom hole pressures (BHP) at the end of injection along with a review of the properties which affect the pressure transient, particularly permeability and thickness. The BHPs at the end of injection for the affected cases are shown in **Figure A5.12**.

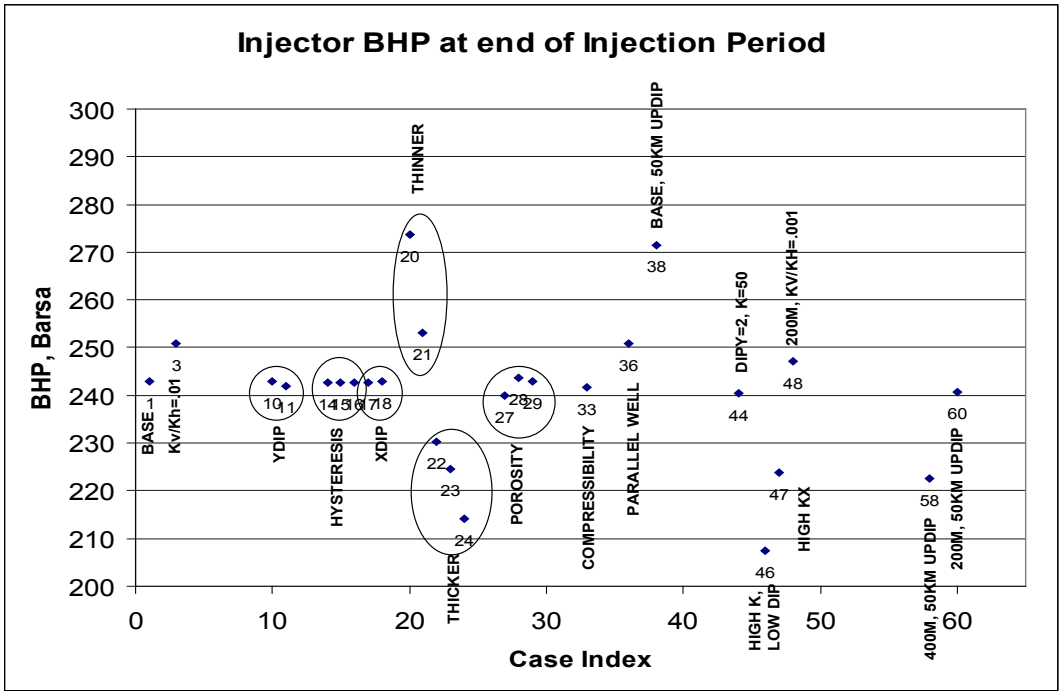

Figure A5.12: Grouping of Calculated BHP to Determine Which Cases to Rerun

5.4 Conclusions

Superposition can be used to upscale the pressure footprint to estimate the overall pressure transient due to a number of injection sites. Simulation has been performed to validate this method in which it has been shown that this approach is likely to underestimate the storage potential. A simple algorithm was developed to populate the simulation model with injection sites until the fracture pressure limit is exceeded.

Typically there is a trade off between the longitudinal and lateral well spacing. In general reduced lateral well spacing results in a reduction of the number of sites which can be

accommodated in the longitudinal direction. This typically involves reducing the number of updip wells.

However, the estimated number of injection sites was found to depend on the proximity of the constant pressure boundary. Where possible simulation has been performed with the constant pressure boundary located at least 50 km from the point of injection. For the base case model, this choice halves the number of injection sites which can be accommodated in the model.

It should be noted that the pressure corrected pore volume utilisation will always be lower than the CO_2 extent value even if there was no significant pressure interference. This occurs because the aquifer is divided up into injection sites which are based on the length of the CO_2 plume and a pressure corrected width in which only an integral number of injection sites are allowed. Typically, the longitudinal direction of the aquifer would not be fully utilised and some unused aquifer extent smaller than the CO_2 plume length remains. More significantly, the pressure corrected width, derived from repeatedly halving the model width, whilst ensuring that the injection site is wider than the CO_2 extent, is up to twice the CO_2 plume width. The effects are directly combined in estimating a pore volume utilisation.

6 Sensitivity Calculations

6.1 Introduction

The cases run are listed in **Table A6.1** and results are given in **Table A6.2** and **Table A6.3**.

Table A6.2 contains the plume size. The width was taken at the end of injection. The downdip extent was defined as the distance downdip from the point of injection such that 99.999% of the CO_2 was stored updip of it. Similarly, the updip limit was defined as the distance updip from the point of injection such that 99% of the CO_2 was stored downdip of it. The migration velocity is the rate at which the updip limit boundary of CO_2 moves away from the point of injection. The simulations attempted to inject 200 Mt. The actual mass of CO_2 injected is given in **Table A6.2** from which it can be seen that some cases did not have sufficient injectivity to meet the target.

A pore volume utilisation is also given in the table. This utilisation is calculated as the mass of CO_2 injected divided by the mass of CO_2 which could be contained in the smallest cuboid which contains 99% of the injected CO_2 with density calculated at the centroid of the CO_2 plume at hydrostatic (initial) conditions. The density is given in **Table A6.2**. The pressure corrected Storage Factors are given in **Table A6.3**.

The impact of key variables on the pressure corrected pore volume utilisation is shown in **Figure A6.1**. The data plotted considers single property variations around the base case values. The base case utilisation is 0.85% as indicated by the black dash.

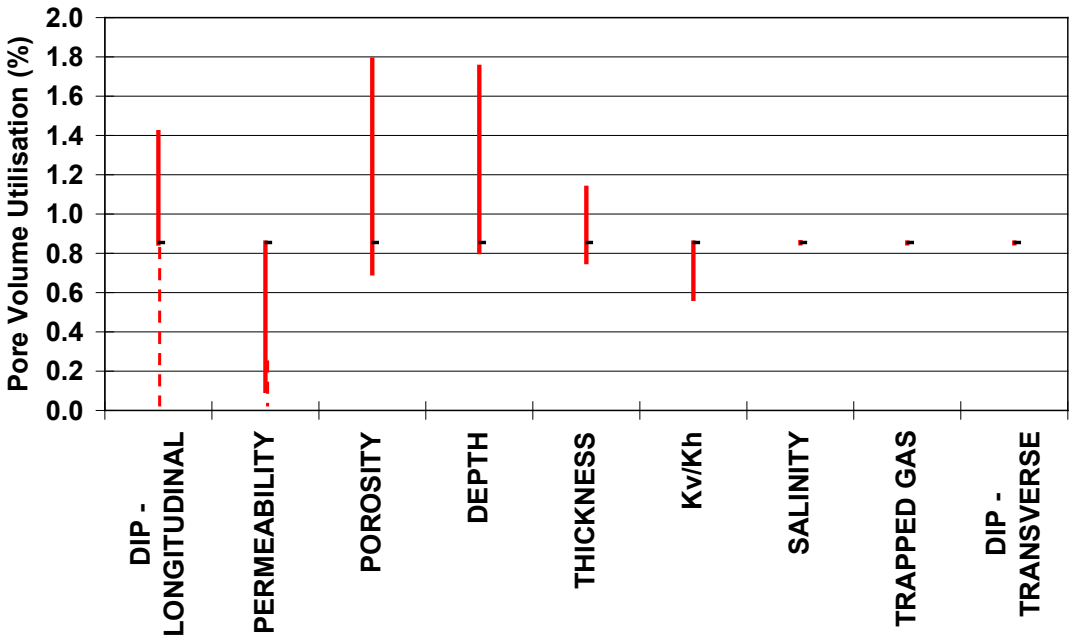

Figure A6.1: Impact of Key Variables on the Pressure Corrected Storage Factor

Figure A6.1 shows that salinity, trapped gas saturation (and hysteresis model) and transverse dip had minimal effect on the utilisation.

The longitudinal dip was found to be very significant. Increasing the dip caused the CO_2 to migrate faster. Increased dip also resulted in less pore volume between the point of injection and the 800 m limit beyond which CO_2 was not allowed to migrate. For dips greater than 1 degree the plume was typically found to be unstable which is why the range of storage factors has been extended (dashed line) down to 0. The highest value corresponded to a dip of 0.1 degrees.

The permeability also had a significant effect on the migration velocity. Increasing the permeability caused the CO_2 to migrate faster affecting the stability of the plume. CO_2 might have also migrated above the 800 m depth limit. Increasing the permeability to 3,000 mD resulted in CO_2 migrating above 800 m and so the range has been extended (dashed line) down to 0. Reducing the permeability typically resulted in insufficient injectivity. Cases with insufficient injectivity resulted in low utilisation when the pressure upscaling was applied.

The porosity had an impact on the utilisation as it affected both the distance and rate at which CO_2 migrated. Higher utilisations occurred for lower porosities. This is because the reduced pore volume resulted in higher CO_2 saturations and higher trapped gas saturations. The extra distance migrated by the CO_2 is typically less than the factor by which the porosity was reduced. The change in porosity did not have a major impact on the pressure upscaling.

The depth at which CO_2 is stored can be significant as it affects the density of the CO_2. However, this effect is not large as the cooler temperatures experienced at lower depths compensate. For the simulations performed, the density varied from 705 to 765 kg/m^3 (base case value of 724 kg/m^3). The utilisation typically increased with the density of the stored CO_2.

The thickness also impacted the utilisation. Typically thicker formations resulted in larger CO_2 plumes (greater updip limits in **Table A6.2**). However, this was more than compensated for in the pressure upscaling as they have smaller pressure transients, which typically allowed more injection sites to be accommodated (**Table A6.3**). Thinner formations may have lower storage factors depending on the pressure upscaling.

The effective k_v:k_h ratio was found to have only a small effect on the plume migration and also on the pressure corrected utilisations.

The impact of the trapped gas saturation was small for the variation around the base case. The variations in **Figure A6.1** correspond to storage regime two (see Section 7.2) in which typically only 35% of the CO_2 has become structurally trapped after 1,000 years (**Figure A4.11**), so on this time scale the significance of the trapped gas saturation was small. However, for storage regime three which requires all of the injected CO_2 to be trapped, the trapped gas saturation is likely to have a significant impact on the pore volume utilisation.

Figure A6.1 shows that the stability of the plume depended mostly on the dip and the permeability.

6.2 Plume Stability

The criterion for plume stability required the CO_2 plume boundary limit to be migrating at less than 10 m/yr and declining. The migration velocities for a range of dips and permeabilities are shown in **Figure A6.2** of the 99% boundary limit of injected CO_2.

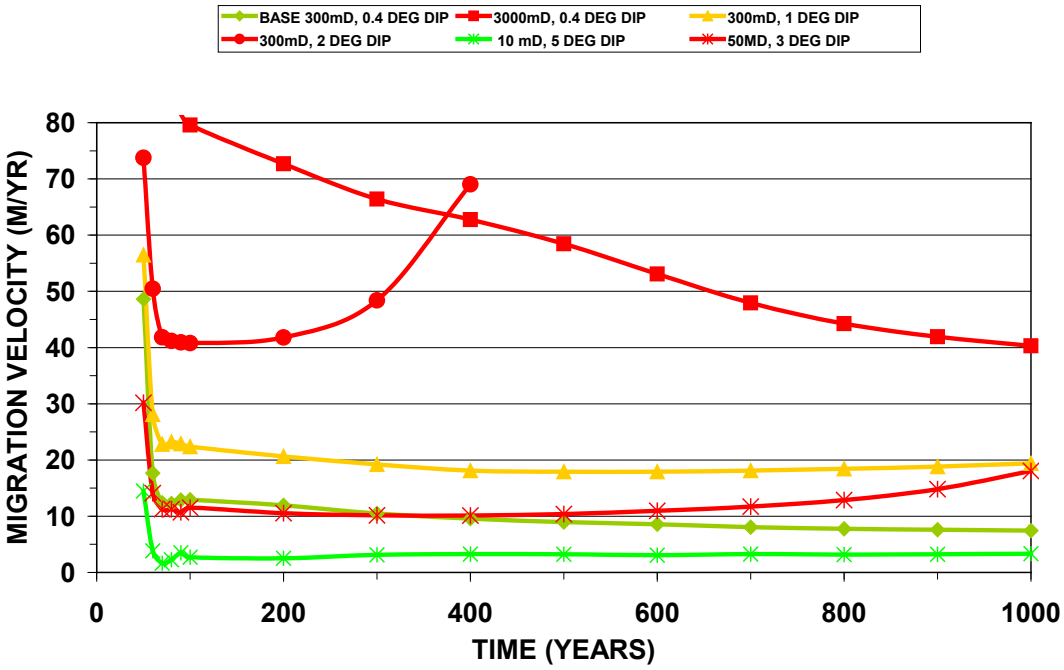

Figure A6.2: Variation of Plume Migration Velocity with Dip and Permeability

The base case velocity was 7.5 m/yr and declining slowly at 1,000 years which satisfied the stability criterion.

However, the 3,000 mD variation of the base case had migration velocity of 40 m/yr which is significantly more than the stability criterion for secure storage.

A variation of the base case with two degree dip had even higher migration velocities which were actually increasing with CO_2 migrating above 800 m at around 450 years. Reducing the dip to one degree resulted in much lower migration velocities. At 1,000 years the velocity was 19 m/yr and increasing which violated the stability criterion.

A case with 10 mD and 5 degree dip was found to have a low migration velocity of 3 m/yr at 1,000 years. Injection was significantly limited due to the low permeability with only 29 Mt injected.

A case with permeability 50 mD and dip 3 degrees resulted in a migration velocity of 18 m/yr at 1,000 years, but 200 Mt of CO_2 was able to be injected.

These results show that there may be only a fairly narrow combination of dips and permeabilities for which the CO_2 plume may be stable. Where the stability criterion is not met, other trapping mechanisms (e.g. structural, residual, solution) need to be considered to ascertain a pore volume utilisation. These mechanisms are being considered as part of Exemplar simulation (see Appendix A5.4).

An analytic expression has been published for the rate at which the tip of the CO_2 plume migrates under incompressible flow (MacMinn et al, 2010):

$$v = \frac{kk_{rCO2}(\rho_w - \rho_{CO2})g\sin\theta}{\mu_{CO2}(1 - S_{wirr})\phi} \qquad (6.1)$$

This expression has been used to calculate a migration velocity for all cases and is compared to the simulation results in **Figure A6.3** with good agreement.

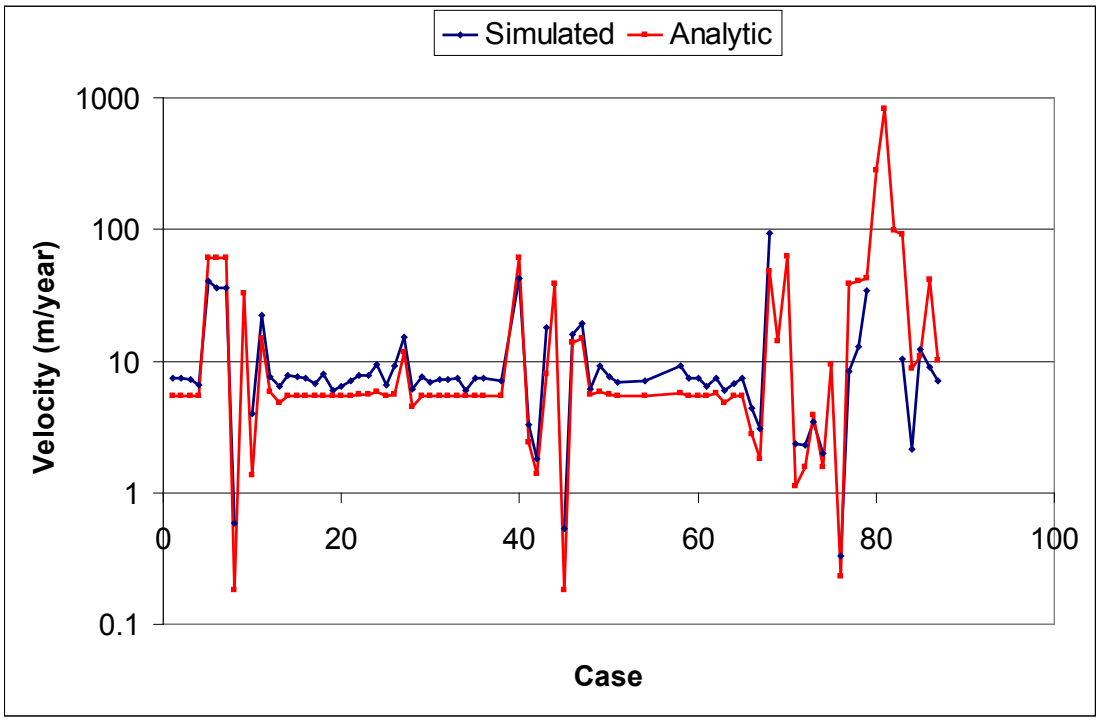

Figure A6.3: Comparison of Analytic Velocity with Simulation

7 Application to CarbonStore

7.1 CarbonStore Units

An interim review of the open aquifers in CarbonStore identified 26 units whose properties are given in **Table A7.1**. Note that the index identifier used here does not correspond to CarbonStore Unit number.

Index	Permeability (mD)	Dip (º)	Net Thickness (m)	Gross Thickness (m)	Vertical NTG (fraction)	Porosity (fraction)	Centroid Depth (m)
1	429	0.5	103	135	0.76	0.26	2195
2	145	0.5	78	122	0.64	0.24	2550
3	250	0.5	50	80	0.63	0.25	2347
4	100	0.9	66	79	0.83	0.23	617
5	5	2.5	421	495	0.85	0.19	2635
6	5	3.3	226	283	0.8	0.13	2105
7	5	3.7	109	109	1.0	0.15	2156
8	12000	0.4	143	250	0.57	0.33	1046
9	897	0.9	295	491	0.6	0.27	1668
10	897	0.9	157	262	0.6	0.27	1389
11	897	0.9	73	122	0.6	0.27	1531
12	6696	0.9	102	175	0.58	0.31	1299
13	1081	1.2	38	60	0.64	0.28	1849
14	721	1.2	53	75	0.7	0.27	1992
15	7000	1.5	58	61.4	0.95	0.31	1193
16	7687	1.6	55	183	0.3	0.18	1257
17	4500	1.7	55	84.1	0.65	0.31	1062
18	400	2.0	16	40	0.4	0.15	2160
19	250	2.5	183	262	0.7	0.15	2623
20	12000	2.8	143	250	0.57	0.33	1034
21	275	3.0	24	34	0.7	0.16	1846
22	275	3.0	12	17	0.7	0.16	2112
23	38	3.2	403	576	0.7	0.17	2574
24	250	4.0	41	55	0.75	0.15	2099
25	10	5.7	76	380	0.2	0.06	1213
26	1	4.5	32	38	0.85	0.25	2847

Table A7.1: Large Open Aquifers from CarbonStore Review

Most of these units fell outside the range set at the original modelling workshop, a number of extra simulations were performed to assess them. The range of dips and permeabilities is shown in **Figure A7.1**.

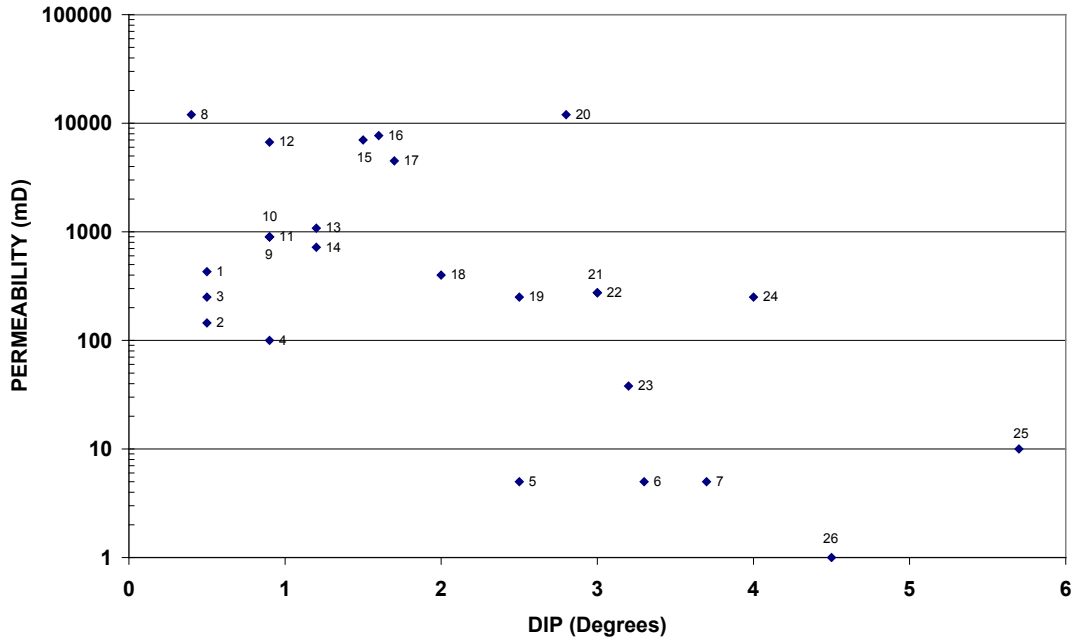

Figure A7.1: Permeability-Dip Combinations for Large Open Aquifers in CarbonStore

These cases can be largely classified as having

- high permeability/dip which fail the velocity stability criterion,
- good injectivity and storage security satisfying the velocity criterion or
- low injectivity, but good security.

The classification is shown in **Figure A7.2** assuming a target injection of 200 Mt of CO_2.

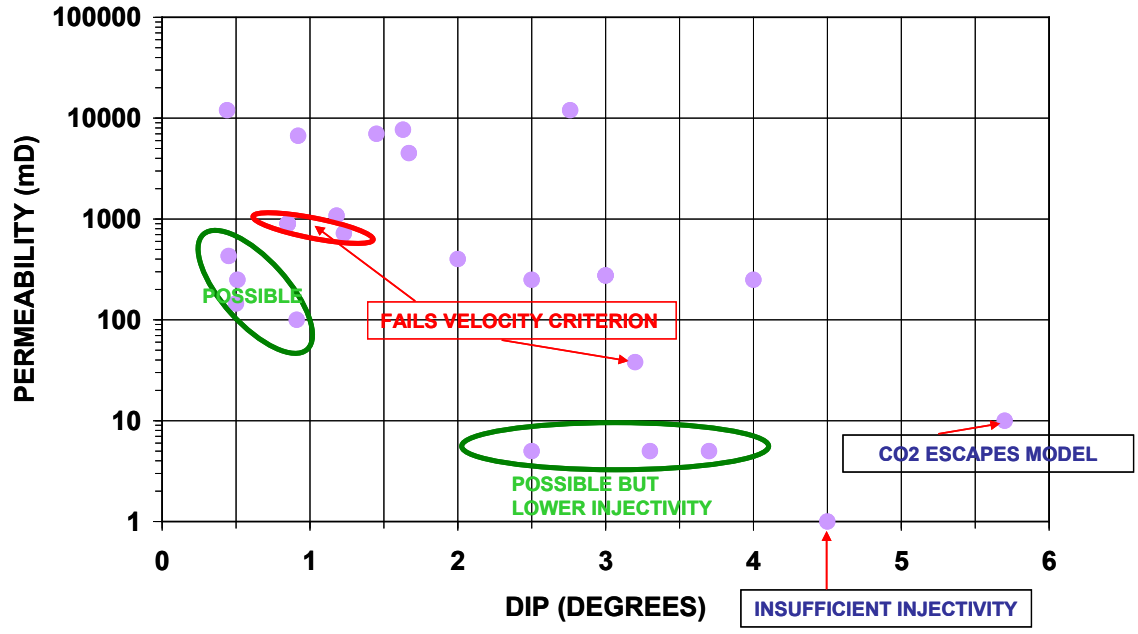

Figure A7.2: Classification of Cases Assuming 200 Mt of CO_2 Injected

All cases above and to the right of the 'fails velocity criterion line' will also fail the stability criterion. For these cases, further simulation was performed assuming an injection target of 20 Mt (i.e. 10% of the base case). This allows more cases to satisfy the stability criterion and storage factors can be calculated for these cases, but it is noted that some cases are still unstable (**Figure A7.3**).

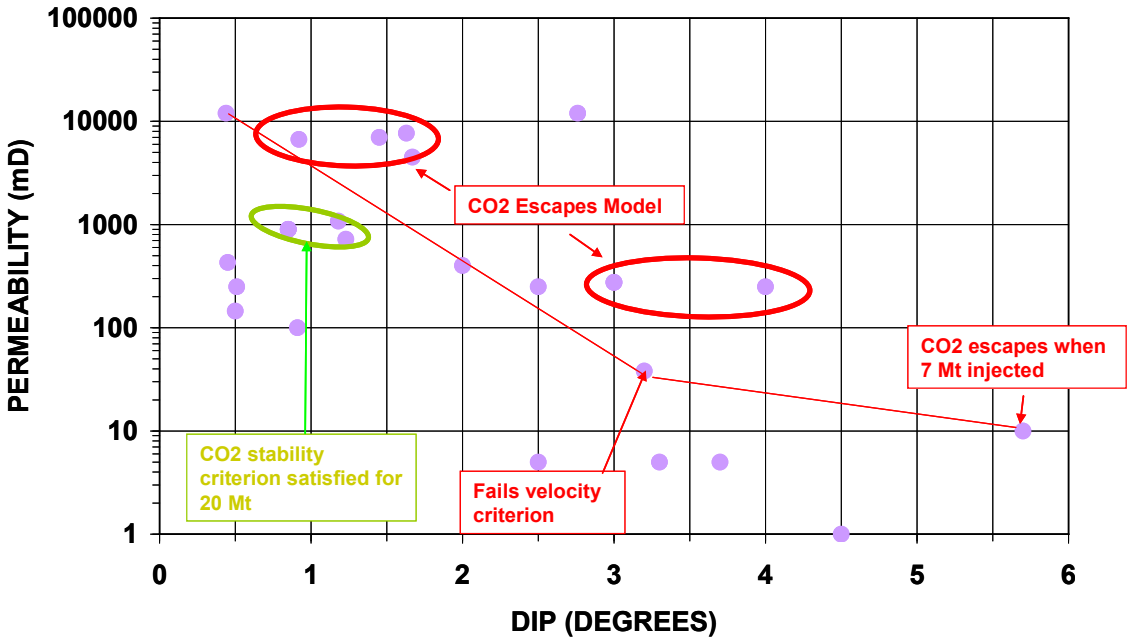

Figure A7.3: Classification of Cases Assuming 20 Mt of CO_2 Injected

Further simulations were run for the lower permeability case 23 injecting only 10 Mt and 1 Mt. For these low injection cases, the injected CO_2 became residually or solution trapped.

Simulations representing the remaining higher dip higher permeability cases were run with decreasing injected CO_2 amounts (<< 20 Mt) until the stability criterion was satisfied. For these simulations, the stability criterion is only met if all of the injected CO_2 is either residually or solution trapped. This requirement resulted in much lower injection.

The migration velocities of the 99% boundary limit of the plume are shown in **Figure A7.4** for a small number of cases assuming an injection target of 200 Mt of CO_2. This figure shows significant differences in the behaviour of the plume. For stable cases (e.g. case 2) the limit of the plume migrated at low velocity which was slowly declining at 1000 years. For unstable cases (e.g. case 14) the limit migrated at tens of metres per year and was actually increasing at 1,000 years. The unstable cases typically terminated before 1,000 years because CO_2 had migrated above the 800 m level.

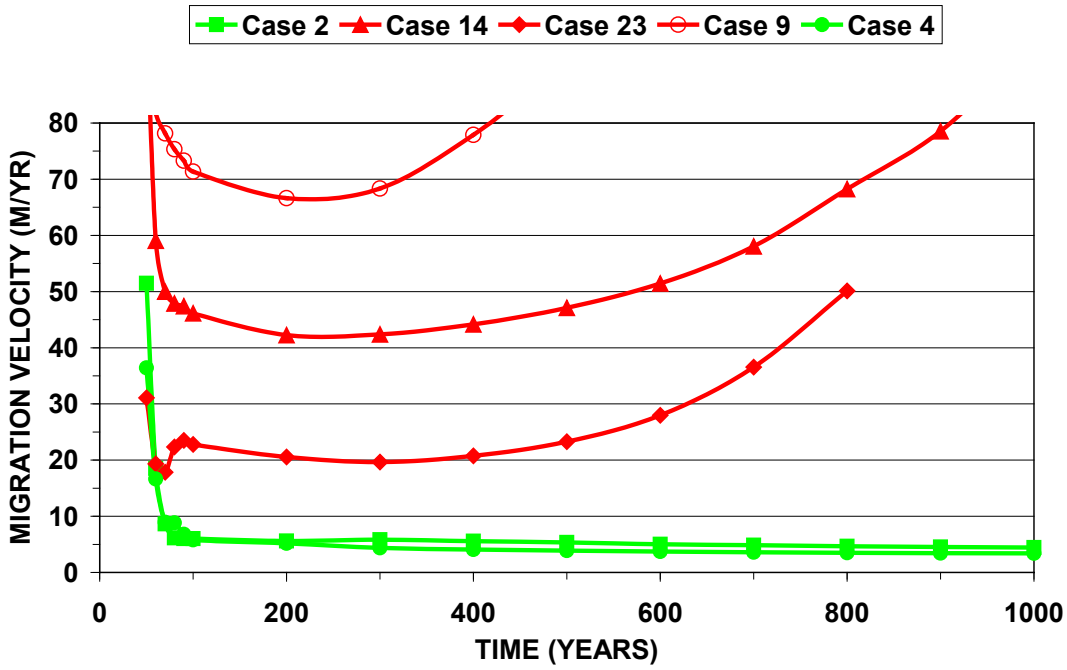

Figure A7.4: Migration Velocities of 99% Limit of CO_2 Plume for Selected Units 200 Mt Injection Target

The velocity of migration for other permeability-dip combinations is shown in **Figure A6.2**.

The mass of CO_2 securely stored for each permeability-dip combination is shown in **Figure A7.5**.

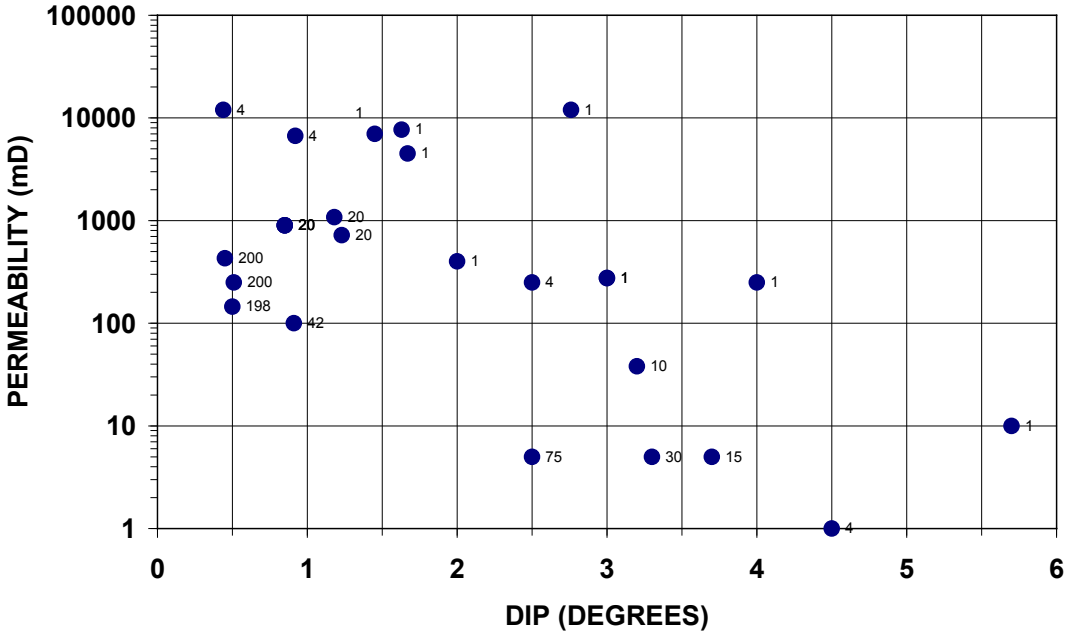

Figure A7.5: Stable Masses of CO_2 Injected (Mt)

The pore volume utilisation for the cases inspired by the interim CarbonStore review was estimated by comparison with the results of all simulations runs. The most appropriate

simulation case was used. The results are given in **Table A7.2** which also specifies which simulation run was used.

Index	Distance from Centroid to 800 m Depth (km)	Mass injected per site (Mt)	Number of Injection Sites	Pressure Corrected Utilisation (%PV)	Simulation Case used for Utilisation	Dynamic Storage Capacity (Mt)	Comment
1	178	200	31	0.85	38	6270	
2	201	198	1	0.38	66	179	
3	174	200	21	1.13	61	4184	
4	-12	42	8	0.26	73	358	Adjusted for unit geometry
5	42	75	52	0.81	71	3871	Adjusted for injectivity
6	23	30	38	0.78	72	1144	Adjusted for injectivity
7	21	15	23	1.02	74	347	Adjusted for injectivity
8	32	4	40	0.47	92	0	4 Mt/injection site
9	59	20	30	0.66	77	605	20 Mt/injection site
10	40	20	10	0.66	77	201	20 Mt/injection site
11	49	20	2	0.66	77	35	20 Mt/injection site
12	31	4	40	0.47	92	174	
13	51	20	2	0.81	86	39	20 Mt/injection site
14	56	20	3	0.81	86	62	20 Mt/injection site
15	16	1	48	0.51	91	200	1 Mt /injection site
16	16	1	48	0.51	91	1030	1 Mt /injection site
17	9	1	48	0.51	91	101	1 Mt /injection site
18	39	1	31	0.40	90	31	1 Mt /injection site
19	42	4	306	0.71	88	1223	4 Mt /injection site
20	5	1		0.39	94	0	1 Mt /injection site
21	20	1	30	0.40	90	30	1 Mt /injection site
22	25	1	11	0.40	90	11	1 Mt /injection site
23	32	10	224	0.80	87	2236	10 Mt/injection site
24	19	1	24	0.40	90	21	1 Mt /injection site
25	4	1	307	1.51	84	307	Adjusted for Injectivity, 1 Mt /injection site
26	26	4	30	0.81	71	103	Adjusted for Injectivity, 4 Mt/injection site

Table A7.2: Dynamic Capacity of Large Open Aquifers in CarbonStore Review

7.2 Storage Regimes for CarbonStore Large Open Aquifers

The cases for which pore volume utilisation have been calculated were divided into two groups as shown in **Figure A7.6**. The red plume stability line is defined by equation 6.1. Above the red line, less CO_2 is injected such that after 1,000 years all of the injected CO_2 is residually trapped and/or dissolved. The injection per well into some of these cases was very constrained, see **Figure A7.5**. This figure also shows that the injection into some cases below the line is significantly constrained due to low injectivity. The cases below the line in **Figure A7.6** were subdivided into 2 groups, those with good injectivity and those with low injectivity. The transition between these two regimes was chosen to be permeability based with the boundary set at 10mD. Consequently, the open aquifers were divided into three storage regimes as defined in **Table A7.3**.

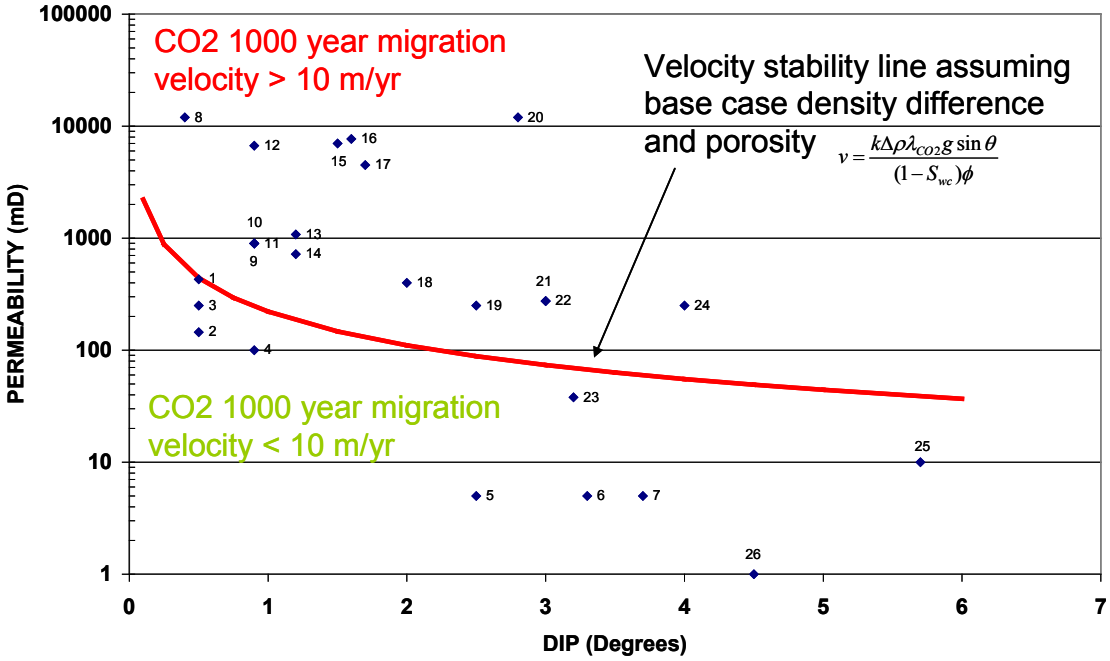

Figure A7.6: Division of Units into Stable and Unstable Plumes

Regime Identifier	Brief Description	Location on Figure 7-6
1	Poor injectivity units	Permeability < 10 mD
2	Good injectivity and security units	Below the red stability line but with permeability > 10 mD
3	Good injectivity but migration limited	Above the red line

Table A7.3: Open Aquifer Storage Regimes

7.3 Implementation in CarbonStore

The CarbonStore Monte Carlo calculation requires the Most Likely, Minimum and Maximum pore volume utilisation for each storage regime. The approach described in section 7.1 was tailored to give a specific utilisation for each unit. The data for each storage regime were analysed to produce a likely range of utilisations and a Most Likely value. All of the cases for which simulation results were available were used for this analysis and the range of utilisations is shown in **Figure A7.7**.

The pressure packing factor is the ratio of the CO_2 storage capacity calculated using the pressure upscaling method to that calculated from the CO_2 plume extent. The nearer the packing factor to one, the smaller the pressure interference between injection sites. Thus for the high permeability units in storage regime three, the packing factor is fairly close to one indicating that there is less pressure interference, but for the other regimes this effect is much stronger. However, regimes one and two typically have higher storage utilisations which emphasises the detrimental impact of significant migration on storage capacity.

The range of values shown in **Figure A7.7** was used as the basis for the storage utilisations input to CarbonStore. They have been compared and contrasted to those produced by

Exemplar modelling of the Forties aquifer. A combined set of utilisations was produced as set out in **Table A7.4**.

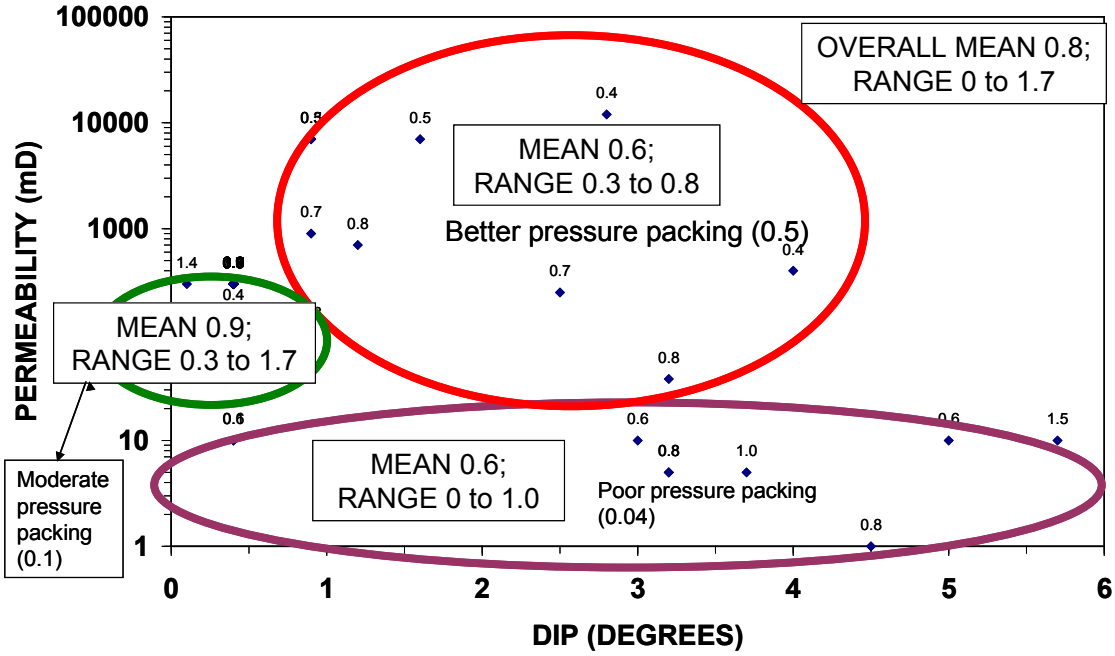

Figure A7.7: Representative Structure Pore Volume Utilisation (%PV)

Storage Regime	Minimum	Most Likely	Maximum
1	0 (E.g. unable to inject CO_2)	0.6 (Mean RS pressure footprint)	1.0 (Max RS pressure footprint)
2	0 (E.g. heterogeneity defeats security)	0.9 (Mean RS pressure footprint)	1.8 (Interpreted max from Exemplar)
3	0 (E.g. heterogeneity defeats security)	0.6 (Mean RS pressure footprint)	1.0 (Max RS pressure footprint)

Table A7.4: Open Aquifer Storage Capacities (%PV)

The minimum utilisation was set to 0 for all regimes to recognise the fact that either heterogeneity or injectivity might preclude storing CO_2 in a unit.

The main extra features modelled in the Exemplar study of part of the Forties aquifer were heterogeneity, structural trapping due to surface topology and partially optimised location and number of injection wells. The Exemplar gave a local utilisation of 5.4% for storage regime two. The Exemplar model was extracted from an optimal downdip region of the Forties aquifer. However the storage capacity method presented in section 5 indicates that due to pressure interference between injection sites it is typically not possible to inject comparable amounts at shallower depths or to utilise the entire aquifer for CO_2 injection. The base case model (index 38) only utilised one third of the aquifer for CO_2 injection (see section 5.3).

Consequently, it is recommended that the Exemplar utilisations corresponding to storage regime two are reduced by a factor of three to 1.8% for estimating the capacity of an entire Unit. No such reduction should be performed for the cases corresponding to storage regime three where there is little pressure interference.

The range for regime three from the RS cases was extended to reflect the potential role the surface topology might make in structurally trapping CO_2 in high permeability units.

It should be noted that whilst regime one and three have the same distribution of utilisations, it is still important to distinguish between them because wells in regime three have a maximum cumulative injection limit. It was recommended that this limit is set to 10 Mt which is a representative value from the simulations in regime three.

The Exemplar study gives conclusions consistent with those from the RS simulations.

CarbonStore also needs to calculate well numbers for use in economics calculations. It was recommended that a modified application of the (Mathias et al, 2009) solution for well numbers is used in which:

- The limiting fracture pressure is calculated at the centroid depth of the unit
- The associated pore volume is calculated from the dynamic capacity pore volume utilisation
- The maximum injected per well is limited to 10 Mt for wells in regime three.

8 Discussion of Results

This study has presented results based on a simple representative model of a large dipping open aquifer. The representative model was characterised by the majority of injected CO_2 remaining close to the point of injection whilst a small fraction typically migrated tens of kilometres updip over thousands of years. Not all of the injected CO_2 had necessarily been trapped (capillary or dissolution) after 1,000 years, which was the limit of simulation, or even after 10,000 years. A pragmatic method for calculating storage potential based on published guidelines was used to estimate secure storage capacity based on plume stability. Pressure interference between injection sites was found to be significant and affected estimates of entire unit capacity based on extrapolating single injection site simulation results.

In this section a brief comparison is made with other studies as a critical review of the results of this study.

8.1 Sleipner

8.1.1 Background

Sleipner was the world's first commercial CO_2 storage project. It commenced in 1996 injecting CO_2 at a rate of 1 Mt/year. There are many studies detailing different aspects of the Sleipner CO_2 storage project (Chadwick et al, 2002, Holloway et al, 2002 etc). Sleipner injects CO_2 into a very large continuous sand body, the Utsira Sand, so might be considered as an example of a large open aquifer. However, studies indicate that the surface topology contains structural trapping of the order of the mass of CO_2 injected and so it should properly be considered as open with structure in terms of the CarbonStore classification. In this section some of the published studies are reviewed and contrasted to this study. Because the geology of the Sleipner storage site plays a key role in CO_2 migration a brief review of the Sleipner site is presented in which the information is mostly drawn from (Chadwick et al, 2002) and (Holloway et al, 2002).

The Utsira Sand comprises a basinally-restricted deposit of Mio-Pliocene age extending for more than 400 km from north to south and between 50 and 100 km from east to west. The top Utsira Sand surface generally varies quite smoothly in the depth range 550 to 1500 m, and is around 800 – 900 m near Sleipner. Thickness is approximately 300 m at Sleipner.

Around Sleipner, the top of the Utsira Sand dips generally to the south, but in detail it is gently undulatary with small domes and valleys. The Sleipner CO_2 injection point is located beneath a small domal feature which rises about 12 m above the surrounding area. The Utsira sands contain thin (~1m thick) layers of shale or clay which constitute important permeability barriers within the reservoir sand. The base of the Utsira Sand is structurally more complex, and is characterised by the presence of numerous mounds, interpreted as mud diapirs.

Around and east of the injection point, a unit termed the Sand-wedge lies just above the top of the Utsira Sand, separated from it by a few metres of shale.

The structural and stratigraphical detail around the injection point is essential to understanding and predicting the long-term behaviour of the CO_2 plume.

Porosity estimates range generally from 27% to 31%, locally up to 42%. The permeability is high in the range 1,000 to 8,000 mD.

The total pore volume of the Utsira Sand, based on regional assessments of porosity and shale volume, is about 6 x 10^{11} m^3. The pore volume enclosed within structural and stratigraphical traps, where CO_2 can be expected to accumulate in the long-term around the Sleipner injection point is 0.11% of the total pore-volume or approximately 20 Mt. Extrapolating these figures over the entire Utsira Sand gives a storage volume in traps of just 6.6 x 10^8 m^3 (approximately equivalent to 460 Mt assuming a storage density of 700 kg/m^3).

The trapping of CO_2 beneath intra-reservoir shale beds has been reported to significantly increase realisable storage volumes. Time-lapse seismic data shows the bulk of the injected CO_2 is currently being trapped beneath the intra-reservoir shales. This has the effect of markedly decreasing migration distances in the short term.

Simple buoyancy-driven migration modelling shows that 2.1 Mt of CO_2 trapped wholly at the top of the reservoir would ultimately migrate more than 4 km from the injection point. This compares with the observed 1999 CO_2 plume (2.35 Mt) whose areal extent, was entirely within 1 km of the injection point. By 2001, 4.36 Mt of CO_2 was still confined to within 1.3 km of the injection point, whereas 4.2 Mt trapped wholly at the top Utsira would be expected to reach an ultimate distance of about 9 km. The intra-reservoir shales are, therefore, providing a mechanism for delaying CO_2 dispersal in the short term (tens of years).

A range of migration models, were constructed taking an injected CO_2 volume of 30 Mm^3 (approximating to the expected final injected mass of 20 Mt). Assuming migration at the top of the Utsira Sand, the preferred model shows migration generally in a westerly direction, to reach a maximum distance from the injection site of about 12 km.

An alternative scenario, that the CO_2 leaks into, and migrates along the top of the Sand-wedge, gives less well constrained results. Migration is northwards then north eastwards, until, with 7.4 Mm^3 injected, the CO_2 front moves out of the area of 3D seismic data coverage.

The long term fate predicted for most of the injected CO_2 is for it to dissolve in the brine over a few thousand years.

It is clear that local permeability heterogeneities, both stratigraphical and structural, can profoundly affect CO_2 distribution and migration within the reservoir. These features were difficult or impossible to detect on the seismic data prior to CO_2 injection; they only became apparent after being effectively 'illuminated' by the CO2 stream.

8.1.2 Application of Representative Structure Modelling to Sleipner

The CO_2 injected into Sleipner is expected to become trapped within local structures. However, the shales are also expected to affect migration of the CO_2 and may act to enhance the mass of CO_2 capillary trapped around the injection site. The structural trapping mechanism was not included in the Representative Structure simulation model of large open aquifers but residual trapping was. If the majority of the injected CO_2 becomes structurally trapped, then this would suggest that Sleipner is not a good analogue for the open aquifer RS model. Conversely, if the majority was residually trapped, then application of the RS model would be appropriate.

A potential analogue for Sleipner within the RS simulations is case 80 which has permeability 7,000 mD, porosity 31% and a dip of 0.9 degrees though this is likely to be higher than the Sleipner value. For case 80, which injected 20 Mt of CO_2, the injected CO_2 migrated more

than 27 km in 150 years and failed to meet the stability criterion. In order to ensure plume stability, the injection had to be limited to 4 Mt (case 92). For this case the CO2 migrated approximately 14 km from the point of injection in 1,000 years. The pressure corrected pore volume utilisation was 0.47%.

The projected CO_2 migration distance for Sleipner for 20 Mt of CO_2 injection is comparable to those found for the 4 Mt injected in the RS model. However, the RS model does not contain the structural traps associated with the surface topography which could trap up to 20 Mt depending on degree of contact. Furthermore, the RS model does not contain the shale barriers which also significantly impact migration distances. The RS analogue case is much thinner than Sleipner and this also results in larger migration distances.

However, the pore volume utilisation of 0.47% is likely to be a reasonable estimate of the residually/ solution trapped CO_2 as it significantly exceeds the structural storage equivalent to a pore volume utilisation of 0.11% estimated to be associated with the surface topography of the Utsira sand.

The effects of surface topography and heterogeneity including shales were considered by Exemplar simulation (see Appendix A5.4). This study produced pore volume utilisations comparable to the RS model but also found that topology could either enhance or reduce storage capacity compared with smooth dipping models..

8.2 CO2Store

The following example storage locations are taken from the CO2STORE project (Torp, 2005). These indicate the importance of structural trapping and the potential for early leakage of CO_2.

8.2.1 Froan Basin area of the Trøndelag Platform

The Froan Basin area (in Norwegian waters) is reported as likely to contain sedimentary sequences with reservoir properties potentially suitable for underground CO_2 storage in the southeastern Trøndelag Platform (Lundin et al, 2005). The potential reservoir constitutes an open, northwestward dipping monocline with a typical migration distance of approximately 60 km from potential injection sites to the subcrop of the reservoir formation below the Quaternary or at the sea floor. Permeability is up to 5000 mD and porosity up to 30%. Reservoir thickness is typically 200 metres. The strata are typically subhorizontal, but vary up to 5% at the edges.

Simulation was performed using ECLIPSE100^{TM}. The injection rate was 2 Mt/year over a period of 25 to 50 years. Up to 100 Mt was injected at a depth of approximately 2000 m. Relative permeability hysteresis was not included in the simulation model. The critical gas saturation was not reported but a graphic of the relative permeability data suggests it might be of the order of 0.1.

Post injection migration was modelled to 5,000 years. The wells were treated as vertical. Perforations were placed immediately above the top of the basement. Two well positions were chosen, one below a domal trap and one in an area without any obvious structural trap, although small surface structures are present.

The simulation cases predicted that injected CO_2 would be expected to move upward in the reservoir unit until it reached the base of the next sealing formation and then migrate laterally below the seal towards the sea floor. All of the injected CO_2 was either trapped locally in structural traps or became dissolved in the formation water before it could come into the proximity of the subcrop. Leakage was not predicted in any of the studied cases for total injected masses of up to 100 Mt injected at a depth of approximately 2000 m. The CO_2 migrated approximately 16 km for the case without the domal trap. Approximately 40% of the injected CO_2 had dissolved in the brine after 5,000 years.

The simulation cases predicted no danger of pressure build-up that would cause fracturing, because the reservoir is not tightly sealed and it has large enough pore volume to accommodate the injected CO_2 volume by water compressibility (an increase in water density). A distribution of pressure increase due to injected CO_2 over large parts of the basin is likely, which will keep the overall increase small. Injection at high rates at several places in the basin may however lead to pressure increases, which should be studied in a comprehensive model for the whole basin.

8.2.2 Frohavet Basin

The reservoir constitutes an open, south-eastward dipping monocline with a typical migration distance of about. 4.5 km from potential injection sites to the subcrop of the reservoir formation below the Quaternary or at the sea floor (Polak et al, 2004). No data about rock properties in the subsurface exist for the Frohavet Basin. The permeability was assumed to be 2,000 mD, porosity 25% and thickness 75m based on outcrops. The dip would appear to be several degrees although it is not specified in the report.

Simulation was performed using ECLIPSE100^{TM}. The injection rate was 2 Mt/year for 25 years. Up to 100 Mt was injected at a depth of approximately 2000 m. Relative permeability hysteresis was not included.

The injection point for the base case was placed vertically beneath a mapped dipping anticlinal structure at a depth of about 600 m. However, the pore volume in the trap was small such that only a small fraction of the injected CO_2 could be stored in it. Consequently, the simulations predicted a very high cumulative volume of CO_2 to migrate from the trap towards the sea floor and to leak from the reservoir.

In the case of high porosity and high permeability (base case) leakage of CO_2 was predicted to start after a few years and most of the injected CO_2 would have leaked after less than 50 years.

Property variations including lower permeability, lower k_v:k_h ratio, high residual gas saturation and a good injection strategy (well placement and number of wells) resulted in delayed leakage and reduced the fraction of CO_2 which leaked. Given a favourable combination of these parameters, the onset of leakage might occur several centuries after the start of injection and leakage rates (annual and average) might be in the order of 0.01% of the total injected mass per year. In extremely favourable parameter combinations, no leakage at all might occur.

The simulation cases predicted no danger of pressure build-up that would cause fracturing, because the reservoir is not tightly sealed and it has large enough pore volume to accommodate the injected CO_2 volume by water compressibility.

The Frohavet Basin may be suitable for safe long-term storage of CO_2, given favourable reservoir properties of the potential storage formations. These reservoir properties are at present not known at all due to the complete lack of well data or subsurface samples.

8.2.3 Comparison with Representative Structure Modelling

The Froan Basin study reported much shorter migration distances than might be expected from the RS modelling. However, it is clear that structural trapping played an important role in determining how far the CO_2 migrates. For the scenario where injection is below an anticline the CO_2 is confined within five kilometres of the point of injection. This scenario would be classed as a structural trap within an open unit in CarbonStore whose storage capacity would be calculated by combining the storage capacity of the trap with the storage potential of the parent unit. The simulated scenario effectively looks at storage in the structure only.

For the case where injection is not below a large structure the migration distance is still much smaller than would be expected from this work. It is not clear what the effective dip is for the region in which CO_2 was injected and so it is not possible to compare directly to an RS simulation. Either surface structural trapping or very low dip might have an important effect in delaying CO_2 migration. Case 46 corresponds to a high permeability (3,000 mD) low dip (0.1º) structure. For this case the plume migration velocity after 1,000 years was 16 m/year with a migration distance of 29.3 km compared to the migration distance of 16 km estimate reported in these studies.

Pressure interference between injection sites was recognized as an issue when attempting to determine how much CO_2 can be injected into an entire aquifer. This issue was addressed in the RS modelling though pressure upscaling of pore volume utilisation to determine storage capacity.

The Frohavet Basin appears to be a high permeability open aquifer. For high permeability scenarios migration of CO_2 to the subcrop could happen in a few tens of years. This is consistent with the results for the high permeability RS cases run to match those in CarbonStore. To ensure safe storage, the modelled mass of CO_2 injected was significantly reduced.

8.3 CASSEM Project

The CASSEM project (CO_2 Aquifer Storage Site Evaluation and Monitoring) reported results for simulation of CO_2 injection into two potential aquifer storage sites (Jin et al, 2010). One site had a simple geology, whilst the other was much more complex. The results showed that the migration of CO_2 is strongly influenced by the local topography of the upper surface of the aquifer. Calculated pore volume utilisations were of the order of 1% for the first site and 2.75% for the second site. The difference in site utilisation is reported as being due to the greater pressure increase possible at a deeper storage location.

The first site has utilisations comparable to RS results, and though the second site utilisation is significantly higher than the RS values, it is still in the range of the Exemplar study (Appendix A5.4). Migration distances are not reported, but CO_2 is contained within the detailed simulation model which has dimensions of the order of 10 to 20 km. The permeability of the sites are 500 mD and 60 mD respectively. Injection into the second site is below a large anticline capable of storing 10% of the injected CO_2. A porous overburden (seal) and

underburden is modelled and a significant fraction of the aquifer brine (up to 23%) is displaced into these layers.

8.3.1 Application of Representative Structure Modelling to Site B

Case 69 has permeability of 38 mD, porosity 0.17, thickness 400 m and a dip of 3.2 degrees. The first three properties are comparable properties to site B but it is not possible to make a comparison of dips, as one has not been reported for site B.

Case 69 suffered from plume stability issues and injection had to be restricted to 10 Mt to achieve stability (case 87). Case 87 had a pore volume utilisation based on the CO_2 plume size of 1.9%. However, pressure upscaling reduced it to 0.8% because shallower regions of the aquifer are seriously impacted by the pressure footprint associated with injecting at many sites.

Whilst potential based on CO_2 plume dimension is comparable to the CASSEM study value, the pressure upscaled utilisation of 0.8% is smaller. However, the CASSEM study modelled both porous seal and basement formations and a significant fraction of brine was expelled into these which would have resulted in lower aquifer pressure. The RS modelling did not include either seal or underburden formations. These were assumed to be impermeable. Including the pore volume of these formations would reduce the CASSEM utilisation to 1.7%, which makes the result comparable to the range in storage regime 2. However, without knowledge of the dip, it is difficult to be sure which regime site B corresponds to.

8.4 Analytic Models

8.4.1 MacMinn et al

MacMinn et al presented an analytic model based on incompressible flow for the migration of CO_2 post injection in dipping aquifers with or without the presence of ground water flow (MacMinn et al 2010). The model includes capillary trapping but not dissolution. It consists of a number of condition dependent scenarios which can be solved to determine migration distance and also the pore volume utilisation for CO_2 storage. Although the equations are not specified in the paper for the scenario corresponding to the open aquifer representative structure model, they are straightforward to solve.

Applying the analytic model to a low permeability case (case 8) corresponding to storage regime one, the analytic model predicted that CO_2 would become residually trapped after 51,000 years. The rate of advance of the CO_2 plume tip would be 0.2 m/yr and the overall distance migrated 13.1 km. The RS simulation model predicted a velocity of migration 0.6 m/yr and a CO_2 extent of 2 km after 1,000 years. The time required to become residually trapped would be much longer than this and so the eventual distance migrated is likely to be comparable to the analytic model. It should be noted that the analytic model assumes an initial CO_2 distribution corresponding to the end of injection. The maximum extent of CO_2 in the analytic model was 2 km at the end of injection.

For the base case (case 38, storage regime two) the analytic model predicted that the CO_2 would become residually trapped after 4,135 years. The rate of advance of the CO_2 plume tip would be 5.5 m/yr and the overall distance migrated 31.7 km. The RS simulation model predicted a migration velocity of 7.1 m/yr and a CO_2 extent of 12.7 km after 1,000 years. By analogy with case 1, the migration velocity would have dropped to about 3 m/yr at 10,000

years at which time it would have migrated about 55 km. The time required for full residual trapping was in excess of 10,000 years. However there is reasonable correspondence between the models.

Applying the analytic model to case 92 (storage regime 3) which was the high permeability analogue used for the Sleipner comparison, the analytic model predicted that the CO_2 would become residually trapped after 6 years and the overall distance migrated 1.7 km. The RS model predicts mobile CO_2 at 1,000 years and a much larger migration distance of 14 km. The reason for this is probably that the analytic model assumes an initial distribution for the injected CO_2 and actually only models the CO_2 post injection. This initial distribution results in faster trapping and less migration. Thus the analytic model provides poor estimates for high permeability units.

8.4.2 Gupta et al

Gupta et al present correlations for the time injected CO_2 takes to migrate to the top seal, the maximum lateral extent of the CO_2 plume at the end of injection and the fraction of mobile CO_2 during the buoyancy dominated post injection period (Gupta et al, 2010). These correlations are based on gravity numbers characteristic of horizontal and vertical flow of CO_2. They assume injection through a partially completed vertical well and so are not directly applicable to the simulation performed in this study.

Nevertheless, applying the second correlation to the base case index 38 predicted a CO_2 plume size of radius 5.9 km which is comparable to the plume dimensions from simulation of 12 by 5 km. Applying the third correlation to determine the fraction of trapped CO_2 produced an anomalous unphysical result.

It is not clear how to estimate storage capacity using these correlations.

9 Conclusions

Dynamic estimates of storage capacity require some constraint determining when the store is 'full'. An operational definition for dipping open aquifers, applicable to numerical simulation, was developed based on the existing UK/EU guidelines.

A novel upscaling technique utilising symmetry, the method of images and superposition was devised to estimate the extent of the pressure footprint from multiple injectors. The technique was programmed and tested and found to be sufficiently accurate for the purposes of this project.

A base model was constructed including targeted local grid refinement. This was checked for areal and vertical gridding resolution and boundary effects. The gridding resolution was found to be sufficient, but the injector was moved updip, 50 km from the lower boundary, to reduce pressure boundary effects.

Typically CO_2 injected formed a thin tongue under the overlying seal and migrated updip tens of kms over thousands of years due to its density being lower than the surrounding brine. During this time injected CO_2 which had remained near the point of injection gradually became residually trapped, though this took several thousand years.

For the base model at the end of 50 years injection, the injected CO_2 was contained within a 5.5 km distance from the injector. The CO_2 became more dispersed with time, with CO_2 migrating 65 km updip after 10000 years. However, after 1000 years 99% of the injected CO_2 had only migrated updip 13 km, with a migration velocity of 7.5 m/yr. The fraction of CO_2 residually trapped after 1000 years was 34%, rising to 60% after 10000 years. After 1000 years, about 10% of the injected CO_2 had dissolved in brine, increasing to 26% after 10000 years.

Representative permeability and mean dip were found to be the most important factors affecting storage security and dynamic storage capacity in dipping open aquifers, as they strongly influence the speed of updip CO_2 migration. In order to facilitate storage capacity estimation, it proved useful to classify the simplified modelled open aquifers into three broad storage regimes using these two key factors:

- Regime 1 has poor well injectivity, but good storage security and is characterised by a low representative permeability.
- Regime 2 is characterised by both good CO_2 injectivity and good storage security and therefore typically has higher storage capacities.
- Regime 3 has good CO_2 injectivity, but storage capacities are strongly constrained by the tendency of CO_2 to migrate updip due to buoyancy forces. Such stores are characterised by either a high representative permeability or significant mean dip, or both.

In order to secure CO_2 injected into modelled regime 3 stores, cumulative injection needed to be restricted to prevent any CO_2 remaining mobile after 1000 years, because mobile CO_2 would exceed the assumed migration velocity criterion.

An analytic formula, which assumes incompressible flow, was shown to provide good estimates of CO_2 migration velocities. This formula was used in storage regime classification.

A pressure packing factor was defined as the ratio of the CO_2 storage calculated using the pressure upscaling method to that calculated from the CO_2 extent. For storage regimes 1 and 2 the packing factor indicates significant pressure interference between injection sites. However, for the higher permeabilities in storage regime 3, the packing factor suggests much less pressure interference.

Porosity and depth were found to affect storage capacity significantly, but formation thickness and permeability anisotropy less so. Salinity and trapped gas saturation had only a negligible effect in storage regime 2. Trapped gas saturation is likely to be significant for storage regime 3.

For each of these storage regimes a range and most likely value of storage capacity were estimated. Typical storage capacities obtained were equivalent to significantly less than the 2% of pore volume figure originally assumed from the literature, for initial CarbonStore estimates.

Results which were compared with those from the open aquifer Exemplar model and a combined set of results agreed for use in CarbonStore. The results were also compared with other studies and while no similar study was available for a good comparison, the project results are consistent with other published results where relevant.

10 References

1. Chadwick RA., Zweigel P, Gregersen U, Kirby GA, Holloway S and. Johannessen PN 2002. Geological Characterisation Of CO2 Storage Sites: Lessons From Sleipner, Northern North Sea, Proceedings of the 6th International Conference on Greenhouse Gas Control, 1–4 October 2002, Kyoto, Japan.
2. Earlougher Jr. RC, 1977. Advances in Well Test Analysis., SPE Monograph Volume 5, 1977, Appendix B.
3. ECLIPSE100TM Technical Description, 2008, Chapter 36 Local Grid Refinement and Coarsening, Schlumberger.
4. European Commission, 2011. Implementation of Directive 2009/31/EC on the Geological Storage of Carbon Dioxide, Guidance Documents 1-4, http://ec.europa.eu/clima/policies/lowcarbon/ccs_implementation_en.htm.
5. Gupta AK and Bryant SL, 2010. Analytical Models to Select an Effective Saline Reservoir for CO2 Storage, SPE134762, 2010.
6. Holloway S, 2004.Best Practice Manual from Sacs 2004 – Saline Aquifer CO2 Storage Project, Issued by Appendix A Statoil, Research Center, N-7005 Trondheim, Norway, Edited by: -, British Geological Survey (BGS) (editor),- Andy Chadwick, British Geological Survey (BGS), Erik Lindeberg, Sintef Petroleum, Isabelle Czernichowski-Lauriol, Bureau de Recherches Geologiques et Minieres (BRGM) and Rob Arts, Netherlands Organisation for Applied Scientific Research (TNO).
7. Intergovernmental Panel on Climate Change, September 2005. IPCC Special Report, Carbon Dioxide Capture and Storage, Summary for Policymakers, Eighth Session of Working Group III, Montreal, Canada.
8. Jin M, Pickup G, Mackay E, Todd A, Monaghan A and Naylor M, 2010. Static and Dynamic Estimates of CO2 Storage in Two Saline Formations in the UK, , SPE 131609, 2010.
9. Kovscek, AR, 2006. GCEP Technical Report 2006Global Climate and Energy Project Rapid Prediction of CO2 Movement in Aquifers, Coal Beds, and Oil and Gas Reservoirs Final Report 2006, Investigators: Anthony R. Kovscek, et al. GCEP Technical Report 2006.
10. Lundin E, Polak S, Bøe R,.Zweigel P and Lindeberg E, 2005. Storage potential for CO2 in the Froan Basin area of the Trøndelag Platform, Mid-Norway, NGU Report 2005.027, 2005.
11. MacMinn CW, Szulczewski ML. and Juanes R, 2010. CO2 Migration in Saline Aquifers I: Capillary Trapping Under Slope and Groundwater Flow, , Journal of Fluid Mechanics (2010), 662: 329-351.
12. Mattax CC.and Dalton RL, 1990. Reservoir Simulation p51, SPE Monograph Volume 13, 1990.
13. Polak S, Lundin E, Zweigel P, Bøe R, Lindeberg E and Olesen O, 2004. Storage potential for CO2 in the Frohavet Basin, Mid-Norway, NGU Report 2004.049, 2004
14. Smith, G, 2010a. Notes of Modelling Workshop held at ETI Loughborough offices 8 June, BGS Keyworth offices 9 June 2010.

15. Smith, G, 2010b. Notes of Modelling Workshop hosted by RPS Energy at Dorset Green Technology Park, 14 July 2010.

16. Torp T, 2005. The CO2STORE project – Status, Statoil, Norway, CSLF International Workshop on CSLF Projects, Potsdam 29 September 2005

11 Glossary

Variable	Meaning	Units
ΔP	Change in pressure	MPa
μ	Viscosity	Pa.s
ρ	Density	Kg/m^3
Φ	Porosity	Fraction
θ	Dip	Degree
BHP	Well bottom hole flowing pressure	MPa
DP	Change in pressure	bars
g	Gravity	m/s
k	Permeability	mD
k_r	Relative permeability	fraction
k_v:k_h	Ratio of vertical to horizontal permeability	fraction
S	Saturation	fraction
S_{wirr}	Residual brine saturation	fraction

12 Simulation Cases and Results

Table A6.1: Definition of DOA Cases Simulated

Index	Width X (km)	Length Y (km)	Depth (m)	Dip in X (deg)	Dip in Y (deg)	k_x (mD)	k_y (mD)	k_z (mD)	k_v / k_h	Salinity (ppm)	Porosity (fraction)	Thickness (m)	Hysteresis Model	Trapped Gas Saturation	Well Orientation	Well bore radius (m)	Well Length (m)	Injection Period (years)	Target Injection Rate (MT/yr)	Compressibility (1/bar)	Distance to CP boundary (km)	Other Changes
1	20	180	2000	3	0.4	30	300	30	0.1	100,000	0.27	100	C	0.3	X	0.1	900	50	4	$5.8x10^{-5}$	10	
2	20	180	2000	3	0.4	30	300	300	1	100,000	0.27	100	C	0.3	X	0.1	900	50	4	$5.8x10^{-5}$	10	
3	20	180	2000	3	0.4	30	300	3	0.01	100,000	0.27	100	C	0.3	X	0.1	900	50	4	$5.8x10^{-5}$	10	
4	20	180	2000	3	0.4	30	300	0.3	0.001	100,000	0.27	100	C	0.3	X	0.1	900	50	4	$5.8x10^{-5}$	10	
5	20	180	2000	3	0.4	300	3000	300	0.1	100,000	0.27	100	C	0.3	X	0.1	900	50	4	$5.8x10^{-5}$	10	
6	20	180	2000	3	0.4	30	3000	300	0.1	100,000	0.27	100	C	0.3	X	0.1	900	50	4	$5.8x10^{-5}$	10	
7	20	180	2000	3	0.4	3000	3000	300	0.1	100,000	0.27	100	C	0.3	X	0.1	900	50	4	$5.8x10^{-5}$	10	
8	20	180	2000	3	0.4	10	10	1	0.1	100,000	0.27	100	C	0.3	X	0.1	900	50	4	$5.8x10^{-5}$	10	
9	20	35	2000	3	2	30	300	30	0.1	100,000	0.27	100	C	0.3	X	0.1	900	50	4	$5.8x10^{-5}$	10	
10	20	180	2000	3	0.1	30	300	30	0.1	100,000	0.27	100	C	0.3	X	0.1	900	50	4	$5.8x10^{-5}$	10	
11	20	69	2000	3	1	30	300	30	0.1	100,000	0.27	100	C	0.3	X	0.1	900	50	4	$5.8x10^{-5}$	10	
12	20	180	3000	3	0.4	30	300	30	0.1	100,000	0.27	100	C	0.3	X	0.1	900	50	4	$5.8x10^{-5}$	10	
13	20	29	1000	3	0.4	30	300	30	0.1	100,000	0.27	100	C	0.3	X	0.1	900	50	4	$5.8x10^{-5}$	10	
14	20	180	2000	3	0.4	30	300	30	0.1	100,000	0.27	100	C	0.3	X	0.1	900	50	4	$5.8x10^{-5}$	10	
15	20	180	2000	3	0.4	30	300	30	0.1	100,000	0.27	100	C	0.3	X	0.1	900	50	4	$5.8x10^{-5}$	10	
16	20	180	2000	3	0.4	30	300	30	0.1	100,000	0.27	100	C	0.3	X	0.1	900	50	4	$5.8x10^{-5}$	10	
17	20	180	2000	1	0.4	30	300	30	0.1	100,000	0.27	100	C	0.3	X	0.1	900	50	4	$5.8x10^{-5}$	10	
18	20	180	2000	5	0.4	30	300	30	0.1	100,000	0.27	100	K	0.15	X	0.1	900	50	4	$5.8x10^{-5}$	10	
19	20	180	2000	3	0.4	30	300	30	0.1	100,000	0.27	100	K	0.3	X	0.1	900	50	4	$5.8x10^{-5}$	10	
20	20	180	2000	3	0.4	30	300	30	0.1	100,000	0.27	25	K	0.375	X	0.1	900	50	4	$5.8x10^{-5}$	10	
21	20	180	2000	3	0.4	30	300	30	0.1	100,000	0.27	50	C	0.3	X	0.1	900	50	4	$5.8x10^{-5}$	10	
22	20	180	2000	3	0.4	30	300	30	0.1	100,000	0.27	75	C	0.3	X	0.1	900	50	4	$5.8x10^{-5}$	10	

Index	Width X (km)	Length Y (km)	Depth (m)	Dip in X (deg)	Dip in Y (deg)	k_x (mD)	k_y (mD)	k_z (mD)	k_v / k_h	Salinity (ppm)	Porosity (fraction)	Thickness (m)	Hysteresis Model	Trapped Gas Saturation	Well Orientation	Well bore radius (m)	Well Length (m)	Injection Period (years)	Target Injection Rate (MT/yr)	Compressibility (1/bar)	Distance to CP boundary (km)	Other Changes
23	20	180	2000	3	0.4	30	300	30	0.1	100,000	0.27	200	C	0.3	X	0.1	900	50	4	$5.8x10^{-5}$	10	
24	20	180	2000	3	0.4	30	300	30	0.1	100,000	0.27	400	C	0.3	X	0.1	900	50	4	$5.8x10^{-5}$	10	
25	20	180	2000	3	0.4	30	300	30	0.1	50,000	0.27	100	C	0.3	X	0.1	900	50	4	$5.8x10^{-5}$	10	
26	20	180	2000	3	0.4	30	300	30	0.1	200,000	0.27	100	C	0.3	X	0.1	900	50	4	$5.8x10^{-5}$	10	
27	20	180	2000	3	0.4	30	300	30	0.1	100,000	0.13	100	C	0.3	X	0.1	900	50	4	$5.8x10^{-5}$	10	
28	20	180	2000	3	0.4	30	300	30	0.1	100,000	0.33	100	C	0.3	X	0.1	900	50	4	$5.8x10^{-5}$	10	
29	20	180	2000	3	0.4	30	300	30	0.1	100,000	L	100	C	0.3	X	0.1	900	50	4	$5.8x10^{-5}$	10	
30	5	180	2000	3	0.4	30	300	30	0.1	100,000	0.27	100	C	0.3	X	0.1	900	50	4	$5.8x10^{-5}$	10	
31	7.5	180	2000	3	0.4	30	300	30	0.1	100,000	0.27	100	C	0.3	X	0.1	900	50	4	$5.8x10^{-5}$	10	
32	10	180	2000	3	0.4	30	300	30	0.1	100,000	0.27	100	C	0.3	X	0.1	900	50	4	$5.8x10^{-5}$	10	
33	20	180	2000	3	0.4	30	300	30	0.1	100,000	0.27	100	C	0.3	X	0.1	900	50	4	$1.5x10^{-4}$	10	
34	20	180	2000	3	0.4	30	300	30	0.1	100,000	0.27	100	C	0.3	X	0.1	900	50	4	$5.8x10^{-5}$	10	
35	20	180	2000	3	0.4	30	300	30	0.1	100,000	0.27	100	C	0.3	X	0.1	900	50	4	$5.8x10^{-5}$	10	
36	20	180	2000	3	0.4	30	300	30	0.1	100,000	0.27	100	C	0.3	Y	0.1	900	50	4	$5.8x10^{-5}$	10	
37	20	180	2000	3	0.4	30	300	30	0.1	100,000	0.27	100	C	0.3	X	0.1	900	50	4	$5.8x10^{-5}$	10	2 wells
38	20	180	2000	3	0.4	30	300	30	0.1	100,000	0.27	100	C	0.3	X	0.1	900	50	4	$5.8x10^{-5}$	50	
39	20	180	2000	3	0.4	30	300	30	0.1	100,000	0.27	100	C	0.3	X	0.1	900	50	4	$5.8x10^{-5}$	50	2 wells
40	20	180	2000	3	0.4	30	3000	3	0.001	100,000	0.27	100	C	0.3	X	0.1	900	50	4	$5.8x10^{-5}$	10	
41	20	24	2000	3	5	10	10	1	0.1	100,000	0.27	100	C	0.3	X	0.1	900	50	4	$5.8x10^{-5}$	10	
42	20	23	2000	3	3	10	10	1	0.1	100,000	0.27	100	C	0.3	X	0.1	900	50	4	$5.8x10^{-5}$	10	
43	20	33	2000	3	3	50	50	5	0.1	100,000	0.27	100	C	0.3	X	0.1	900	50	4	$5.8x10^{-5}$	10	
44	20	45	2000	3	2	30	300	30	0.1	100,000	0.27	100	C	0.3	X	0.1	900	50	4	$5.8x10^{-5}$	10	
45	40	180	2000	3	0.4	10	10	1	0.1	100,000	0.27	100	C	0.3	X	0.1	900	50	4	$5.8x10^{-5}$	10	
46	20	180	2000	3	0.1	300	3000	300	0.1	100,000	0.27	100	C	0.3	X	0.1	900	50	4	$5.8x10^{-5}$	10	
47	20	69	2000	3	1	300	300	30	0.1	100,000	0.27	100	C	0.3	X	0.1	900	50	4	$5.8x10^{-5}$	10	

Index	Width X (km)	Length Y (km)	Depth (m)	Dip in X (deg)	Dip in Y (deg)	k_x (mD)	k_y (mD)	k_z (mD)	k_v / k_h	Salinity (ppm)	Porosity (fraction)	Thickness (m)	Hysteresis Model	Trapped Gas Saturation	Well Orientation	Well bore radius (m)	Well Length (m)	Injection Period (years)	Target Injection Rate (MT/yr)	Compressibility (1/bar)	Distance to CP boundary (km)	Other Changes
48	20	180	2000	3	0.4	30	300	0.3	0.001	100,000	0.27	200	C	0.3	X	0.1	900	50	4	$5.8x10^{-5}$	10	
49	5	180	2000	3	0.4	30	300	30	0.1	100,000	0.27	400	C	0.3	X	0.1	900	50	4	$5.8x10^{-5}$	10	
50	10	180	2000	3	0.4	30	300	30	0.1	100,000	0.27	200	C	0.3	X	0.1	900	50	4	$5.8x10^{-5}$	10	
51	30	180	2000	3	0.4	30	300	30	0.1	100,000	0.27	75	C	0.3	X	0.1	900	50	4	$5.8x10^{-5}$	10	
52	10	180	2000	3	0.4	30	300	30	0.1	100,000	0.27	100	C	0.3	X	0.1	900	50	4	$5.8x10^{-5}$	10	2 wells
53	5	180	2000	3	0.4	30	300	30	0.1	100,000	0.27	100	C	0.3	X	0.1	900	50	4	$5.8x10^{-5}$	10	2 wells
54	10	180	2000	3	0.4	30	300	30	0.1	100,000	0.27	100	C	0.3	X	0.1	900	50	4	$5.8x10^{-5}$	50	
55	5	180	2000	3	0.4	30	300	30	0.1	100,000	0.27	100	C	0.3	X	0.1	900	50	4	$5.8x10^{-5}$	50	
56	10	180	2000	3	0.4	30	300	30	0.1	100,000	0.27	100	C	0.3	X	0.1	900	50	4	$5.8x10^{-5}$	50	2 wells
57	5	180	2000	3	0.4	30	300	30	0.1	100,000	0.27	100	C	0.3	X	0.1	900	50	4	$5.8x10^{-5}$	50	3 wells
58	20	180	2000	3	0.4	30	300	30	0.1	100,000	0.27	400	C	0.3	X	0.1	900	50	4	$5.8x10^{-5}$	50	
59	20	180	2000	3	0.4	30	300	30	0.1	100,000	0.27	100	C	0.3	Z	0.1	100	50	4	$5.8x10^{-5}$	10	
60	20	180	2000	3	0.4	30	300	30	0.1	100,000	0.27	200	C	0.3	X	0.1	900	50	4	$5.8x10^{-5}$	50	
61	20	180	2000	3	0.4	30	300	30	0.1	100,000	0.27	50	C	0.3	X	0.1	900	50	4	$5.8x10^{-5}$	50	
62	20	180	3000	3	0.4	30	300	30	0.1	100,000	0.27	100	C	0.3	X	0.1	900	50	4	$5.8x10^{-5}$	50	
63	20	180	1000	3	0.4	30	300	30	0.1	100,000	0.27	100	C	0.3	X	0.1	900	50	4	$5.8x10^{-5}$	150	
64	20	180	2000	3	0.4	30	300	30	0.1	100,000	0.27	75	C	0.3	X	0.1	900	50	4	$5.8x10^{-5}$	50	
65	20	180	2000	3	0.4	30	300	30	0.1	100,000	0.27	150	C	0.3	X	0.1	900	50	4	$5.8x10^{-5}$	50	
66	20	180	2500	3	0.4	15	150	1.5	0.01	100,000	0.27	75	C	0.3	X	0.1	900	50	4	$5.8x10^{-5}$	50	
67	20	180	2000	3	0.4	10	100	10	0.1	100,000	0.27	100	C	0.3	X	0.1	900	50	4	$5.8x10^{-5}$	50	
68	20	126	2000	3	0.9	90	900	90	0.1	100,000	0.27	50	C	0.3	X	0.1	900	50	4	$5.8x10^{-5}$	50	
69	20	77	2500	3	3.2	3.8	38	3.8	0.1	100,000	0.17	400	C	0.3	X	0.1	900	50	4	$5.8x10^{-5}$	50	
70	20	126	2000	3	0.9	90	900	90	0.1	100,000	0.27	300	C	0.3	X	0.1	900	50	4	$5.8x10^{-5}$	50	
71	20	77	2500	3	3.2	5	5	0.5	0.1	100,000	0.19	400	C	0.3	X	0.1	900	50	4	$5.8x10^{-5}$	50	
72	20	77	2000	3	3.2	5	5	0.5	0.1	100,000	0.13	200	C	0.3	X	0.1	900	50	4	$5.8x10^{-5}$	50	

Index	Width X (km)	Length Y (km)	Depth (m)	Dip in X (deg)	Dip in Y (deg)	k_x (mD)	k_y (mD)	k_z (mD)	k_v / k_h	Salinity (ppm)	Porosity (fraction)	Thickness (m)	Hysteresis Model	Trapped Gas Saturation	Well Orientation	Well bore radius (m)	Well Length (m)	Injection Period (years)	Target Injection Rate (MT/yr)	Compressibility (1/bar)	Distance to CP boundary (km)	Other Changes
73	20	67	1000	3	0.9	10	100	10	0.1	100,000	0.23	66	C	0.3	X	0.1	900	50	4	$5.8x10^{-5}$	50	
74	20	68	2000	3	3.7	5	5	0.5	0.1	100,000	0.15	109	C	0.3	X	0.1	900	50	4	$5.8x10^{-5}$	50	
75	20	55	1250	3	5.7	10	10	0.1	0.01	100,000	0.06	76	C	0.3	X	0.1	900	50	4	$5.8x10^{-5}$	50	
76	20	78	3000	3	4.5	1	1	0.1	0.1	100,000	0.25	32	C	0.3	X	0.1	900	50	4	$5.8x10^{-5}$	50	
77	20	126	2000	3	0.9	90	900	90	0.1	100,000	0.27	50	C	0.3	X	0.1	900	5	4	$5.8x10^{-5}$	50	
78	20	126	2000	3	0.9	90	900	90	0.1	100,000	0.27	50	C	0.3	X	0.1	900	10	4	$5.8x10^{-5}$	50	
79	20	126	2000	3	0.9	90	900	90	0.1	100,000	0.27	50	C	0.3	X	0.1	900	25	4	$5.8x10^{-5}$	50	
80	20	77	1300	3	0.9	700	7000	700	0.1	100,000	0.31	100	C	0.3	X	0.1	900	5	4	$5.8x10^{-5}$	50	
81	20	65	1300	3	1.6	700	7000	700	0.1	100,000	0.18	55	C	0.3	X	0.1	900	5	4	$5.8x10^{-5}$	50	
82	20	67	2000	3	4	25	250	25	0.1	100.000	0.15	40	C	0.3	X	0.1	900	5	4	5.8x10-5	50	
83	20	73	2000	3	3	27.5	275	27.5	0.1	100.000	0.16	24	C	0.3	X	0.1	900	5	4	5.8x10-5	50	
84	20	55	1250	3	5.7	10	10	1	0.1	100000	0.06	76	C	0.3	X	0.1	900	5	4	5.8x10-5	50	
85	20	77	2500	3	3.2	3.8	38	3.8	0.1	100000	0.17	400	C	0.3	X	0.1	900	5	4	5.8x10-5	50	
86	20	106	2000	3	1.2	70	700	70	0.1	100000	0.27	50	C	0.3	X	0.1	900	5	4	5.8x10-5	50	
87	20	77	2500	3	3.2	3.8	38	3.8	0.1	100000	0.17	400	C	0.3	X	0.1	900	3	4	5.8x10-5	50	
88	20	86	2500	3	2.5	25	250	25	0.1	100000	0.15	180	C	0.3	X	0.1	900	1	4	5.8x10-5	50	
89	20	42	2000	4	4	40	400	40	0.1	100000	0.15	20	C	0.3	X	0.1	900	1	4	5.8x10-5	25	
90	20	42	2000	4	4	40	400	40	0.1	100000	0.15	20	C	0.3	X	0.1	900	0.25	4	5.8x10-5	25	
91	20	65	1300	3	1.6	700	7000	700	0.1	100000	0.18	55	C	0.3	X	0.1	900	0.25	4	5.8x10-5	25	
92	20	77	1300	3	0.9	700	7000	700	0.1	100000	0.31	100	C	0.3	X	0.1	900	1.00	4	5.8x10-5	25	
93	20	77	1300	3	0.9	700	7000	700	0.1	100000	0.31	100	C	0.3	X	0.1	900	0.25	4	5.8x10-5	25	
94	20	28	1034	3	2.8	1200	12000	1200	0.1	100000	0.33	143	C	0.3	X	0.1	900	0.00	4	5.8x10-5	25	

C Carlson Hysteresis model, K Killough Hysteresis model

X,Y,Z Direction of well completion (X = transverse to dip, Y = parallel to dip, Z= Vertical)

Table A6.2: CO_2 Plume Dimensions and Migration Results

Index	Mass Injected (Mt)	CO_2 Density at centroid of plume (kg/m^3)	Plume Width (km)	Downdip Limit of Plume (km)	Updip Limit of Plume (km)	Velocity of Migration (m/yr)	Pore Volume Utilisation (%) (Using CO_2 Extent)
1	200	722	5.50	7.33	12.93	7.45	9.21
2	200	722	5.50	7.38	13.01	7.44	9.14
3	200	722	4.50	6.81	12.25	7.22	11.96
4	200	723	4.00	5.79	9.90	6.56	16.32
5	200	683	5.50	7.59	61.11	40.31	2.87
6	200	683	3.50	10.15	63.52	35.91	4.20
7	200	682	6.50	6.83	60.19	36.05	2.49
8	58	725	3.50	2.60	1.76	0.59	19.09
9	200	654	5.50	5.55	>24	>100	-
10	200	725	5.50	10.05	9.52	3.94	9.48
11	200	698	5.50	6.18	22.54	22.54	6.71
12	200	704	5.50	7.21	13.53	7.65	9.22
13	200	763	5.50	6.60	11.97	6.44	9.49
14	200	721	5.50	7.34	13.17	7.77	9.10
15	200	722	5.50	7.30	13.05	7.59	9.16
16	200	722	5.50	7.26	12.96	7.49	9.22
17	200	722	5.50	7.10	12.36	6.74	9.58
18	200	721	5.00	7.57	13.39	7.92	9.79
19	198	727	7.50	10.15	13.17	5.94	23.19
20	200	726	6.00	10.00	13.00	6.50	14.78
21	200	723	5.50	7.62	12.72	7.10	12.20
22	200	718	4.50	7.07	13.45	7.79	7.44
23	200	716	5.00	7.09	13.54	7.74	5.01
24	200	703	4.00	6.77	15.55	9.48	2.95
25	200	722	5.00	7.18	12.04	6.64	10.66
26	200	720	5.50	7.72	14.68	9.09	8.34
27	200	717	7.50	10.15	23.09	15.31	8.60

Index	Mass Injected (Mt)	CO_2 Density at centroid of plume (kg/m^3)	Plume Width (km)	Downdip Limit of Plume (km)	Updip Limit of Plume (km)	Velocity of Migration (m/yr)	Pore Volume Utilisation (%) (Using CO_2 Extent)
28	200	722	5.00	6.78	11.11	6.13	9.37
29	200	721	5.50	7.34	13.17	7.67	9.09
30	200	724	4.50	9.52	10.99	6.92	11.07
31	200	723	5.00	8.42	11.99	7.20	10.03
32	200	722	5.00	7.98	12.33	7.32	10.09
33	200	722	5.50	7.54	12.82	7.38	9.15
34	200	721	5.00	6.41	12.29	6.00	10.97
35	200	721	5.50	6.60	13.33	7.48	9.36
36	200	721	5.00	7.34	13.71	7.40	9.75
37	-	-	-	-	-	-	-
38	200	724	5.00	7.40	12.70	7.14	10.17
39	-	-	-	-	-	-	-
40	200	685	3.00	9.38	60.33	42.43	5.17
41	58	703	3.50	2.05	4.10	3.32	14.04
42	58	718	3.50	2.08	3.00	1.80	16.69
43	200	666	7.50	3.56	13.85	18.06	8.51
44	200	584	5.50	5.59	33.54	>100	5.89
45	58	725	3.50	2.57	1.81	0.53	19.40
46	200	722	5.50	10.15	29.32	16.03	4.72
47	200	696	7.50	4.48	21.98	19.27	5.36
48	200	718	3.50	4.63	7.12	6.16	12.53
49	200	704	2.35	7.39	14.81	9.30	5.04
50	200	716	4.50	7.42	13.20	7.65	5.57
51	200	723	5.50	7.39	12.69	6.90	12.36
52	-	-	-	-	-	-	-
53	-	-	-	-	-	-	-
54	200	725	5.00	7.74	12.36	7.07	10.16
55	-	-	-	-	-	-	-

Index	Mass Injected (Mt)	CO_2 Density at centroid of plume (kg/m^3)	Plume Width (km)	Downdip Limit of Plume (km)	Updip Limit of Plume (km)	Velocity of Migration (m/yr)	Pore Volume Utilisation (%) (Using CO_2 Extent)
56	-	-	-	-	-	-	-
57	-	-	-	-	-	-	-
58	200	706	3.50	6.79	15.32	9.29	3.39
59	200	722	5.00	7.62	13.22	7.35	9.84
60	200	722	4.00	7.16	13.25	7.44	6.28
61	200	726	5.50	8.90	12.43	6.40	17.39
62	200	705	5.00	7.38	13.36	7.42	10.12
63	200	765	5.00	6.40	12.00	5.99	10.52
64	200	725	5.00	7.77	12.41	6.71	13.49
65	200	722	4.50	7.19	13.19	7.49	7.45
66	198	715	4.50	7.79	9.48	4.43	17.58
67	196	727	4.50	7.01	7.35	3.08	15.50
68	200	623	6.00	7.00	>62.60	94.59	5.70
69	200	519	3.00	3.23	>26.29	>80	6.40
70	200	496	4.50	5.16	>75.17	>126.36	1.38
71	82	698	3.00	1.76	2.35	2.35	12.67
72	36	710	3.00	1.79	3.17	2.31	13.44
73	42	786	3.50	3.13	6.32	3.41	10.68
74	24	715	3.00	1.76	2.90	1.98	14.15
75	14	789	4.00	2.10	4.33	>8	14.63
76	4	707	2.10	1.22	0.70	0.33	15.75
77	20	703	3.00	2.54	19.35	8.43	3.19
78	40	691	3.50	3.38	26.52	12.89	4.10
79	100	668	3.50	5.16	41.11	34.40	6.84
80	20	680	3.00	2.82	>26.27	~100	1.09
81	20	698	3.50	3.88	>14.29	~100	4.55
82	18	660	3.50	3.18	>16.28	~100	6.77
83	12	574	3.50	3.19	>22.17	10.30	6.14

Index	Mass Injected (Mt)	CO_2 Density at centroid of plume (kg/m^3)	Plume Width (km)	Downdip Limit of Plume (km)	Updip Limit of Plume (km)	Velocity of Migration (m/yr)	Pore Volume Utilisation (%) (Using CO_2 Extent)
84	1	808	2.10	1.18	1.72	2.14	4.55
85	20	646	1.70	1.53	12.24	12.24	1.94
86	20	692	3.00	2.45	19.79	9.04	3.21
87	10	672	1.30	1.35	7.46	7.12	1.91
88	4	677	1.70	1.70	10.91	2.37	1.02
89	3	613	2.10	2.28	16.83	>27.695	4.12
90	1	693	1.70	1.69	7.58	1.27	2.68
91	1	725	1.70	3.19	7.24	0.00	0.79
92	4	713	2.10	2.52	14.16	1.06	0.51
93	1	739	1.30	2.37	3.13	0.00	0.61
94	1	786	0.90	3.58	1.56	0.00	0.58

No storage Factors calculated for cases with more than one well

Table A6.3: Pressure Corrected Storage Factors

Index	Transverse spacing 20 km		Transverse spacing 10 km		Transverse spacing 5km		Max no Wells	Pressure Corrected Utilisation (%)	Modified Max no of wells	Modified Pressure Utilisation (%)	Reason for Modification
	Max no. Wells	Long Spacing (km)	Max no. Wells	Long Spacing (km)	Max no. Wells	Long Spacing (km)					
1	6	20.3	3	20.3	0	0.0	6	1.71	3	0.85	Simulated as case 38
2	6	20.4	3	20.4	0	0.0	6	1.71	3	0.85	Very similar to 1
3	5	19.1	3	19.1	1	19.1	6	1.71	3	0.85	Higher bhp/smaller footprint than 1. Expect upscale the same
4	4	15.7	2	15.7	1	15.7	4	1.14	2	0.57	Set in proportion to case 1
5	3	68.7	3	68.7	0	0.0	6	1.81	0	0.00	Unstable
6	2	73.7	2	73.7	2	73.7	8	2.41	0	0.00	Unstable
7	3	67.0	3	67.0	0	0.0	6	1.81	0	0.00	Unstable
8	1	4.4	0	4.4	0	0.0	1	0.08	1	<0.08	Pfrac exceeded overestimate
9	1	29.3	1	29.3	0	0.0	2	-	-	-	ignored as very unstable
10	9	19.6	4	19.6	0	0.0	9	2.55	5	1.42	Estimated as 5@19.6 in 20 km width by adjusting bhps comparable to 1
11	2	28.7	2	28.7	2	0.0	8	6.15	0	0.00	Estimated as 2@28.7 in 20 km width by adjusting bhps comparable to 1
12	9	20.7	9	20.7	4	20.7	18	5.26	6	1.75	Simulated as case 62
13	2	18.6	2	18.6	0	0.0	4	6.69	5	8.36	Simulated as case 63
14	6	20.5	3	20.5	0	0.0	6	1.71	3	0.85	Very similar to 1
15	6	20.4	3	20.4	0	0.0	6	1.71	3	0.85	Very similar to 1
16	6	20.2	3	20.2	0	0.0	6	1.71	3	0.85	Very similar to 1
17	6	19.5	3	19.5	0	0.0	6	1.71	3	0.85	Very similar to 1
18	6	19.5	3	19.5	0	0.0	6	1.71	3	0.85	Very similar to 1
19	0	0.0	0	0.0	0	0.0	0	0.00	1	<1.13	Pfrac limit exceeded overestimate
20	2	21.3	1	21.3	0	0.0	2	1.13	2	1.13	Simulated as case 61
21	4	20.3	2	20.3	0	0.0	4	1.52	2	0.76	Simulated as case 64
22	8	20.5	6	20.5	3	20.5	12	2.29	5	0.95	Simulated as case 65
23	9	20.6	8	20.6	4	20.6	16	2.30	7	1.01	Simulated as case 60

Index	Transverse spacing 20 km		Transverse spacing 10 km		Transverse spacing 5km		Max no Wells	Pressure Corrected Utilisation (%)	Modified Max no of wells	Modified Pressure Utilisation (%)	Reason for Modification
	Max no. Wells	Long Spacing (km)	Max no. Wells	Long Spacing (km)	Max no. Wells	Long Spacing (km)					
24	8	22.3	8	22.3	8	22.3	32	2.34	14	1.02	Simulated as case 58
25	6	19.2	4	19.2	2	19.2	8	2.28	3	0.85	Very similar to 1
26	5	22.4	3	22.4	0	0.0	6	1.71	3	0.86	Estimated as 3@22.4km by adjusting bhp comparable to 1
27	4	33.2	3	33.2	0	0.0	6	3.57	3	1.79	Estimated as 3@33.2km by adjusting bhp comparable to 1
28	6	17.9	4	17.9	2	17.9	8	1.86	3	0.70	Very similar to 1
29	6	20.5	3	20.5	0	0.0	6	1.71	3	0.85	Very similar to 1
30	0	0.0	0	0.0	2	20.5	2	2.27	0	0.00	Simulated ac case 55 but failed
31	0	0.0	0	0.0	3	20.4	3	2.27	1	0.76	Extrapolated from widths
32	0	0.0	4	20.3	2	20.3	4	2.28	1	0.57	Simulated as case 54
33	7	20.4	4	20.4	0	0.0	8	2.28	4	1.14	Estimated as 3@20.4km by adjusting bhp comparable to 1
34	1	18.7	0	0.0	0	0.0	1	0.28	1	0.28	No need to adjust
35	4	19.9	2	19.9	0	0.0	4	1.14	3	0.86	Estimated as 3@19,9km by adjusting bhp comparable to 1
36	5	21.1	3	21.1	1	21.1	6	1.71	3	0.86	Very similar to 1
37	-	-	-	-	-	-	-	-	-	-	
38	3	20.1	1	20.1	0	0.0	3	0.85	3	0.85	Simulated
39	-	-	-	-	-	-	-	-	-	-	
40	3	69.7	3	69.7	0	0.0	6	1.80	0	0.00	Unstable
41	1	6.1	0	0.0	0	0.0	1	0.63	1	<0.63	Pfrac exceeded overestimate
42	0	5.1	0	0.0	0	0.0	0	0.00	1	<0.65	Pfrac exceeded overestimate
43	1	17.4	0	0.0	0	0.0	1	1.68	0	0.00	Unstable
44	1	39.1	1	39.1	0	0.0	2	2.82	0	0.00	Unstable
45	0	4.4	0	0.0	0	0.0	0	0.00	1	<0.04	Pfrac exceeded overestimate
46	5	39.5	3	39.5	0	0.0	6	1.71	0	0.00	Unstable
47	3	26.5	3	26.5	0	0.0	6	4.62	0	0.00	Unstable

Index	Transverse spacing 20 km		Transverse spacing 10 km		Transverse spacing 5km		Max no Wells	Pressure Corrected Utilisation (%)	Modified Max no of wells	Modified Pressure Utilisation (%)	Reason for Modification
	Max no. Wells	Long Spacing (km)	Max no. Wells	Long Spacing (km)	Max no. Wells	Long Spacing (km)					
48	10	11.8	6	11.8	3	11.8	12	1.72	7	1.00	Set to case 60
49	0	0.0	0	0.0	7	22.2	7	2.04	3	0.88	Taken from case 58
50	0	0.0	8	20.6	4	20.6	8	2.30	3	0.86	Taken from case 60
51	5	20.1	3	20.1	2	20.1	8	2.02	3	0.76	Taken from case 64
52	-	-	-	-	-	-	-	-	-	-	
53	-	-	-	-	-	-	-	-	-	-	
54	0	0.0	1	20.1	0	0.0	1	0.57	1	0.57	Simulated
55	-	-	-	-	-	-	-	-	-	-	Simulation failed
56	-	-	-	-	-	-	-	-	-	-	
57	-	-	-	-	-	-	-	-	-	-	
58	8	22.1	7	22.1	3	22.1	14	1.02	14	1.02	Simulated
59	4	20.8	3	20.8	1	20.8	6	1.71	6	1.71	Simulated
60	7	20.4	3	20.4	1	20.4	7	1.00	7	1.00	Simulated
61	2	21.3	1	21.3	0	0.0	2	1.13	2	1.13	Simulated
62	6	20.7	3	20.7	1	20.7	6	1.75	6	1.75	Simulated
63	5	18.4	1	18.4	0	18.4	5	1.34	3	0.81	Adjusted because extra 100 km downdip
64	2	20.2	1	20.2	0	0.0	2	0.76	2	0.76	Simulated
65	5	40.7	2	20.4	1	20.4	5	0.95	5	0.95	Simulated
66	1	17.3	0	0.0	0	0.0	1	0.38	1	0.38	Simulated
67	0	14.4	0	0.0	0	0.0	0	0.00	1	<0.28	Pfrac exceeded overestimate
68	2	69.6	1	69.6	0	0.0	2	1.89	0	0.00	Note CO_2 above 800 m after ~ 900 years
69	2	29.5	2	29.5	0	0.0	4	1.47	0	0.00	Note CO_2 above 800 m after ~ 900 years
70	2	80.3	2	80.3	2	80.3	8	1.58	0	0.00	Note CO_2 above 800 m after ~ 700 years

Index	Transverse spacing 20 km		Transverse spacing 10 km		Transverse spacing 5km		Max no Wells	Pressure Corrected Utilisation (%)	Modified Max no of wells	Modified Pressure Utilisation (%)	Reason for Modification
	Max no. Wells	Long Spacing (km)	Max no. Wells	Long Spacing (km)	Max no. Wells	Long Spacing (km)					
71	8	4.1	4	4.1	1	4.1	8	0.81	8	0.81	NB Close well spacing allows lots of wells to be inserted downdip
72	6	5.0	3	5.0	1	5.0	6	0.78	6	0.78	NB Close well spacing allows lots of wells to be inserted downdip
73	3	9.5	2	9.5	1	9.5	4	1.05	1	0.26	NB Adjusted for actual Spilsby geometry
74	7	4.7	3	4.7	1	4.7	7	1.02	7	1.02	
75	8	6.4	7	6.4	6	6.4	24	8.21	0	0.00	Note CO_2 above 800 m after ~ 450 years
76	12	1.9	10	1.9	3	1.9	20	0.82	20	0.82	Note rate per well very low at 0.036 Mt/yr
77	6	21.9	4	21.9	2	21.9	8	0.66	8	0.66	Note only injected for 5 years
78	4	29.9	3	29.9	1	29.9	6	1.02	0	0.00	Unstable
79	3	46.3	2	46.3	1	46.3	4	1.76	0	0.00	Unstable
80	3	29.1	3	29.1	3	29.1	12	0.74	0	0.00	Note CO_2 above 800 m after ~ 200 years
81	4	18.2	4	18.2	4	18.2	16	3.56	0	0.00	Note CO_2 above 800 m after ~ 30 years
82	2	19.5	2	19.5	2	19.5	8	2.75	0	0.00	Note CO_2 above 800 m after ~ 250 years
83	2	25.4	2	25.4	1	25.4	4	1.49	0	0.00	Note CO_2 above 800 m after ~400 years
84	17	2.9	17	2.9	15	2.9	60	1.51	60	1.51	Only 1 M Tonnes per injection site
85	5	13.8	5	13.8	4	13.8	16	0.47	32	0.95	Unstable.
86	4	22.2	4	22.2	2	22.2	8	0.81	8	0.81	20 M Tonnes per injection site
87	7	8.8	7	8.8	7	8.8	28	0.40	56	0.80	10 M Tonnes per injection site
88	7	12.6	7	12.6	7	12.6	28	0.36	56	0.71	Only 4 Mt/well
89	1	19.1	1	19.1	1	19.1	4	0.79	0	0.00	CO_2 escaped after 250 years
90	2	9.3	2	9.3	2	9.3	8	0.40	8	0.40	Only 0.9 Mt/injection site
91	6	10.4	6	10.4	6	10.4	48	0.51	48	0.51	1MT/injection site

Index	Transverse spacing 20 km		Transverse spacing 10 km		Transverse spacing 5km		Max no Wells	Pressure Corrected Utilisation (%)	Modified Max no of wells	Modified Pressure Utilisation (%)	Reason for Modification
	Max no. Wells	Long Spacing (km)	Max no. Wells	Long Spacing (km)	Max no. Wells	Long Spacing (km)					
92	5	16.7	5	16.7	5	16.7	40	0.47	40	0.47	4MT/injection site.
93	14	5.5	14	5.5	14	5.5	112	0.32	112	0.32	1MT/injection. All dissolved
94	5	5.1	5	5.1	5	5.1	200	0.39	80	0.39	1MT/injection. All dissolved

No storage Factors calculated for cases with more than one well.